DESIGN AND DEVELOPMENT OF UNDULATING FIN

ANDRE WILLY

SCHOOL OF MECHANICAL & AEROSPACE ENGINEERING

A thesis submitted to the Nanyang Technological University
In fulfilment of the requirement for the degree of
Master of Engineering

2006

Abstract

Recently researchers and scientists have been more vocal than in the past in promoting an awareness to preserve environment. One of their main concerns is the sustainability of underwater ecology, especially marine environment, which is deteriorating due to extensive use of propellers. Imitating natural propulsion system (*biomimetic*) is an alternative to solve the concern mentioned above, which is to replace propellers. Thorough examination into the locomotion of living creatures reveals their oscillatory pattern. The research leads to the development of an environment friendly propulsion system, which mimics undulating fin of narrow-finned fish such as cuttlefish and knifefish. A nonconventional mechanical system comprises several fin segments was designed and fabricated to mimic the actual flexible fin. Each fin segment is an independent oscillating foil, which is a two-degree-of-freedom slider mechanism driven by two servomotors.

A mechanical undulating fin was successfully designed and constructed. The undulating fin is controlled by several microcontrollers, which are arranged in parallel processing for faster command execution. The control architecture can be easily extended to accommodate any number of actuators required to drive the undulating fin. Lighthill's elongated body theory was generalized to suit the mechanical undulating fin and it can be used to model any swimming method of Body/Caudal Fin (BCF) and Median/Pectoral Fin (MPF) swimmers.

An undulating fin having several actuators was designed and fabricated, and it was integrated with a floating cylindrical tank to give it the shape of a biomimetic robot fish. Several underwater experiments on the undulating fin were successfully conducted and the results were found consistent with the undulatory swimming fish found in nature.

Acknowledgement

The author would like to express his appreciation and gratitude to his supervisor, A/P Low Kin Huat for giving him the opportunity to work on this interesting project. He would also like to extend his thanks to all the technical staffs of the following laboratories:

1. Robotics Research Center: Mr. Lim Eng Cheng,
2. Manufacturing Workshop: Ms. Tan How Jee, Esther,
3. Mechatronics and Control Laboratory: Ms. Lee Koon Fong,
4. Mechanics of Machines Laboratory: Mr. Poon Weng Wai,
5. Thermofluids Laboratory: Mr. Cheong Yuen Kong,
6. CAD/CAM Laboratory: Mr. Leong Tuk Weng, Mike.

Thanks are also due to Mr Eng You Hong, Mr Aw Wai Leong, and Mr. Pattathil Anjan Prabhat for their valuable help in experiments. The author wishes to acknowledge A/P Gerald Seet's generosity in providing research facility and equipment, and Dr. F.M.J. Nickols for his valuable guidance at the early development of the undulating fin described in this thesis. Above all, the author thanks School of Mechanical and Aerospace Engineering (MAE) and Nanyang Technological University (NTU) for granting the author this research opportunity and supportive environment for knowledge and interpersonal skill development.

Table of Contents

Appendices

List of Figures

List of Tables

Chapter One
Introduction

1.1 Background

Recently researchers and scientists have been more vocal than in the past in promoting an awareness to preserve environment. One of their main concerns is the sustainability of underwater ecology, especially marine environment, which is deteriorating due to extensive use of propellers and has recently gained public and government attention.

Despite its versatility, propeller has created a certain concern for marine life; it produces greater amount of marine debris, continued mortality of marine creatures such as manatees as a result of propeller strikes, and disturbance of shallow waters ecosystem.

Engineered counterpart or biomimetic [1] of natural locomotion could be the solution of the above addressed concern. Each species has its own unique and optimum way of interacting with its environment, which then dictates the species' body shape, body size, and the way it propels itself, as proposed by Darwinian process of natural selection [2]. This leads to the development of an environment friendly propulsion system, which mimics lateral undulating fins of cuttlefish or pectoral fins of stingray.

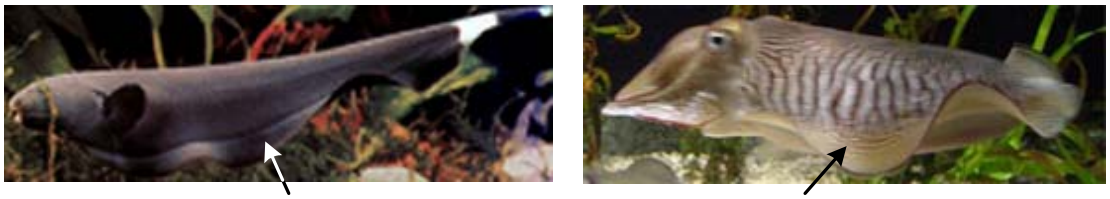

Figure 1.1. (a) Black ghost knifefish and (b) cuttlefish swimming with undulating fins.

1.2 Potential Applications

1.2.1 Industrial and Commercial

Autonomous underwater vehicles (AUV's) are an interesting area of application that could also greatly benefit from biomimetic mechanical systems, as there is an increased demand for improved efficiency to allow for longer missions to be undertaken. Oil and gas companies, for example, are now using underwater robots to perform pipe inspection and repair [3].

1.2.2 Entertainment and Education

It is very interesting to observe how underwater species interact with an undulating finned robotic fish; its deployment in an existing *sea world* has a potential to attract more tourists [4]. In the area of education, robots present an excitement for young minds to do research and innovate.

1.2.3 Field Service and Research

In this field, undulating-finned robot offers exceptional advantage over propeller in preserving an undisturbed condition of its surroundings for data acquisition. This robot can also replace human divers to dive beyond 100 feet, thus removing the divers from a danger known as "the bends" or decompression sickness, which can be fatal [5].

1.2.4 Military and Defense

Most important areas where biomimetic robot finds its significant role in ensuring safe waters; the undulating fin robot might be undetected when swim with a school of fish and therefore may act as a spy. The underwater robot can also be used to guard underwater natural resources of a country [6].

1.3 Objectives and Scope

Fish swim by undulation and/or oscillation of their body and/or fin(s). The objective of this research was to build an environment friendly propulsion system by mimicking the undulating fins of cuttlefish and stingray. The research was focused on developing a prototype that can be implemented on an underwater robot (AUV). In the course of the research it was realized that there are vast array of fishes swimming with undulating fins. Black ghost knifefish and banded knifefish are just two examples of the many types of knifefishes swimming by undulations of their fins.

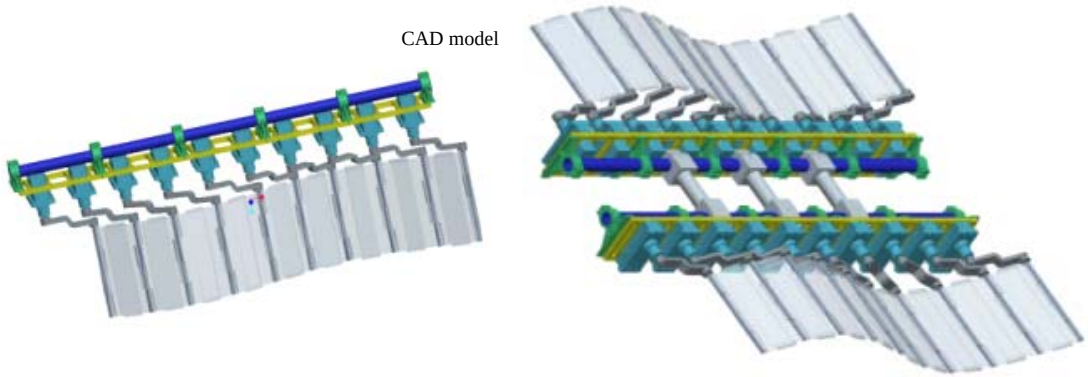

(a) (b)

Figure 1.2. (a) Independent single unit of a mechanical undulating fin mimicking the anal fin of the knifefish in Figure 1.1(a). (b) Two units of undulating fins arranged side-by-side in horizontal plane mimicking the lateral fins of cuttlefish shown in Figure 1.1(b).

The development of the prototype was then carried out to build a modular cuttlefish robot whose fins are two separate independent units. A single fin unit is shown in Figure 1.2(a). With that unit, we were able to mimic the propulsion system of black ghost knifefish swimming with an undulating long-based anal fin, while its body remains straight. With two units of the undulating fin shown in Figure 1.2(a), and by putting them side-by-side in a horizontal plane, we were able to construct and mimic the lateral fins of a cuttlefish, shown in Figure 1.2(b).

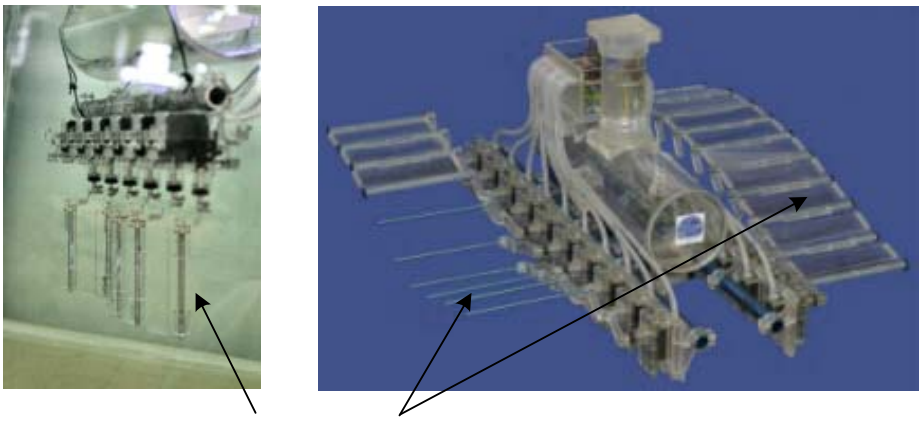

(a) (b)

Figure 1.3. Mechanical counterpart, biomimetic robots, of the undulating fins of the black ghost (a) and cuttlefish (b) shown in Figure 1.1(a) and Figure 1.1(b), respectively.

The scope of the research work was:

1. To study various fish swimming modes, focusing on undulatory swimming modes.
2. To design and build a mechanical counterpart of an undulating fin.
3. To design and apply control to the undulating fin.
4. To construct robots swimming with undulating fins, such as knifefish and cuttlefish.
5. To conduct experiment with the implemented control system in order to obtain qualitative data such as the behavior of the undulating fin, and quantitative data such as velocity of the undulating fin in various swimming modes.

1.4 Thesis Organization

This thesis reviews several fish swimming modes following classical classification scheme and nomenclature proposed by Breder [7]. The mechanical design of the undulating fin will be discussed, as well as factors involved in the design. Control architecture of the undulating fin was designed in parallel processing. Theory developed for undulating fin will be generalized for programming purpose. Lastly, the experimental results will be presented.

Chapter Two
Literature Review

2.1 Brief History of Robot

The word *robot* comes from Czech *robota*, which means servitude, forced labor. Modern dictionary [8] defines robot as a mechanical device that sometimes resembles a human and is capable of performing a variety of often complex human tasks on command or by being programmed in advance. The device may operate automatically or by remote control.

The history of robots can be traced back to the year 270 BC when ancient Greek engineer named Ctesibus made organ and water clocks with movable figures [9, 10]. Throughout centuries many had worked on the filed of robotics based on the technology and socioeconomic needs of their time. Leonardo da Vinci (1452-1519) who wrote many documents on Anthrobotics, and Nikola Tesla (1856-1943) who made a remote controlled submersible boat, are two noteworthy great inventors and engineers of the past. In the early years of the twentieth century, many science fiction books about robotics were published. In 1959, MIT demonstrated computer-assisted manufacturing, and in 1961, the first industrial robot was online in General Motors automobile factory in New Jersey. Since then, robots were developed to assist human and to have intelligence.

Recently robots are widely used in the industry, which requires non-stop operation, mass production, high repeatability, small variation in one product batch, and high precision. In the field of research, robots are often deployed to area inaccessible to human or that which might pose danger.

2.2 Biomimetic Robots

2.2.1 Fish Robots

In the field of underwater robotics, engineers are looking into propulsive mechanisms other than propeller. Tuna have long attracted the attention of many researchers including those in MIT [11]. Nature works for maximum achievement with minimum effort. Tunas' streamline body shape, swimming method, and lunar-shape of the tail make them fast as well as efficient swimmers in water. Previous research on carangiform swimmers was also done by Mason and Burdick [12, 13].

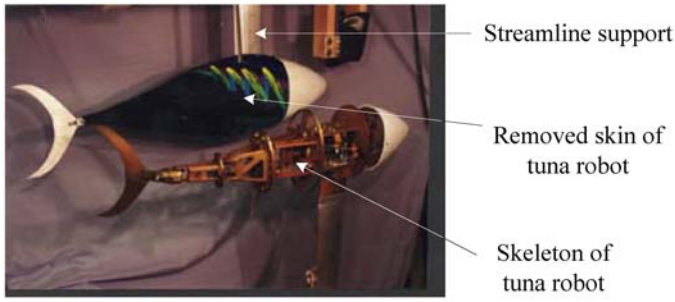

Figure 2.1. MIT RoboTuna with streamline support structure that also passes all tendons and sensor wires [11].

University of Essex also developed a robotic fish, which has its own intelligent guidance system. When the fish gets near the end of the pool, it slows down and stops and turns looking for a new direction. It then turns and swims in the new direction. It does this itself. It is not radio-controlled [14].

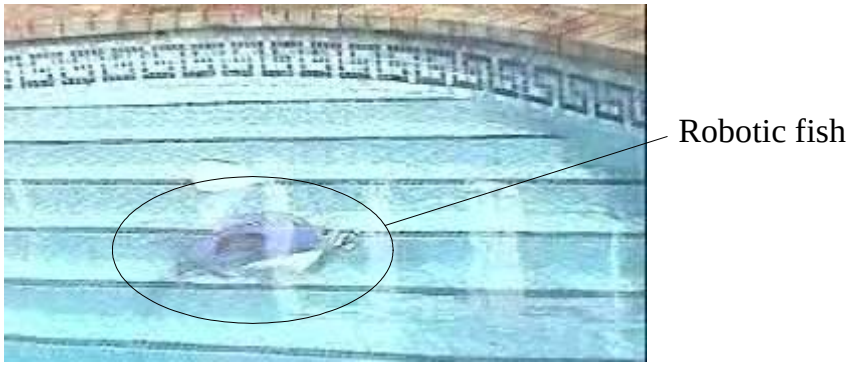

Figure 2.2. Robotic fish of the University of Essex. The fish is shown turning and swimming for new direction at the end of the pool [14].

Figure 2.3. Coelacanth robotic fish of Mitsubishi Heavy Industry (MHI) [4].

Mitsubishi Heavy Industries, Ltd. (MHI), has produced the world's first, radio-controlled lifelike robotic fish to be made available on the market, called "Mitsubishi Animatronics." The robot is in the likeness of a coelacanth, an ancient fish called a "living fossil." MHI is creating the lifelike creature in the hopes of marketing it and similar animatronic system to amusement parks and aquariums. The artificial coelacanth, measuring 70 centimeters long and weighing 12 kg, is powered by an internal battery and controlled automatically by a computer [4]. The robot is also equipped with an intelligence to swim to a recharging unit when its battery runs low.

Figure 2.4. Robotic fish developed by BUAA and CAS of China. The technicians are sending the fish into the swimming pool for testing [15].

In China, a robotic fish was co-developed by the Institute of Robot under Beijing University of Aeronautics and Astronautics (BUAA) and the Automation Research Institute under Chinese Academy of Sciences (CAS). With a black body, the 1.23-meter-long robot is much like a real fish in shape and movement. The robot is controlled through a palm-size remote control pad.

The robotic fish is equipped with automatic navigation control and is able to swim at about 1.5 m/s for two to three hours. The robot is flexible in action, easy to operate and makes little disturbance to surrounding environment. The robot had been tested in an underwater search of a sunken ancient warship in August 2004 [15].

2.2.2 Undulating-Finned Systems

Other underwater robots include lamprey robot which uses shape memory metal to mimic the function of real muscles in mediating undulations as means of propulsion.

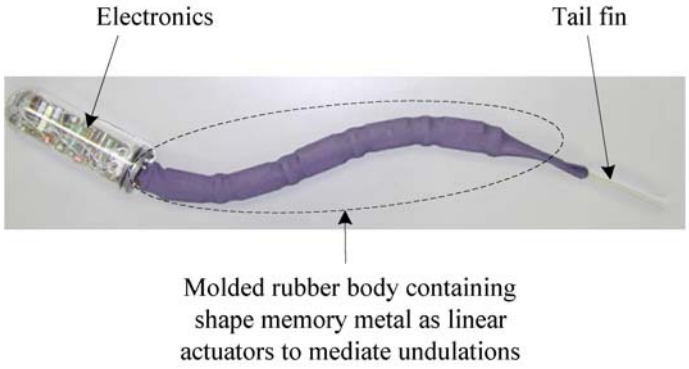

Figure 2.5. Lamprey-based undulatory robot for underwater remote sensing [16].

Other undulatory propulsion mechanism was developed for a black ghost knifefish. The mechanism consists of thirteen servomotors, thirteen fin rays, and a flexible material that connects all fin rays. The amplitude of the traveling wave is 5% of the total length of the fin [17]. The mechanism was designed to have three full sinusoidal wavelengths along the fin, with rays positioned every 90° along the wavelength.

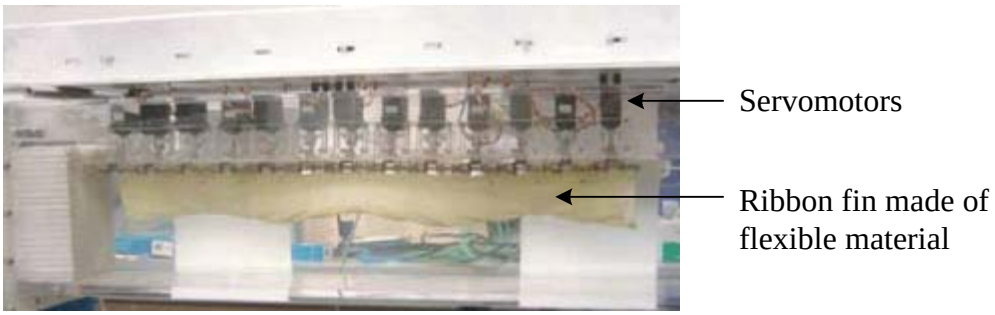

Figure 2.6. Ribbon fin structure mimicking the undulations of a knifefish [18].

Undulatory motion can also be generated by PBA (Parallel Bellow Actuator) element deflections, rather than by links and joints. Such flexible robotic structures offer attractive possibilities for use in the ocean. Producing movements by bending as an elastic continuum, without the need for an additional skeletal structure, results in natural passive compliance to correct for positioning inaccuracies, with simplicity of design and a minimum of moving parts. Benefits are also expected in reducing actuator complexity, weight and local disturbance, as well as increasing robustness and dexterity [19]. To investigate undulating median fin propulsion and its potential for implementation in man-made underwater vehicles, a 'fin actuator' has been developed.

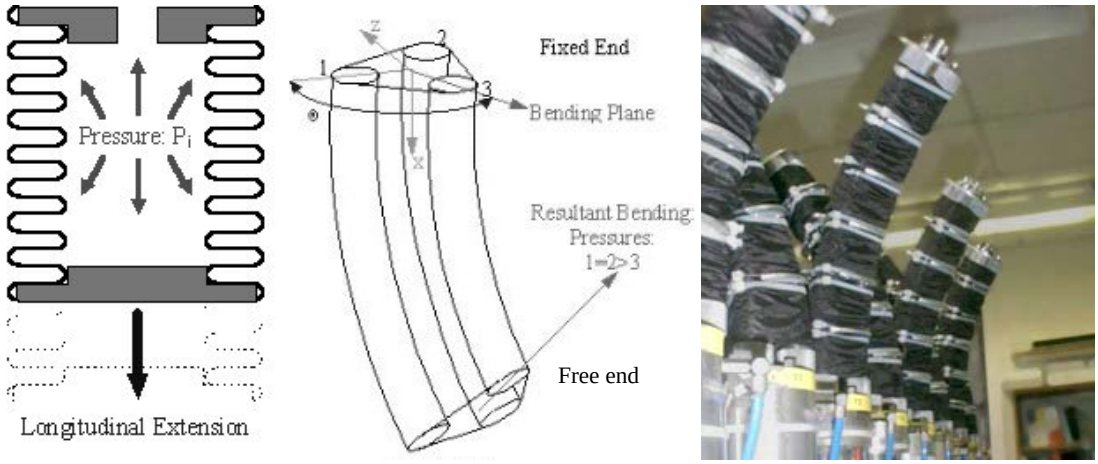

(a) (b) (c)

Figure 2.7. (a) Parallel bellow actuator, PBA, (also referred to as elephant's trunk) actuated pneumatically. (b) Three PBAs joined together to form a 'fin ray'. It can achieve bending movements in any orientation plane. (c) PBAs are arranged in series and connected by a flexible material to mimic fish fin undulation. [19]

The device consists of eight Parallel Bellows Actuators ('fin rays') arranged in a series and interconnected via a flexible material ('fin membrane'). The PBAs are pneumatically driven and allow for bending movements in any orientation plane [20]. Recently, the use of oscillating foils as propulsors has attracted much interest, due to demands for increased propulsion efficiencies of autonomous underwater vehicles. The PBA could be used as a muscle structure, with a hydrofoil attached to it, to better emulate the body flexions involved in fish swimming. The later have been shown to play a significant role to fish achieving increased swimming efficiencies.

2.3 Fish Swimming Modes

Fish exhibit a variety of swimming movements which employ their fin(s) and/or body to produce propulsive and maneuvering force. The classification of swimming movements presented here follows the nomenclature originally established by Breder [7].

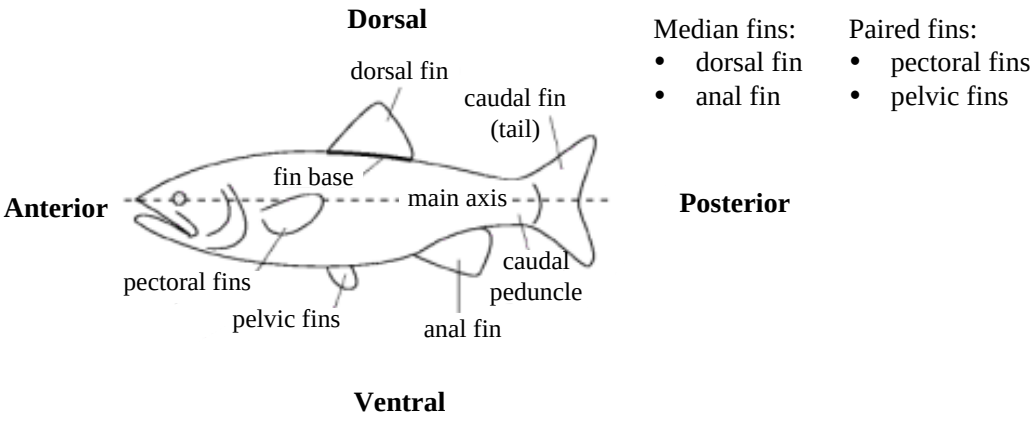

Figure 2.8. Fish morphology and fins used in different swimming modes [21].

Breder [7] proposed two swimming modes of fish based on the propulsive structure used: *body and/or caudal fin* (BCF) locomotion and *median and/or paired fin* (MPF) locomotion. Fish under BCF locomotion generate thrust by bending their body into a backward-moving propulsive wave that extends to its caudal fin, which is shown in Figure 2.8. BCF locomotion is further classified into five subcategories, based on the degree of body undulation, as shown in Figure 2.9.

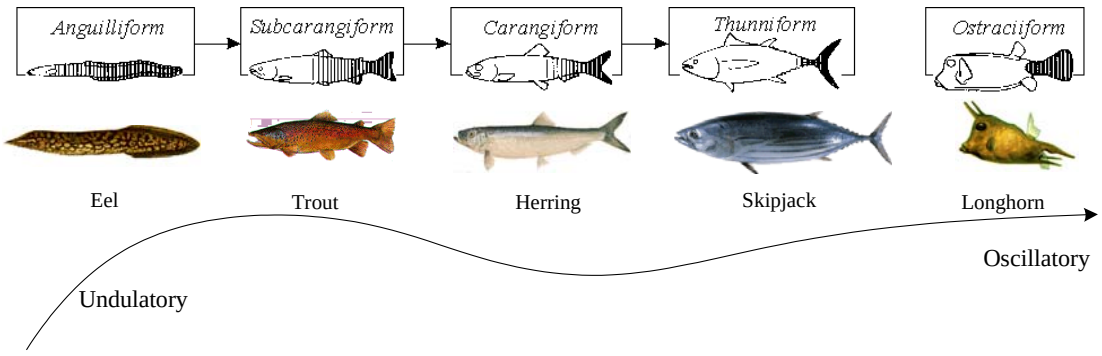

Figure 2.9. Swimming modes and fishes associated with BCF propulsion. Shaded area shows propulsive structure that contributes to thrust generation [22].

In *anguilliform* mode, found in eel, lamprey and needlefish, the whole body participates in large amplitude undulations that increase toward the tail and at least one complete wavelength of the propulsive wave is present along the body [21]. The inclusion of at least one wavelength of the propulsive wave along the body, means that lateral forces are adequately cancelled out, minimizing any tendencies for the body to yaw [21]. On the other end of the BCF subcategories, *ostraciiform* is the only purely oscillatory BCF mode. Fish with ostraciiform mode swim by oscillating the caudal fin, while the body remains essentially rigid.

Body movements in subcarangiform swimmers are very similar to anguilliform mode, the main difference being that the wave amplitude is small in the anterior, and expands significantly only in the posterior half or one-third of the body. Trout is an example of *subcarangiform* swimmer. For *carangiform* swimming the body undulations are further confined to the last third of the body length, and thrust is provided by a rather stiff caudal fin.

Thunniform mode is by far the most efficient locomotion mode evolved in the aquatic environment, where thrust is generated with a lift-based method, allowing high cruising speeds to be maintained for long periods; 90% of the thrust is produced by its caudal fin [21]. Although thunniform swimmers are very efficient at high-speed cruising, they are particularly inefficient for other actions such as slow swimming, turning maneuvers and rapid acceleration from stationary, as well as for turbulent water [21]. Figure 2.10 depicts the gradation of undulatory BCF swimming modes from anguilliform to ostraciiform.

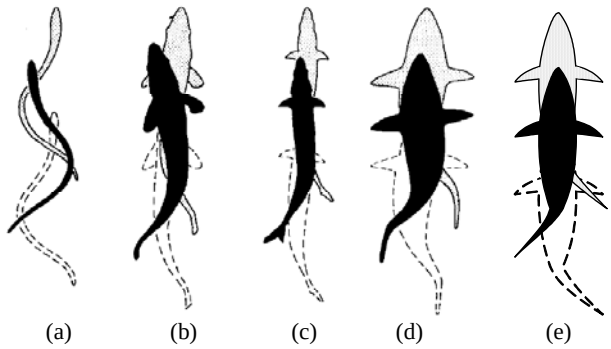

Figure 2.10. Gradation of undulatory swimming modes: (a) anguilliform, (b) subcarangiform, (c) carangiform, (d) thunniform, (e) ostraciiform [modified from 22].

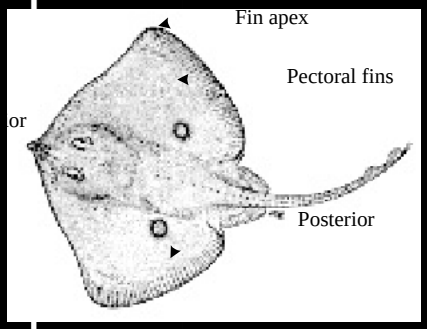

Morphology of
iew) of the undula
pe. The undulations ar

Rajiform mode is found in fish such as rays, skates, and mantas, whose swimming is very similar to the flight of birds. Thrust is produced by large undulations along pectoral fins, which span from the anterior to the posterior of the fish. The amplitude envelope of the undulations increases from the anterior part to the fin apex and decreases toward the posterior as shown in Figure 2.12. Such amplitude envelope can be explained from its triangular-shaped pectoral fins; they are narrower toward anterior and posterior of the fish. The fins may also be flapped up and down similar to the wings of birds. In amiiform mode, fish swim by undulations of long-based dorsal fin, while the body remains straight. Amiiform mode is found in gymnarchus niloticus. Its anal and caudal fins are missing, while the dorsal fin extends along most of the body length, tapering to a posterior point. Locomotor waves may pass in either direction along the dorsal fin, and may show widely varying amplitude, particularly during turning or braking [21]. Gymnotiform mode can be considered as the upside-down equivalent of amiiform mode, since propulsion is obtained by undulations of a long-based anal fin. Gymnotiform fish, such as knifefish, do not have dorsal and caudal fins.

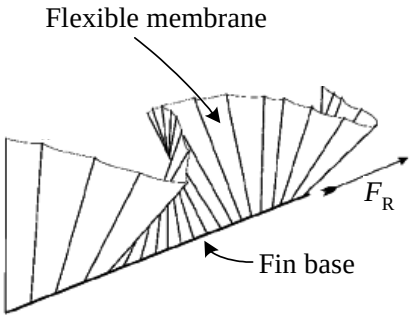

Figure 2.13. Undulations of dorsal or anal fin found in amiiform or gymnotiform mode, respectively. The undulations of the flexible membrane produce resultant force (F_R) parallel to the fin base, which is the body of the fish [21].

Figure 2.13 shows fin undulations of amiiform or gymnotiform fish. The undulations produce propelling force, which is parallel to the fin base. This research work was aimed at analyzing undulating fin of rajiform and gymnotiform swimmers as means of propulsion by designing and constructing a mechanical undulatory propulsion system or mechanical fin. The mechanical modeling of the mechanical fin adapts unconventional method by using rigid linkages, which will be discussed in Chapter 3.

Chapter Three
Design of Undulating Fin

3.1 Undulating-Finned Fish

Cuttlefish is a marine cephalopod of the order *Sepioidea*, related to the octopus and squid and characterized by a thick, internal, calcified shell called the cuttlebone. Amazingly, this animal can regulate fluid to air ratio in its cuttlebone, and therefore alter the level of buoyancy. For defense, cuttlefish has a fascinating capability to change its skin texture (camouflage) to fit environment; ink is the last resort to blind its enemy and escape. There are approximately 100 species of cuttlefish range between 2.5 and 90 centimeters and have somewhat flattened bodies with a pair of narrow fins that extend along the body.

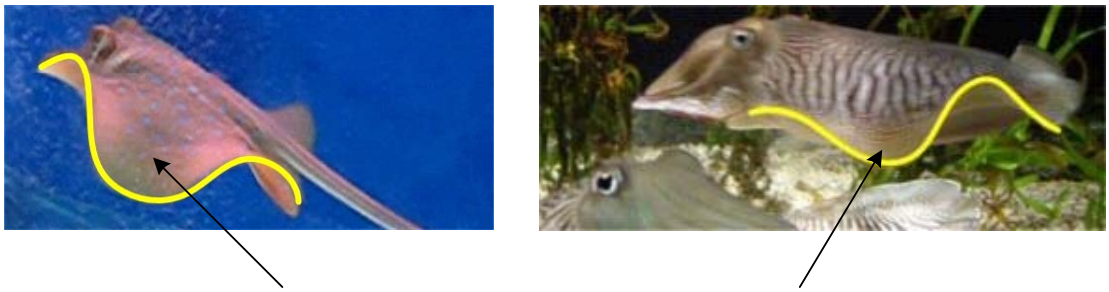

Figure 3.1. Undulatory swimming methods of (a) stingray and (b) cuttlefish. The direction of swimming is the opposite of the direction of fin wave propagation.

The fins of stingray and cuttlefish produce rhythmic undulatory waves, as shown in Figure 3.1, which are used in locomotion and hovering. Although much of the thrust is given by contracting its mantle during jet propulsion, the fins aid in producing thrust at low swimming speeds, in rendering stability, and in supplying lift for hovering.

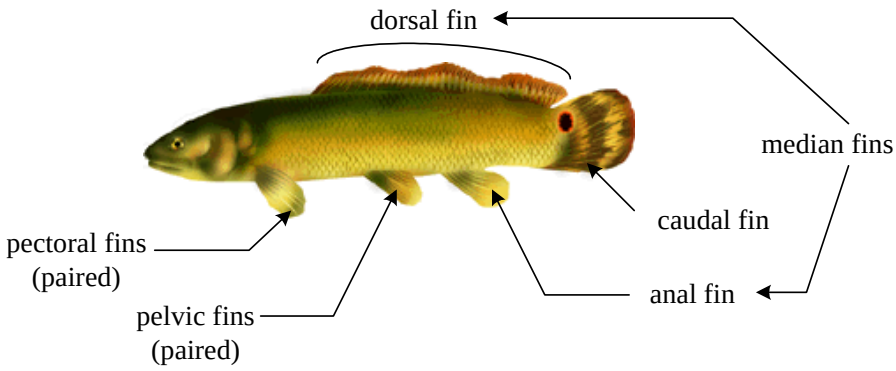

Figure 3.2. Bowfin (*Amia Calva*) swims mostly by undulations of its (usually long-based) dorsal fin. The dorsal fin along most of the body length and display a large number of very closely spaced fin-rays [19].

Figure 3.2 shows an example of a ray-finned fish, a bowfin, with a long-based dorsal fin. The fin consists of fin-rays and a flexible membrane connecting them together. In median fins (dorsal and anal fins) a set of muscles (usually six) for each fin-ray provide the latter with two degrees-of-freedom movement capability, while it has been suggested that certain fish can actively bend the rays of their median fins [21].

Unlike ray-finned fish whose fins are supported by bones, the fins of cuttlefish lack rigid supportive elements; they instead contain three-dimensional array of musculature termed a ‘muscular hydrostat’. The muscle in the fin enables the cuttlefish to fully control undulations amplitude, wavelength, and speed of its fins accordingly depending on its activity; gentle, low amplitude, low frequency fin movements are observed during hovering or when the animals rest on the substratum. Brief bursts of high amplitude and high frequency fin movements are observed during rapid locomotion and maneuvering. It is important to note that this animal changes the wavelength of its fins undulations, which serves the same purpose as a gearbox in car, from short wavelength to longer ones as it is moving faster [23].

3.2 Mechanical Modeling of Undulating Fin

3.2.1 Kinematics of Undulating Fin

Kier and Thompson [23] suggest that fins of cuttlefish are supported by three-dimensional array of muscle; no fin ray is found in the fins of cuttlefish. Both linear and rotary actuators are however unable to model the complex musculature of the fins of the cuttlefish. Despite the complexity of the actual musculature, the fins of cuttlefish exhibit much the same undulations as that displayed by the fins of ray-finned fish with undulatory swimming mode. In order to simplify our modeling, the fin of cuttlefish is divided into many segments such that the fin looks similar to that of ray-finned fish.

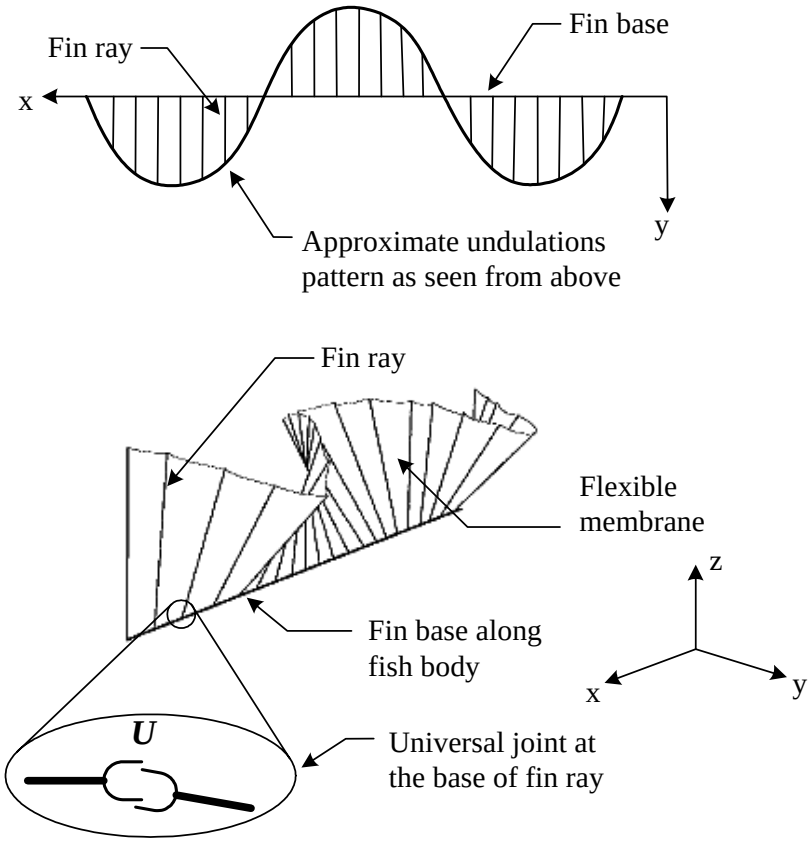

Figure 3.3. Fin diagram of ray-finned fish. The diagram may also represent cuttlefish fin which has been divided into many segments. The base of each fin ray can be modeled by a universal joint (***U***) allowing two degrees of freedom movement for each fin ray [21, 22].

We may therefore conclude from the mechanical point of view that the fins of cuttlefish can also be supported by rigid structure such as fin rays as far as to perform undulatory movements. Figure 3.3 shows fin diagram of any fish, including that of cuttlefish, performing undulations. Universal joint (***U***) is one possible joint that permits two-degree-of-freedom movement at the base of each fin ray.

At the present stage, mechanical modeling of undulating fins, which include those of cuttlefish and ray-finned fish, is simplified to one degree of freedom from originally two degrees of freedom at the base of each fin ray. A servomotor serves as a muscle producing one degree of freedom at the base of each ray. A crank is attached at each servomotor to function as a fin ray. In order for the fin to exhibit undulations similar to that of any undulating fin, each servomotor is programmed so that the crank attached to the servomotor oscillates based on a sinusoidal function.

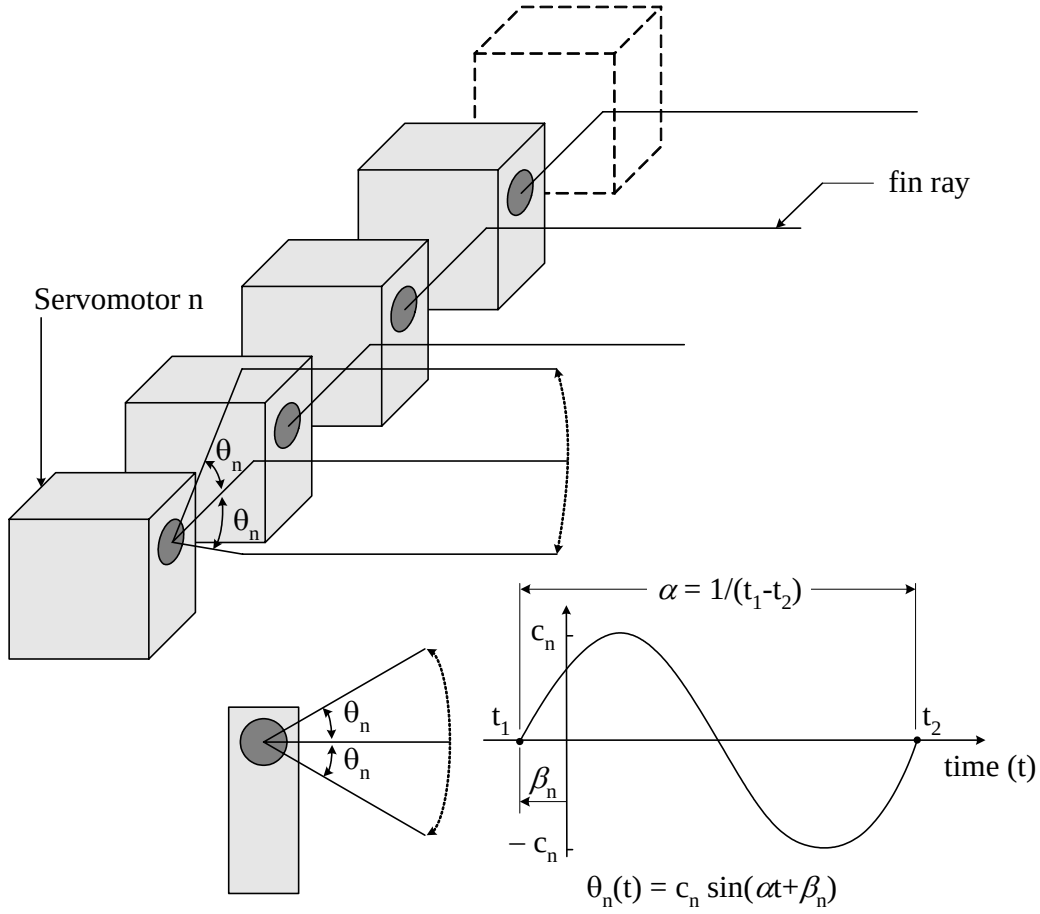

Figure 3.4. The mechanical design to model fin rays of a fish swimming by fin undulations. Servomotors, which serve the same function as the muscle at the base of fin rays, are equally spaced.

In total there are 10 servomotors used to actuate 10 fins rays represented by cranks in Figure 3.4. The servomotors are spaced equally and they oscillate with a certain phase difference in order to achieve a certain wavelength. Figure 3.5 shows that a servomotor on the right of its adjacent one is leading at 45°. The servomotors can be programmed with other phase lead or lag in order to achieve different wavelengths and different directions of wave propagation as will be elaborated in Chapter 4.

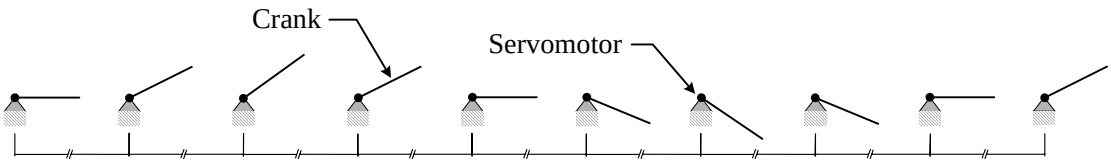

Figure 3.5. Ten servomotors, representing ten fin rays, are spaced equally. The servomotors on the right of their adjacent ones are shown leading at 45° phase difference.

3.2.2 Design of Flexible Membrane

If we ever noticed a fish swimming in a pond or in an aquarium and realized that they swim very gracefully, and when they are not moving they seem to put no effort to maintain their position in still water; they are in harmony with their surroundings.

The propulsion mechanism is one part which must be in harmony with its surroundings. By harmony we mean having the same or almost the same density as the surroundings. It cannot be imagined when the fins of a fish is made of a material which is heavier or lighter than the water in which the fish is swimming; the fish must put a lot of effort to lift and orientate its fin besides propelling itself in water.

It would be wrong when it is said that fins of fish are made of thin and light material. Bigger fish surely have thicker and heavier fins. A heavy object in air having density the same as water would be weightless in water. Proper material selection is therefore inevitable in the design of the flexible membrane. Material density, strength, and water absorption capability are important criteria for selection. The material is required to have a density near that of water so that no or little work is done to lift and orientate the membrane [24]. Take note that some materials are water absorbent, and they become weak after absorbing water.

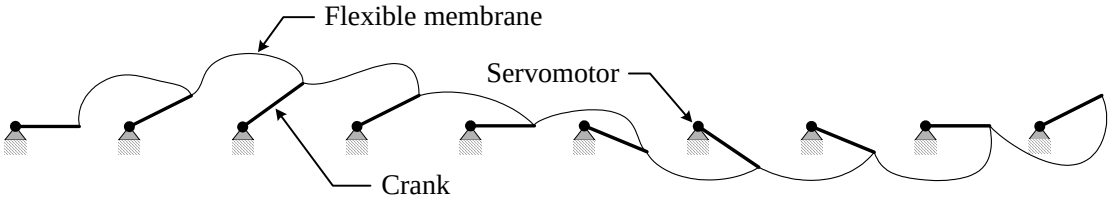

Figure 3.6. The cranks, representing actual fin rays, are connected by a membrane made of flexible material such as plastic sheet, cloth, or a thin sheet of rubber.

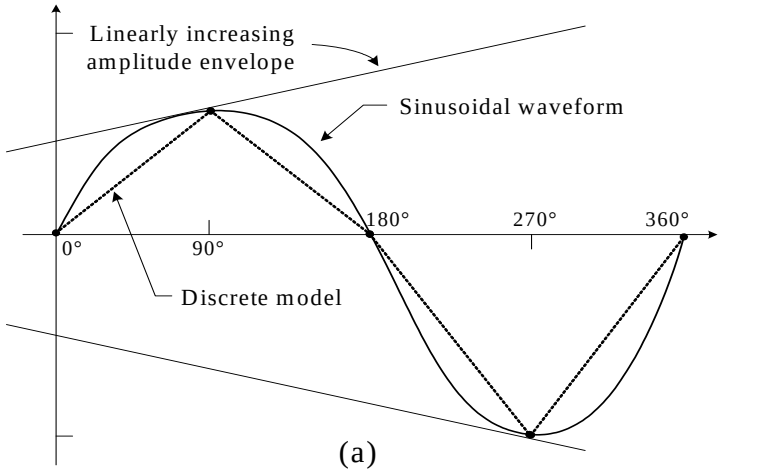

(a)

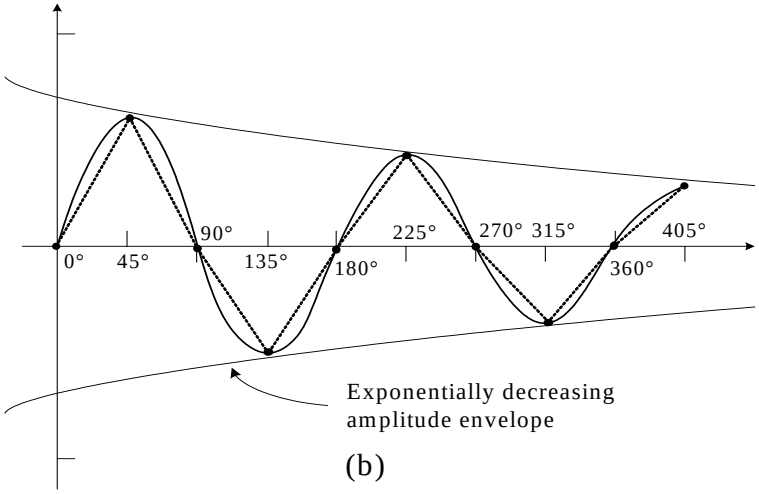

(b)

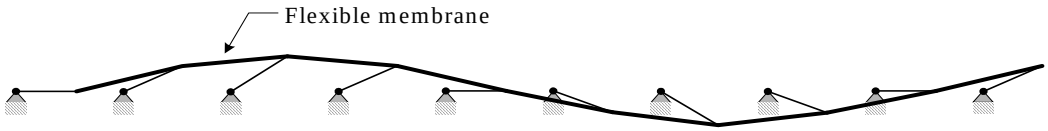

(c)

Figure 3.7. Discrete model of sinusoidal waveforms developed by series of straight-lines joining two points every (a) 90° and (b) 45°. (c) Flexible membrane connecting all cranks in (b) attached to servomotors. The membrane always forms a straight line in joining two cranks.

Flexible materials such as plastic sheet, cloth, and thin rubber sheet are conventionally considered to model a membrane and connect all the cranks. Figure 3.6 shows the main disadvantage of such materials when used a flexible membrane: they assume any unpredictable shape, which can disturb the water flow and movement of the fin. Thin rubber sheet may be an ideal material, which could be used to model a flexible membrane. In this application, however, the rubber is required to elongate, and extra power is needed therefore in addition to the power required to push water. To overcome this situation, the cranks must be closely spaced, such as found in fish, and therefore a lot more actuators are required in order to have at least one smooth wavelength in undulating fin [21].

It is desirable that the membrane material to posses a certain rigidity to push the water, thus create reaction force, and to have certain flexibility that allows it to extend. The following sections will discuss how a rigid material, such as acrylic, can be used to accomplish our objective of having a certain degree of rigidity and flexibility.

3.2.3 Mechanism Design

In order to maintain good model of sinusoidal waveform while undulating, the fin must be made of several segments made of rigid material. These segments were designed to accommodate various sinusoidal waveforms as shown in Figures 3.7 (a) and (b). The designed flexible membrane shown in Figure 3.7(c) always forms a straight-line between two cranks at any time. In addition to that, it is required that the membrane be extendible since the distance between two cranks changes as they oscillate. As no conventional material can accomplish the task, a linkage was designed to allow flexible movement of the membrane while the cranks are oscillating.

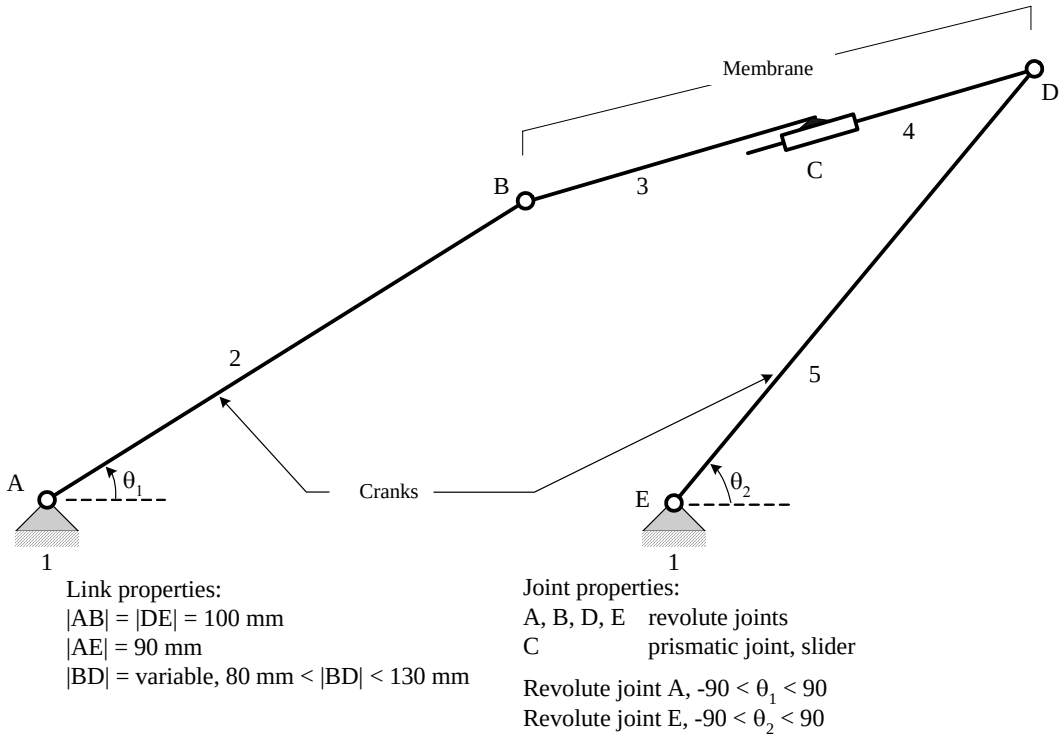

Figure 3.8. Kinematic diagram of two cranks and the membrane. The linkage consists of five links (1, 2, 3, 4, 5) and five lower pairs (four revolute joints: *A*, *B*, *D*, *E*, and one prismatic joint: *C*).

Figure 3.8 shows the kinematic diagram of a linkage representing two cranks and a membrane. The linkage consists of five links and five lower pairs. Gruebler's equation [25] stated that degrees of freedom of a mechanism could be found as follows:

$$dof = 3(n-1) - 2l - h \tag{3.1}$$

dof total degrees of freedom

n number of links, including frame

l number of lower pairs (one degree of freedom joint)

h number of higher pairs (two degrees of freedom joint)

Kutzbach's criterion [25] defined degrees of freedom as the number of actuators to be independently controlled in a mechanism. Equation 3.1 correctly anticipates that the linkage in Figure 3.8, which has five links (n = 5) and five lower pairs (l = 5), possesses two degrees of freedom, since points A and E are each driven by a servomotor.

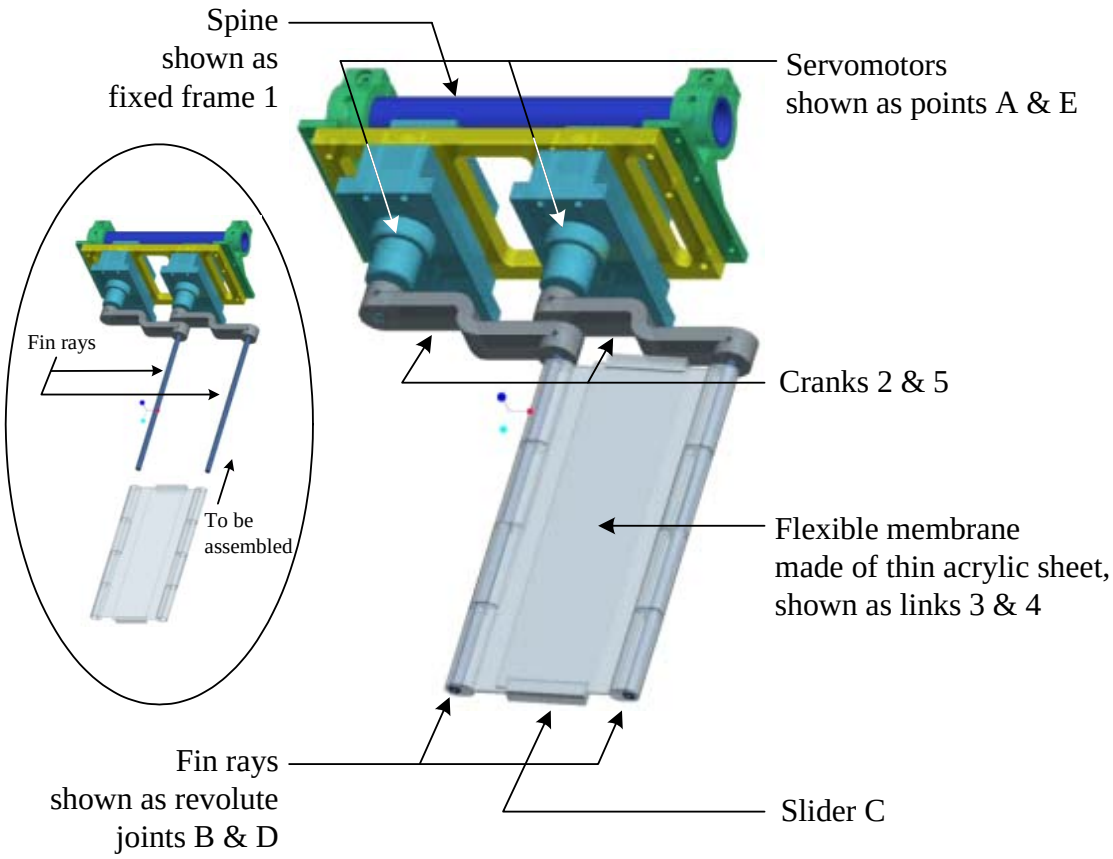

Figure 3.9. CAD model of two-degree-of-freedom mechanism in Figure 3.8.

An important advantage possessed by the mechanism shown in Figure 3.8 is that it will not assume any unpredictable shape. It will always join points *B* and *D* with a straight line. The mechanism design allows the flexible membrane, represented by links 3 and 4 and the slider *C*, to contract to a minimum length of 80 mm and to be stretched up to 130 mm. This therefore poses a certain constraint in the workspace of the mechanism, as shown by the grey area in Figure 3.10. There are two scenarios that will happen due to the mechanical limitation:

a. The slider C will hit end of track when the mechanism tries to contract to a length less than 80 mm, and
b. The slider C will run off track when the mechanism tries to extend beyond 130 mm.

Scenario *a* and Scenario *b* are the boundaries of the workspace shown as grey line and dashed-black line, respectively.

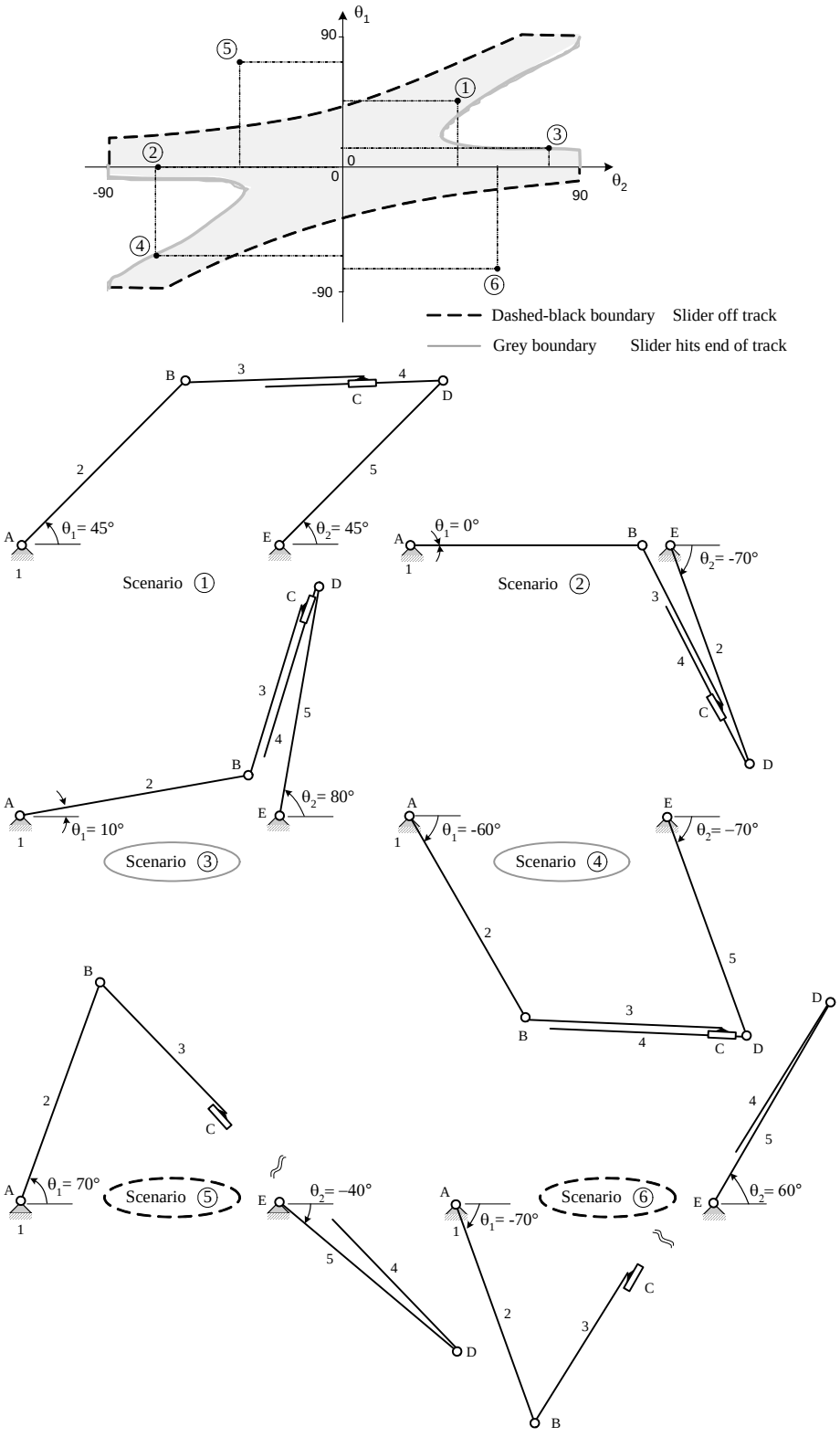

Figure 3.10. Workspace of the mechanism in Figure 3.8, shown by grey area enclosed by grey and black boundaries which signifies two mechanical limitations of the mechanism.

Several fin segments, as shown in Figure 3.9, are joined by a spine to form one module of undulating fin. Figure 3.11 shows an example of an undulating fin having nine fin segments. The module shown in Figure 3.11 will be able to recover various undulatory swimming methods of fish. This module can then serve as a platform for experimental studies to investigate which is the most efficient swimming method.

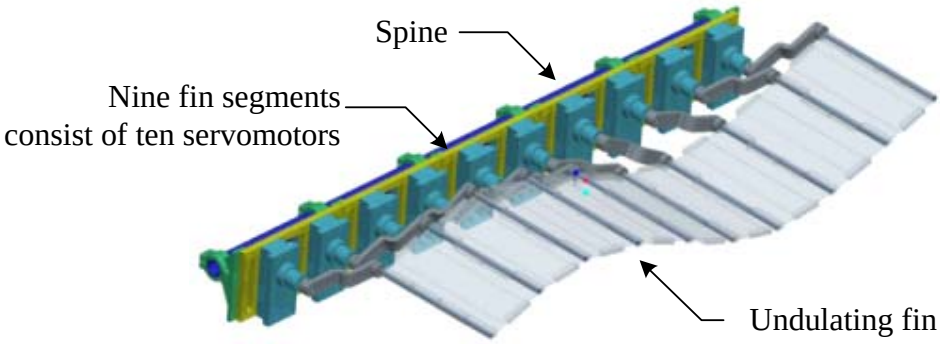

Figure 3.11. One module of undulating fin consists of nine fin segments joined together by a spine. Ten servomotors are used to actuate the undulating fin.

3.3 Undulating-Finned Biorobots

3.3.1 Knifefish Robot

Biorobot counterparts of various fish swimming with undulating fin(s) were considered, such as stingray, cuttlefish, and knifefish. At the early stage of the development of the undulating fin described in this thesis, swimming method of an underwater species, such as knifefish, was successfully mimicked. The Fish swims by undulations of its long-based anal fin. Several servomotors were used to provide the undulatory motion of the fins and also to accommodate various swimming modes. One module of undulating fin was attached to a buoyant tank as shown in Figure 3.12; the buoyant tank was floating on water surface, while the fin module was completely submerged. An experiment on the fin module was conducted in a water tank. The undulating fin was able to provide sufficient thrust for forward and backward propulsion.

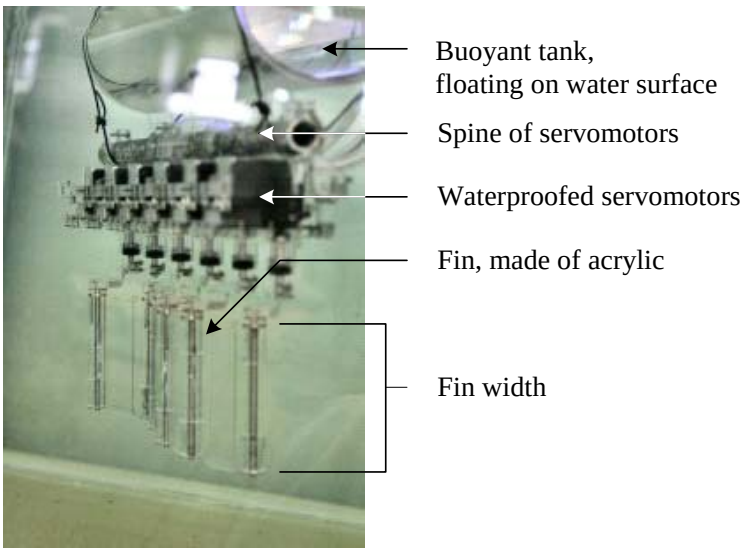

Figure 3.12. Biomimetic of knifefish swimming by undulations of its anal fin.

3.3.2 Cuttlefish Robot

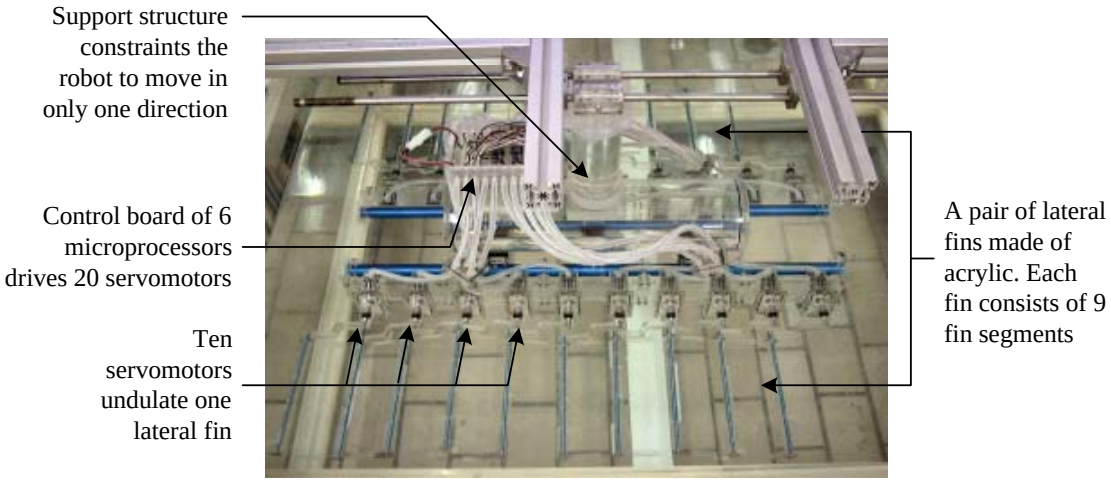

Figure 3.13. Cuttlefish robot in a water tank suspended by an experimental rig.

The success of one fin module drove the research further to constructing a prototype having two fin modules. The two fin modules were attached to a buoyant tank, which was floating on water surface, in order to mimic a cuttlefish, a marine animal that rhythmically undulates its fins for locomotion and maneuvering. This cuttlefish robot was constructed completely untethered by having on board power supply and controller. Twenty servomotors (Futaba S3801) were controlled by a customized control board comprising six microcontrollers (Basic Stamp BS2sx), which were arranged and synchronized in parallel processing for efficient programming.

The microcontrollers were proven sufficient in performing all the required calculations, which accommodate all fin parameters such as amplitude envelope, peak-to-peak amplitude, speed, and wavelength. Control aspect of this research will be discussed in Chapter 4.

Chapter Four
Control of Undulatory Propulsor

4.1 Undulatory Swimming Gaits

According to the classic classification proposed by Breder [7], there are a number of species that can be mentioned swimming with different degree of body and/or fin(s) undulations. Among those species swimming with body undulations are eel, needlefish, and shark. They are categorized into BCF swimmers. Those swimming with fin(s) undulations such as cuttlefish, stingray, and South American electric fish are categorized into MPF swimmers. Fish swimming modes is discussed in Chapter 2.

BCF swimmers undulate from one-third to almost all of their bodies, depending on the speed, often with one or more complete waves present at a time. Lighthill's elongated body theory [26] focusing on swimming gait of eel, proposed the following equation to represent body undulations of a swimming eel shown in Figure 4.1:

$$y = Ae^{\gamma(s-1)} \sin k(s - Vt) \tag{4.1}$$

A Tail beat amplitude [m]

γ Amplitude growth from head to tail

k Number of waves present (equal to 2π/wave length)

V Body wave propagation speed [m/s]

Interested reader may refer to Lighthill [26] for detail discussion on elongated body theory. Note that U in Figure 4.1 is the forward speed of the anguilliform swimmer.

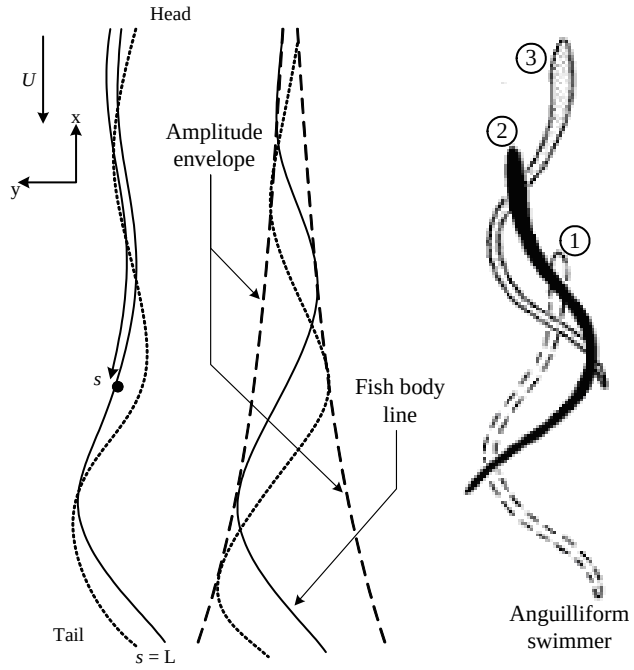

Figure 4.1. Amplitude envelope of body undulations found in anguilliform swimmers, such as eel and needlefish, suggested by elongated body theory.

Cuttlefish, although not included by Breder [7] in his classification, is also observed using its fin for low speed swimming. Besides using water jet propulsion, some wide-finned cuttlefish however swim like a rajiform swimmer i.e. by passing large amplitude undulations along their fins and also flapping their fins to for high-speed locomotion. The amplitude envelope of the fin undulations of those cuttlefish is similar to that of rajiform swimmers. It is however observed that in smaller and narrow-finned cuttlefish, the amplitude envelope is fairly constant along the fins, as shown in Figure 4.2. In proceeding discussions, Lighthill's Theory [26] will be generalized to include all possible MPF swimming methods.

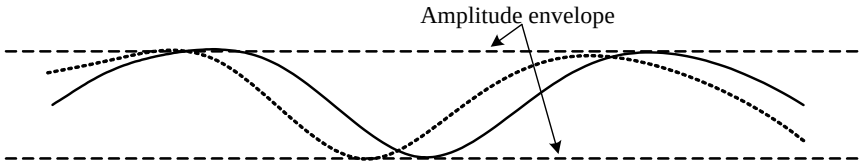

Figure 4.2. Constant amplitude envelope observed in small and narrow-finned cuttlefish when cruising at low speed or hovering.

4.2 Control

4.2.1 Introduction to Control

An environment friendly propulsion system has been designed and constructed to model undulating fins of underwater creatures, such as cuttlefish, stingray, knifefish, and many others, in order to investigate various swimming methods.

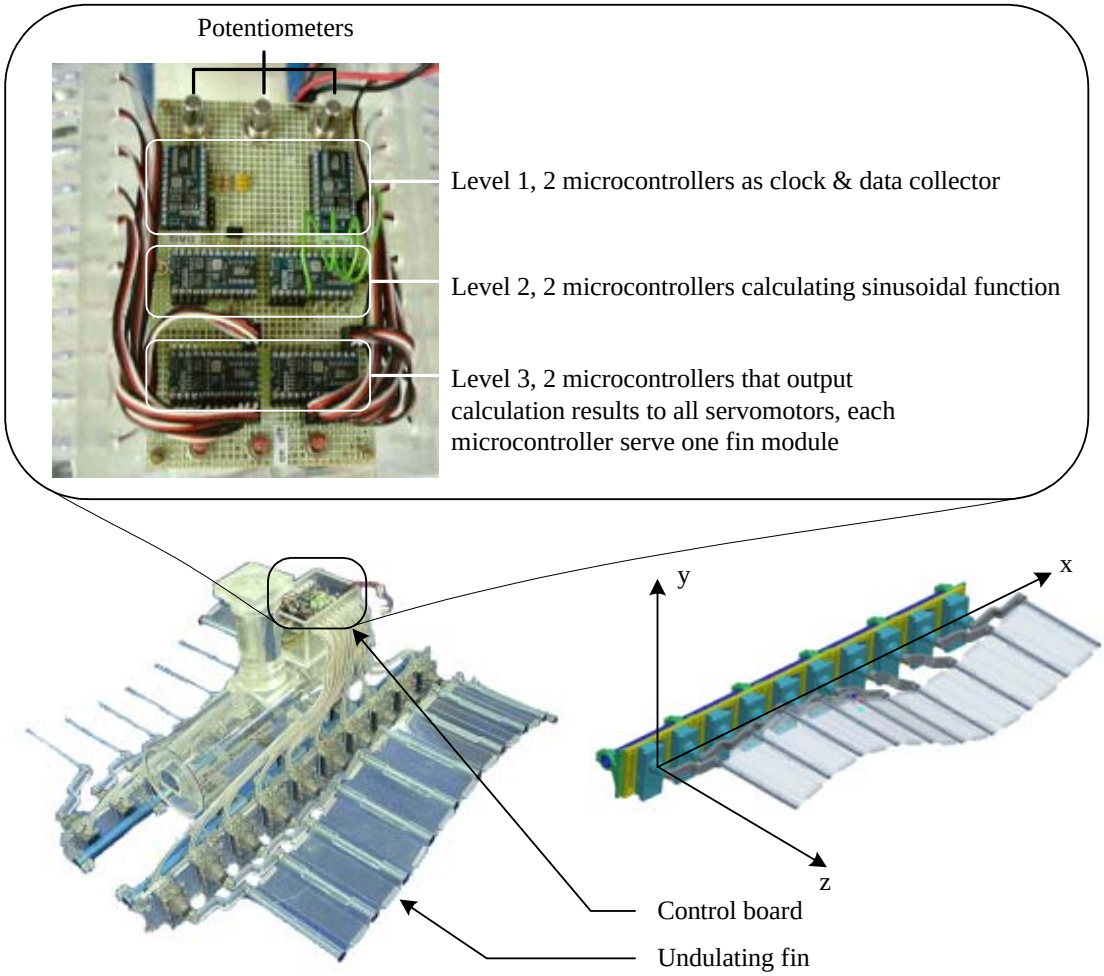

Figure 4.3. Layout of control board consisting of six microcontrollers, arranged in three levels of communications, and three potentiometers that alter some parameters of undulating fin.

Twenty servomotors are controlled by six microcontrollers, shown in Figure 4.3, divided in three levels of communication for efficient programming. In Level 1, shown in figure 4.4, there are two microcontrollers acting as a data miner and a clock.

The data miner is used to obtain user input command, and the clock is used to synchronize processes of all microcontrollers. A 25-millisecond clock time was specified by the servomotors as the maximum time to process one cycle of instructions.

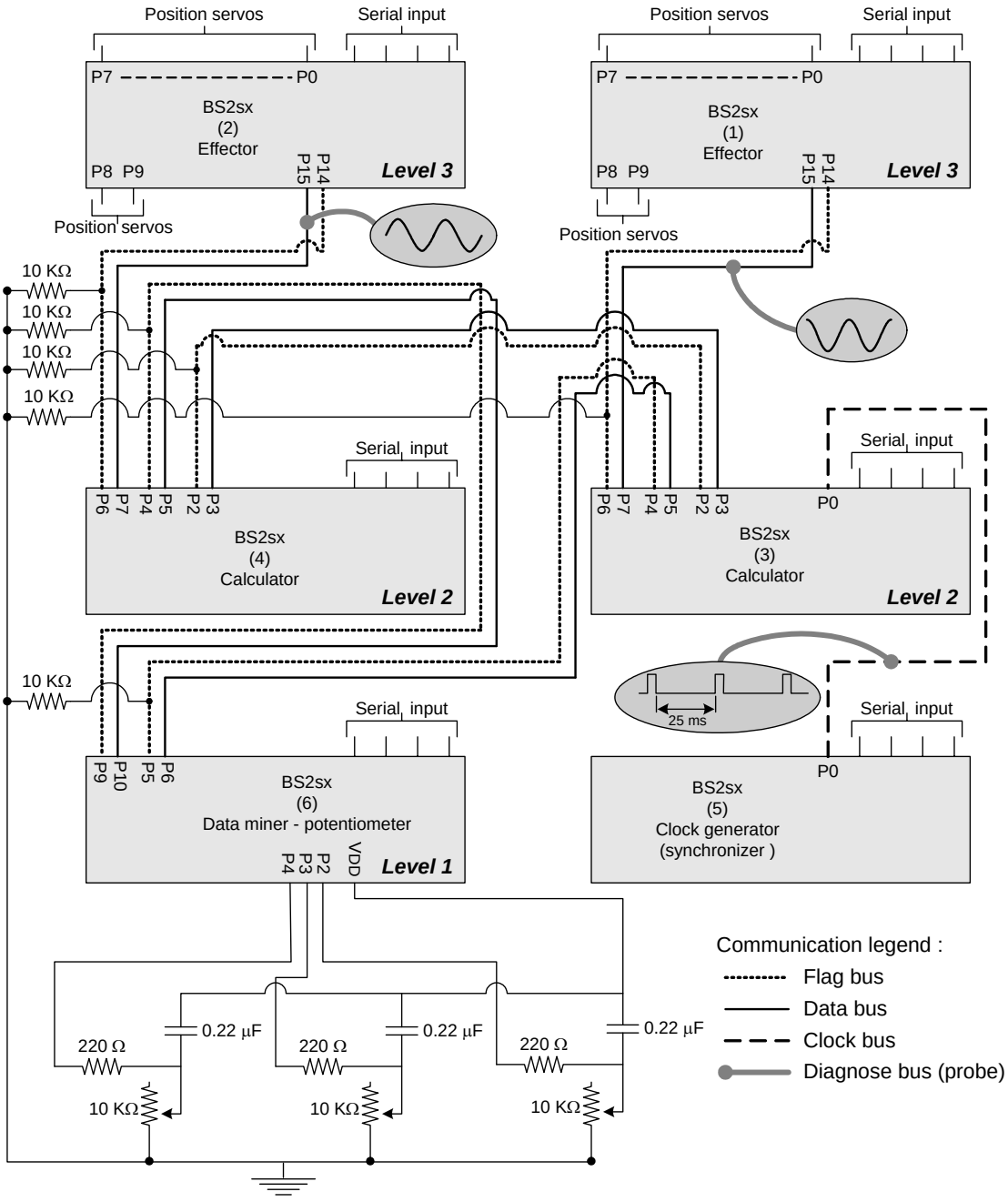

Figure 4.4. Detailed circuitry for controlling two fins.

The inputs collected are then communicated to Level 2, where there are two microcontrollers computing the required pulse needed to be supplied to the servomotors in order to generate undulating effects based on the inputs. Each microcontroller is dedicated to one module of undulating fin consisting of ten servomotors. Each microcontroller transmits the results to a corresponding microcontroller in Level 3. In Level 3, each microcontroller supplies the results to ten servomotors. Each microcontroller in Level 2 does independent computation such that the two lateral fins of the cuttlefish robot can be independently controlled for maneuvering.

4.2.2 Parameters Definition

The fin can accommodate various amplitude envelopes, tail beat frequencies, and wavelengths. In line with Lighthill's conclusion in his elongated body theory [26], we formulate the following equation to fit our programming purpose:

$$\theta_n(t) = g_n \sin\big((\alpha\, t \times 360°) + (n-1)\beta\big), \tag{4.2}$$

whose parameters are summarized in Table 4.1. As shown in Equation (4.2), a variable called *n* appear in place of *x*, while *n* is used to indicate the number of a servomotor along the *x*-axis, and therefore makes Equation (4.2) a discrete model of an undulating fin.

Instead of $y(x,t)$, as in Lighthill's proposal, $\theta_n(t)$ is used to characterize an undulating fin because the output of a servomotor is in terms of angular position θ. By eliminating the time factor in Equation (4.2), the servomotors are programmed to accept time-independent inputs that allow the fin to act as a control surface or hydrofoil [27]. Being modular, some of the fin segments can be detached from the module, and hence changing the effective fin length.

Table 4.1. Summary of parameters required for discrete modeling of undulating fin.

Parameter	Description	Value / Unit
n	Position of a servomotor along x-axis, as shown in Figure 4.3	$1 \le n \le 10$; n = integer
t	Time	Second
g_n	Multiplication factor for a servomotor based on an amplitude envelope	Unit in degrees.
α	Tail beat frequency	$\alpha_{\max}$ = 1.2 Hz
β	Phase difference between consecutive servomotors.	$\beta_{\max} = 90°$
$\theta_n(t)$	Angular position of a crank attached to n^{th} servomotor at time t	$-90° \le \theta_n(t) \le 90°$

Figure 4.5 shows a diagram of parameters designation in Equation (4.2). Six servomotors are used, as an example, and they are programmed to oscillate and hence undulate the flexible membrane with a constant amplitude envelope g_n, which can be described as follows:

$$g_1 = g_2 = g_3 = ... = g_n = \text{constant}. \tag{4.3}$$

Such amplitude envelope then defines the oscillation path of the cranks of the servomotors which can be mapped into one circular path. Other amplitude envelope such as linearly increasing amplitude envelope, which can be described as follows:

$$g_1 = c,\ g_2 = 2g_1,\ g_3 = 3g_1,\ ...,\ g_n = ng_1, \tag{4.4}$$

where c is any constant. Note that this amplitude envelope would have n number of circular paths of n different diameters depending on the specified oscillation amplitude of each crank.

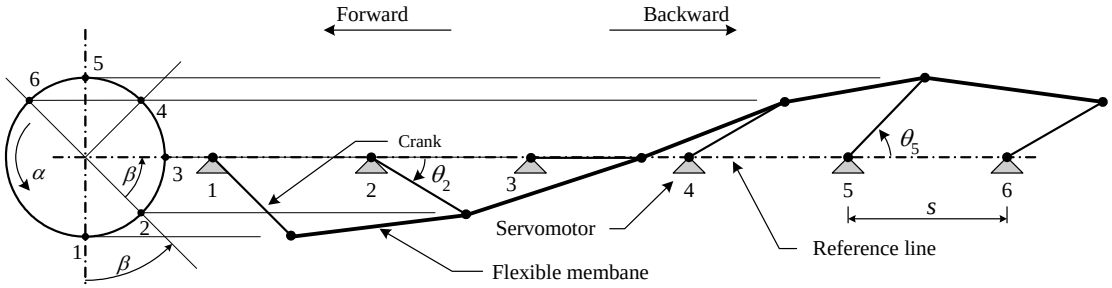

Note: 1. Angular positions are measured counter-clockwise as positive
2. θ_n is measured from reference line
3. β is phase difference between two servomotors, in this example $\beta = 45°$
4. s is spacing between two servomotors
5. α is frequency of undulations

Figure 4.5. Parameters designation of undulating fin.

In order to synchronize the motion, all cranks must oscillate with the same angular frequency α. Lighthill's elongated body theory describes α as body wave propagation speed V in Equation (4.1). The direction of the angular rotation α of the circular path in Figure 4.5 determines the direction of propagation of the wave of the undulating fin, and thus the motion of the whole system. If α rotates counter-clockwise, the wave will propagate to the right, and thus the whole system will swim forward. On the other hand, if α rotates clockwise, the wave will propagate to the left, and the whole system will swim backward.

One important characteristic of an undulating fin is its wavelength. In case of discrete modeling, wavelength l is determined by the phase difference β between consecutive servomotors. Assuming constant phase difference β and spacing between any two servomotors is s, the wavelength l can be expressed as follows:

$$l = \frac{360°}{\beta} \times s\,, \tag{4.5}$$

Note that β is in degree. Presented in Figure 4.5 is an undulating fin driven by servomotors in which $\beta = 45°$. The mechanical design arranged all the servomotors equally spaced at $s = 180\,\text{mm}$. It is therefore expected from Equation (4.5) that the wavelength l be 1440 mm. Note that the angular output of the shaft θ_n of a servomotor n is measured with respect to a reference line shown in Figure 4.5. The role of each

parameter will be elaborated in the following section as the control program is explained.

4.3 Control Program Manual

Figure 4.4 shows a detailed layout of the circuitry used for controlling the two lateral fins of the cuttlefish robot in Figure 4.3. It consists of six microcontrollers (Basic Stamp BS2sx), three potentiometers, 20 output pins to servomotors, and powered by a 7.5 V NiMh battery. The microcontrollers can communicate with one another via a communication line incorporating a data bus and a flag bus. One data bus can be used for two-way communication between two microcontrollers, and it is used for transmitting data from one microcontroller to the other. Flag bus is used for obtaining the state of readiness of the two microcontrollers to perform communication.

4.3.1 Communication Level 1 – Data Acquisition

The Control starts by collecting user input from three potentiometers connected to p2-p4 of BS2sx, which are automatically set as input pins. Note that potentiometers are used to simulate the situation which will happen when RF receivers are used. The potentiometers will be used as parameters of undulating fin discussed in the preceding section. Each potentiometer is a ten-turn pot, for example, which gives variable resistance from 0 Ω to 10 KΩ.

Basic Stamp however does not measure the value of resistance of each potentiometer directly. Instead, it measures charging time required by a capacitor connected in series with the potentiometer. The charging time is stored in terms of the number of counts based on the internal clock of BS2sx. Interested readers may refer to basic stamp manual [28].

4.3.1.1 Data Mining

Data mining starts by discharging all the capacitors connected to the potentiometers for 10 ms to ensure the capacitors are reasonably empty so that the charging time can

be measured correctly. The command RCTIME charges the corresponding capacitor and store the number of counts in the respective variables.

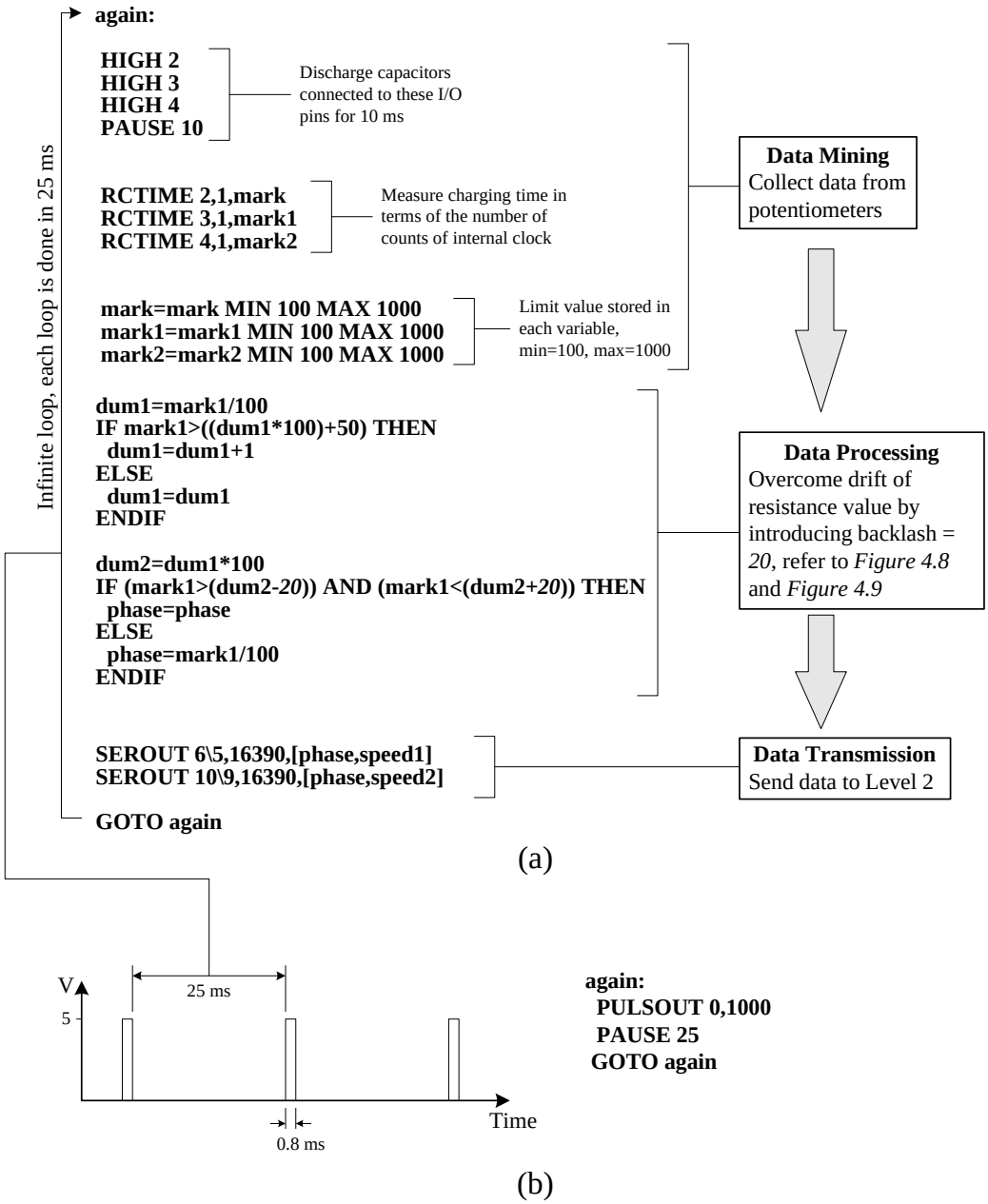

Figure 4.6. (a) Program flowchart of BS2sx(6) for collecting user input. Processes are done within 25-millisecond time limit specified by clock pulse. (b) 25-millisecond clock pulse generated by BS2sx(5).

Although for 10 KΩ the number of counts is up to 1900, however for simplicity, the program limits the value that each variable can store, in this case from 100 to 1000 counts.

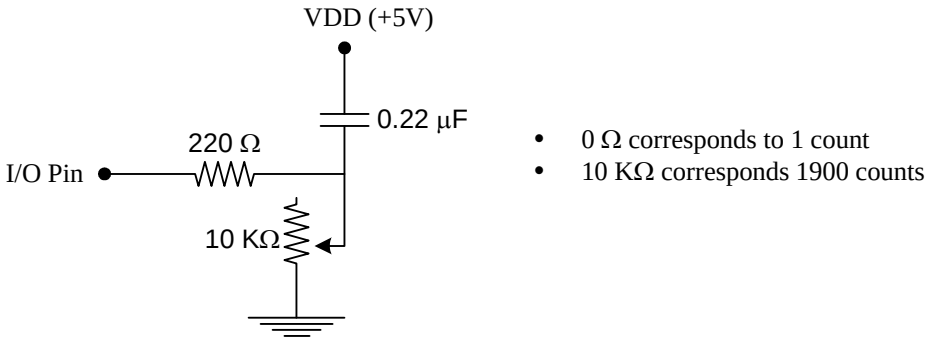

Figure 4.7. One input module of ten-turn potentiometer providing range from 0 Ω to 10 KΩ corresponding to the number of counts from 1 to 1900, respectively.

4.3.1.2 Data Processing

The number of counts stored in each variable, which is any value from 100 to 1000, is then divided into segments numbered from 1 to 10 in the manner shown in Figure 4.8(a). Note that Basic Stamp process number in integer, no floating-point number. Therefore, when a number is divided by 100 for example, the result will be rounded-off to the lower integer.

The method proposed in Figure 4.8(a) however does not work well as the potentiometer is not an ideal one. At one angular position of its input knob, the potentiometer can have different value at different time, although the drift is small. Similar drift can also be noticed with the data received from an RF receiver. In terms of the number of counts, such drift was observed within ±10 of the ideal value. Using the method proposed in Figure 4.8(a), the number can easily hop from one segment to a higher or lower one. Say for instance that the potentiometer is positioned at 602 counts, which is in segment 6. Due to slight drift, the number of counts drops to 596, which makes it fall to segment 5. Shortly thereafter, another small drift occurs and the number of counts increases to 609, which in segment 6. Such situation however will not happen when the potentiometer is not positioned near the segment boundary, which is a vertical line connecting one segment to another as shown in Figure 4.8.

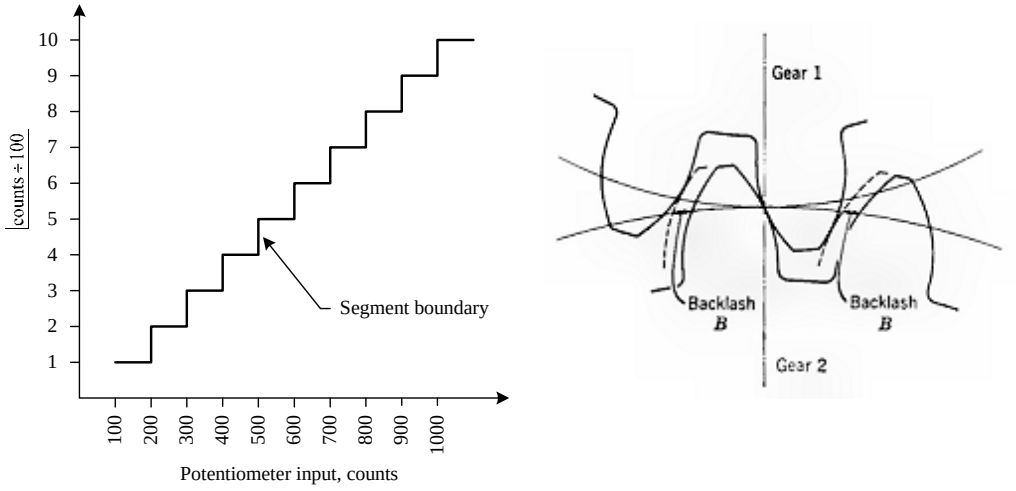

(a) (b)

Figure 4.8. (a) Conventional method of segmenting numbers. (b) Backlash is incorporated in segmenting number such that small drift of counts can be tolerated.

Backlash is a well-known term used to designate a situation when there is a play resulting from loose connections between gears or other mechanical elements. Backlash is therefore a disadvantage in mechanical system. Nevertheless, backlash is purposely introduced to tackle the problem when a potentiometer is positioned near or at the segment boundary.

In the case of the potentiometer used on the control board shown in Figure 4.4, the answer to near-segment-boundary problem due to resistance drift is by introducing a backlash of ±20 counts at the segment boundary. Take for example the following scenario. A potentiometer has a current value of 532 counts, which is in segment 5. In order to move to lower segment, which is segment 4, the potentiometer has to pass below 480 counts. In order to move up, the potentiometer must be turned to a count value of more than 520. Hence, there is a 40-count backlash at segment boundary 5, which is at the number of counts of 500. The same situation and rule applies to other segment boundary, as shown in Figure 4.9, backlash is shown in gray.

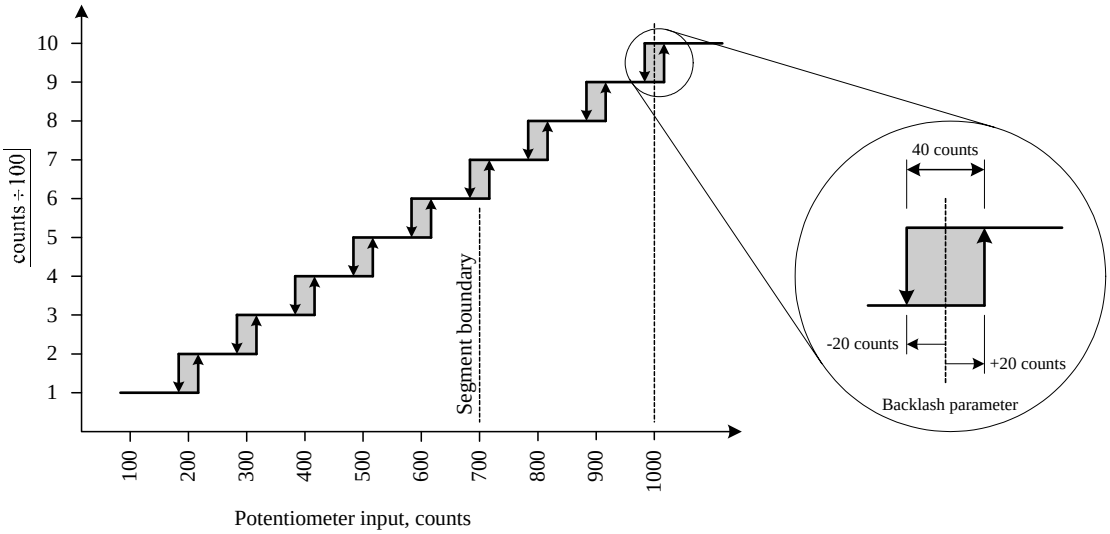

Figure 4.9. Segment chart upon introducing backlash at segment boundary.

4.3.1.3 Data Transmission

When data is ready, the value of each variable will be transferred to two microcontrollers at Level 2 for further processing, which will be discussed in the proceeding sections. Data transmission is done by serial communication between two microcontrollers. The command SEROUT *Tpin/Fpin, Baudrate,[Variable]* transfers value stored in the variable through *Tpin*. *Fpin* is a flag bus used for synchronizing communication between two microcontrollers. *Fpin* checks whether the receiving microcontroller is ready to receive. Data will only be sent if *Fpin* signals the sending microcontroller to send out data. Otherwise, the sending microcontroller will wait until there is a ready signal. After sending the data, *Fpin* will receive another signal indicating that data has been received by the recipient. Upon receiving the signal, the program will move to the next command.

Figure 4.6 demonstrates that there are only three values sent based on the values obtain from the three potentiometers. The three values are the wavelength for the undulating fins, phase, and the oscillation frequency of each fin. Upon sending all data to Level 2, the values of each variable will be updated by performing infinite loop, as demonstrated in Figure 4.6. All those processes are performed within the time limit of 25-millisecond specified by a clock pulse generated by a microcontroller at Level 1, shown in Figure 4.4.

4.3.2 Communication Level 2 – Computation

Level 2 consists of two microcontrollers, BS2sx(3) and BS2sx(4), which produce sinusoidal effect for each undulating fin of the cuttlefish robot. Two microcontrollers are used to overcome RAM limitation of Basic Stamp microcontroller, which is reserved for variables. Since both microcontroller contain the same program, we will now discuss only the content of BS2sx(3). One undulating fin module consists of ten servomotors, and each is represented by a 16-bit variable in the program. Therefore, ten 16-bit registers are allocated for ten servomotors as shown in Figure 4.10. The remaining registers are used by intermediary variables.

The size of RAM of the microcontroller determines the number of servomotors it can serve. Therefore, more than one microcontroller is needed, if one fin module consists of more than ten servomotors.

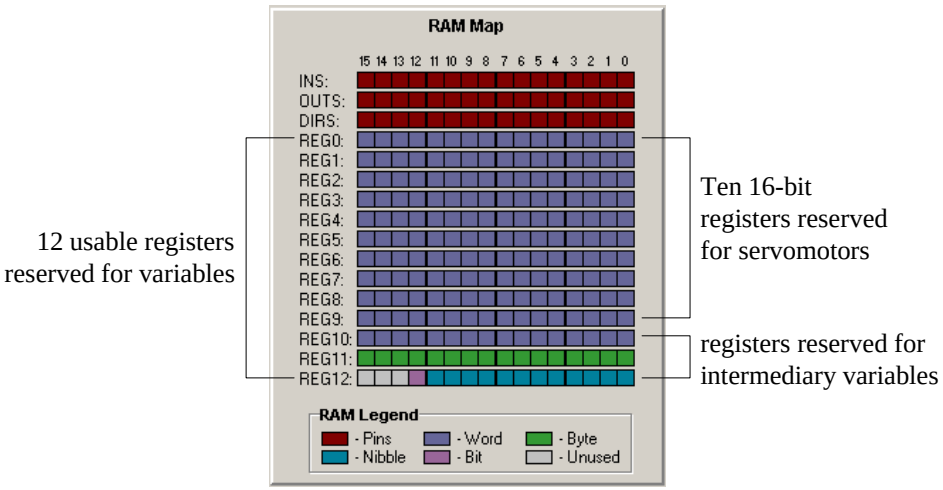

Figure 4.10. BS2sx microcontroller has twelve usable registers.

Computation in Level 2 is executed based on the data obtained from a microcontroller in Level 1, BS2sx(6). When no data is obtained, the computation will proceed based on predefined values. Each microcontroller in Level 2 is an independent unit, and they may perform computation at different speeds. It is therefore required that they be synchronized in order to have synchronized motion of the two undulating lateral fins. The synchronization is done by establishing a communication between the two microcontrollers, which checks the readiness of each microcontroller. Computation will be executed only when both microcontrollers are ready.

The undulating effect of a lateral fin is achieved by oscillating all servomotors following a predefined sinusoidal waveform of a certain frequency. However, each servomotor may oscillate at different amplitudes depending on the amplitude envelope desired for the undulating fin.

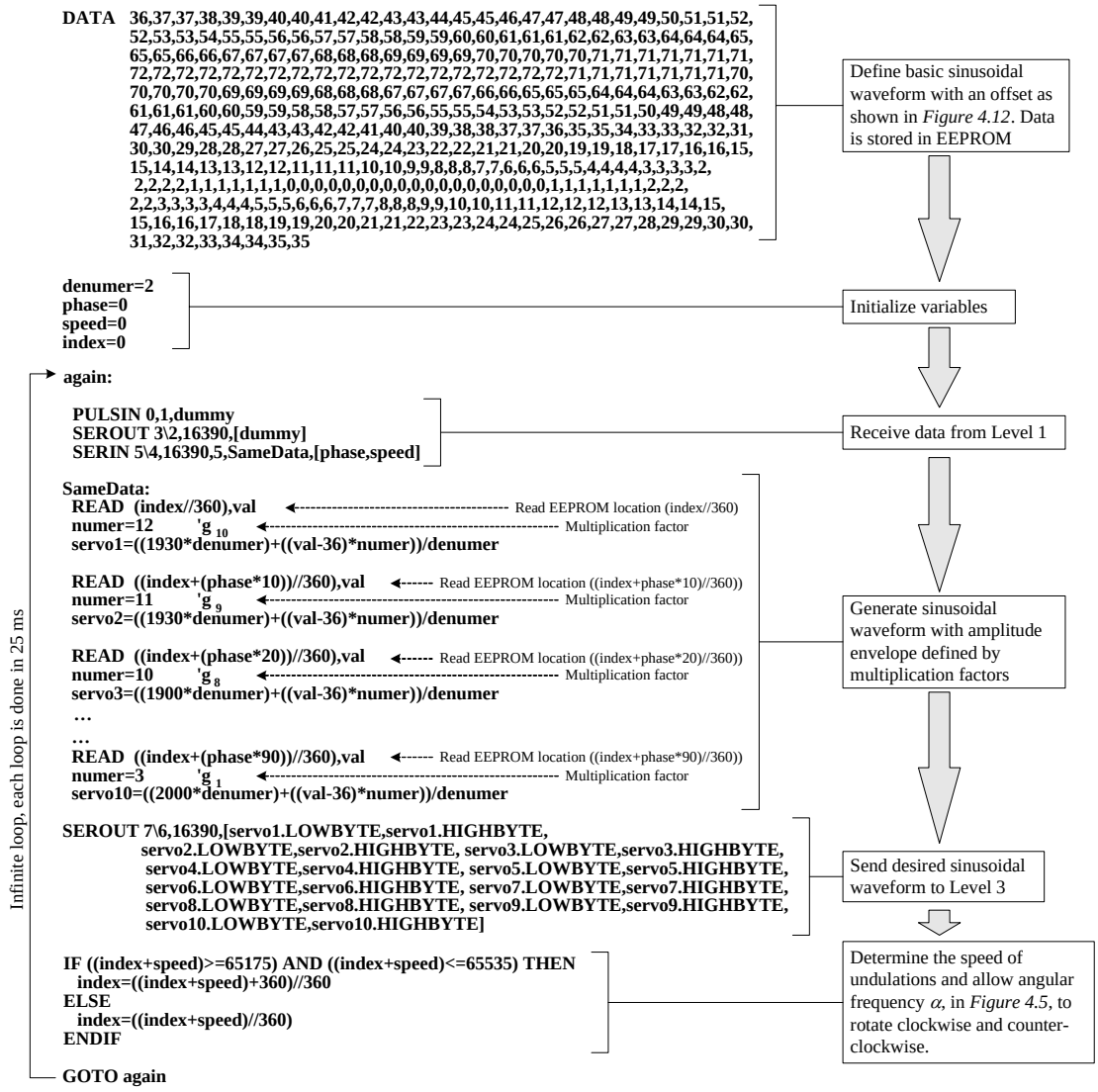

Figure 4.11. BS2sx(3) and BS2sx(4) create undulating effect based on predefined sinusoidal waveform stored in EEPROM.

The program in Figure 4.11 starts by defining a basic sinusoidal waveform with a certain offset, and the program consists of 360 points to represent one revolution or 360 degrees. All those points are stored in the EEPROM of the microcontroller in sequential manner starting from the lowest address. Note that offset is necessary to have all values greater or equal to zero.

The microcontroller does not recognize a negative and floating-point number; a value must be zero, positive and/or integer. Figure 4.12 shows an offset sinusoidal wave of the points stored in the EEPROM of BS2sx(3) and BS2sx(4).

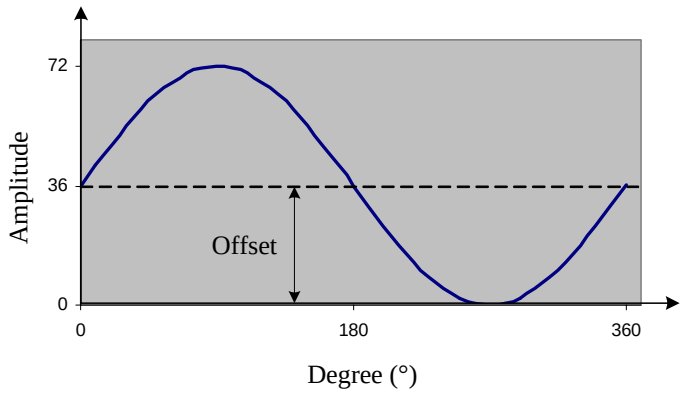

Figure 4.12. Offset sinusoidal waveform must be traced by all servomotors in order to produce undulating effect.

The speed of oscillation, thus the frequency of undulation or tail beat frequency, is determined by a variable called *speed* in Figure 4.11. *speed* is the increment or decrement, depending on direction of oscillation, when reading the data stored in the EEPROM. The bigger the value of *speed* is, the higher is the oscillation frequency, and thus frequency of undulation. Note that the duration of computation in the microcontroller has been conditioned according to the 25-millisecond clock pulse. Therefore each loop cycle in Figure 4.11 is executed every 25 milliseconds. The Oscillation frequency α, or tail beat frequency, of each servomotor is therefore:

$$\alpha = \frac{1}{\tau}\,\text{Hz} \tag{4.6}$$

where $\tau = (360/speed) \times 25\,\text{ms}$, is the period or the time required to perform one complete revolution. The multiplication factors g_n in Figure 4.11 are the same as those described in Table 4.1. They will then determine the amplitude envelope of fin undulations. Figure 4.13 shows surfaces traced by undulating fin at various oscillation frequencies α and phase differences β. The graphs in Figure 4.13 are plotted with the same scale.

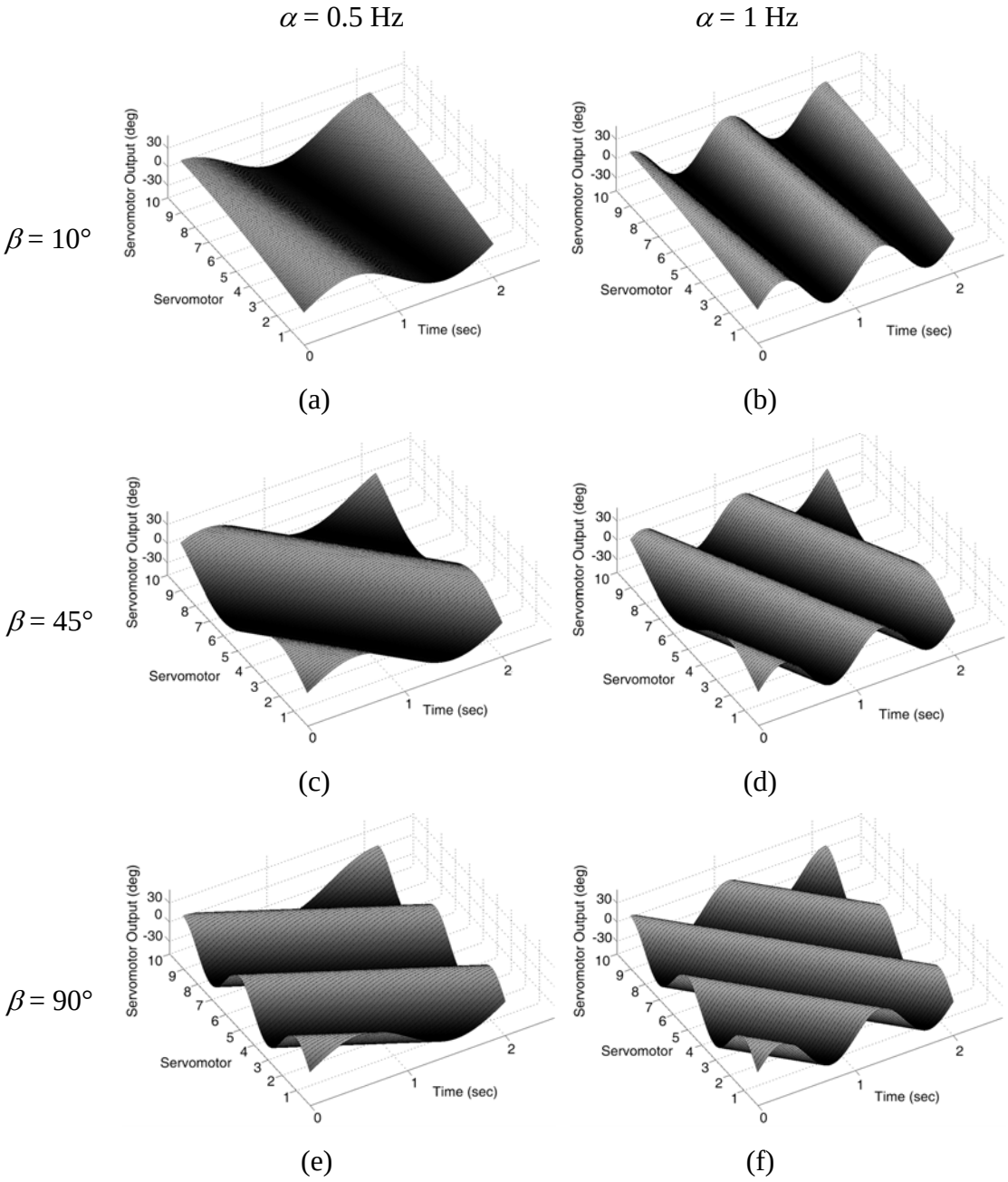

Figure 4.13. Surface traced by undulating fin at various frequencies α and phase differences β, by using Eq. (4.2). (a) α = 0.5 Hz & β = 10°, (b) α = 1 Hz & β = 10°, (c) α = 0.5 Hz & β = 45°, (d) α = 1 Hz & β = 45°, (e) α = 0.5 Hz & β = 90°, (f) α = 1 Hz, β = 90°.

Undulations are at constant amplitude envelope: $g_1 = g_2 = g_3 = ... = g_n = 30°$.

4.3.3 Workspace of Mechanism

After the desired amplitude envelope and phase difference have been determined, it is important to check whether the undulating fin mechanisms will encounter any mechanical limitations, which is discussed in Chapter 3. For the mechanisms to work properly, the angular positions of all fin segments must lay in the workspace defined in Chapter 3. The surfaces shown in Figures 4.13(c-d) are generated by a fin undulating at constant amplitude envelope and 45° phase difference. The workspace of all the fin segments to generate such surface is found to be a closed-loop trajectory which stands inside the workspace defined in Chapter 3, as shown in Figure 4.14. Figure 4.15 shows trajectories traced at various β.

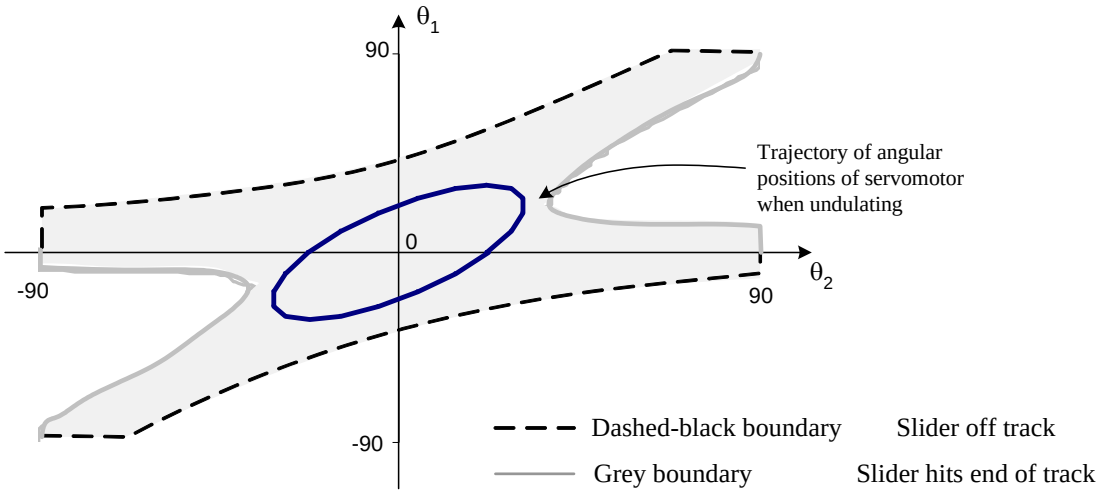

Figure 4.14. Workspace of undulating fin mechanisms of constant amplitude envelope and 45° phase difference β. All fin segments trace the same trajectory due to constant amplitude envelope. Note that the positions of servomotors refer to points B and D in Figure 3.8.

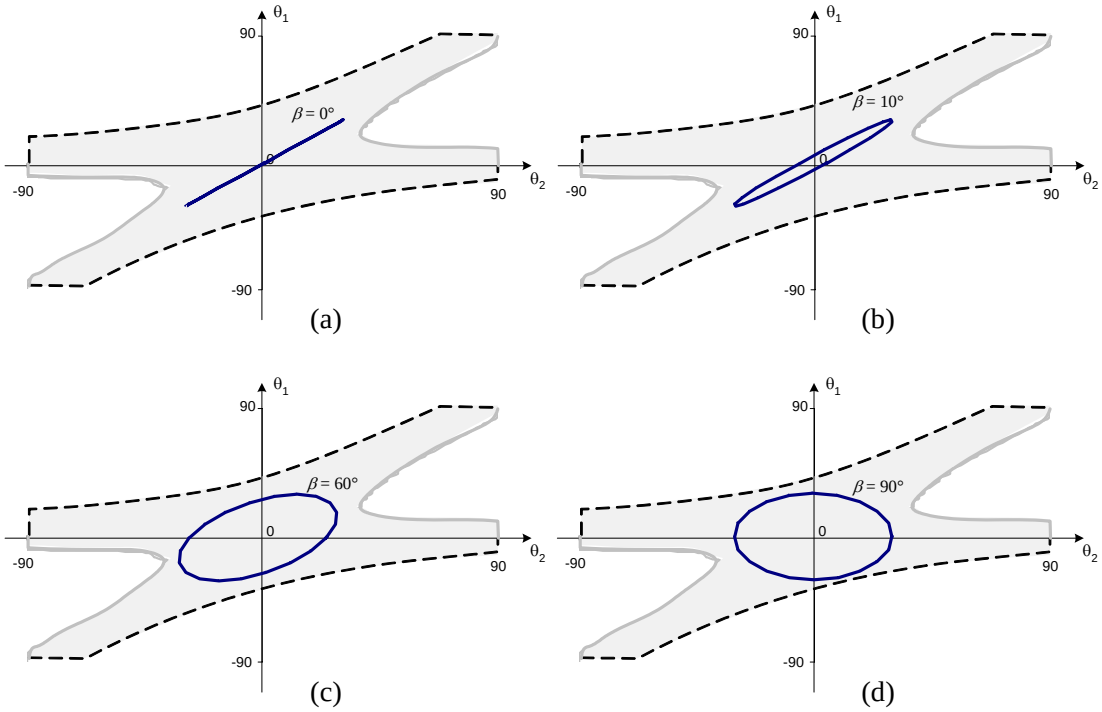

Figure 4.15. Trajectories traced by undulating fin mechanisms at various β. (a) $\beta = 0°$. (b) $\beta = 10°$. (c) $\beta = 60°$. (d) $\beta = 90°$. The size of the trajectory is proportional to the size of amplitude envelope.

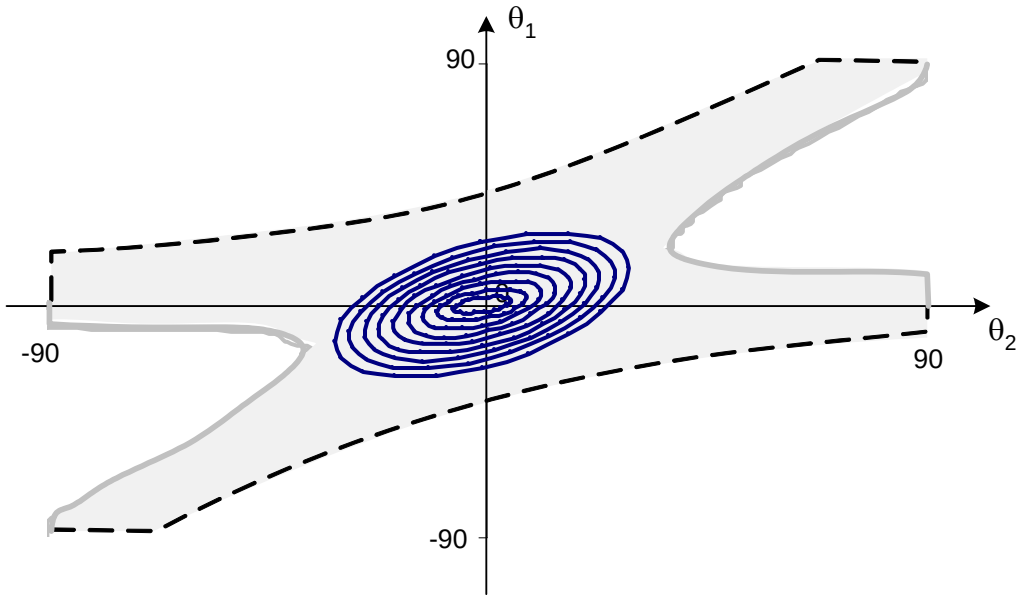

Figure 4.16. Trajectories traced by a fin undulating with a linearly increasing amplitude envelope of $g_1 = c, g_2 = 2g_1, g_3 = 3g_1, ..., g_n = ng_1$ and $\beta = 60°$. There are nine trajectories for nine fin segments. The traced trajectories increase from g_1 to g_n; g_1 be the minimum and g_n the maximum.

Amplitude envelope also affects the trajectory of the undulating fin mechanisms in the workspace. Figure 4.16 shows the trajectories traced by the fin segments of the undulating fin with a linearly increasing amplitude envelope. The number of trajectories is equal to the number of fin segments. Note that the size of trajectory is independent of oscillation frequency α.

4.4 Control Summary

The computations in Level 2 are done in 15 milliseconds, and the data is transferred thereafter to a corresponding microcontroller in Level 3. The technique described in this Chapter can be called parallel processing because all microcontrollers are doing different task at the same time, and they are all synchronized by a clock. The overall operation of the control architecture in this chapter is summarized in Table 4.2.

Table 4.2. Summary of control architecture using parallel processing technique.

Clock BS2sx(5)	Level 1 BS2sx (6)	Level 2 BS2sx(3) & BS2sx(4)	Level 3 BS2sx(1) & BS2sx(2)
$t_0 = 0$	Collect data from potentiometer, and transfer data to Level 2.	Compute based on predefined values, and transfer results to Level 3.	Waiting for results from Level 2.
$t_1 = 25$ ms	Collect new data from potentiometer, and transfer data to Level 2.	Receive data from Level 1, compute based on values at t_0, and transfer data to Level 3.	Control servomotors based on results at t_0.
$t_2 = 50$ ms	Collect new data from potentiometer, and transfer data to Level 2.	Receive data from Level 1, compute based on values at t_1, and transfer data to Level 3.	Control servomotors based on results at t_1.
t_x	Collect new data from potentiometer, and transfer data to Level 2.	Receive data from Level 1, compute based on values at t_{x-1}, and transfer data to Level 3.	Control servomotors based on results at t_{x-1}.

Chapter Five
Theory and Experiment

5.1 Theoretical Analysis Based on Single Oscillating Foil

A mechanical undulating fin has been constructed as a means of propulsion. The undulating fin was designed on modular basis, and it was able to mimic the swimming method of stingray, cuttlefish, and knifefish, as described in Chapter 3. The undulating fin is controlled by ten equally spaced servomotors to which are connected cranks of the same length, as shown in Figure 5.1. Each fin consists of nine fin segments, and one fin segment, shown as link BD in Figure 5.1, is controlled by two servomotors. Each fin segment is connected to the adjacent one by a revolute joint.

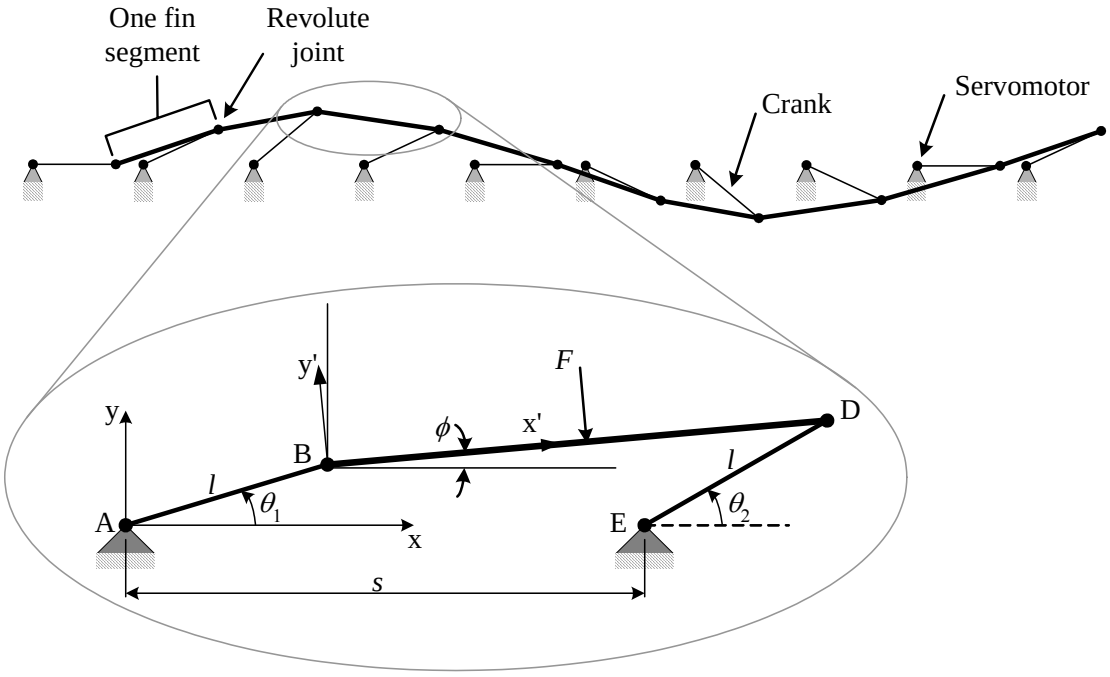

Figure 5.1. Side view of a fin controlled by ten equally spaced servomotors. The fin consists of nine fin segments.

The analysis of the fin will be simplified to one fin segment, which is controlled by two servomotors A and E whose angular displacements with respect to x-axis are specified by θ_1 and θ_2, respectively, as shown in Figure 5.1.

Note that the linkage in Figure 5.1 has two degrees of freedom and *BD* is a link whose length varies according to the orientations of cranks *AB* and *DE*. Mechanical constraints of link *BD* is discussed in Chapter 3.

If θ_1 and θ_2 are functions of time, the position of points *B* and *D* at any point in time is given by:

$$\begin{aligned} P_B(t) &= l\left(\cos\theta_1 \hat{i} + \sin\theta_1 \hat{j}\right), \\ P_D(t) &= l\left[\left(s/l + \cos\theta_2\right)\hat{i} + \sin\theta_2 \hat{j}\right]. \end{aligned} \tag{5.1}$$

Accordingly, the length of link *BD* is:

$$BD(t) = \sqrt{\left[l\left(s/l + \cos\theta_2 - \cos\theta_1\right)\right]^2 + \left[l\left(\sin\theta_2 - \sin\theta_1\right)\right]^2}\,, \tag{5.2}$$

and its orientation with respect to any horizontal line:

$$\phi(t) = \tan^{-1}\frac{\sin\theta_2 - \sin\theta_1}{s/l + \cos\theta_2 - \cos\theta_1}. \tag{5.3}$$

Consider the fin segment in Figure 5.1 moving forward in a certain medium at constant speed *V*, and the two servomotors performing *harmonic oscillations* according to the following functions:

$$\begin{aligned} \theta_1(t) &= a\sin\alpha(t), \\ \theta_2(t) &= b\sin\left(\alpha(t) + \beta\right), \end{aligned} \tag{5.4}$$

where *a* and *b* are the maximum angular oscillations of θ_1 and θ_2, respectively; β is the phase difference between θ_1 and θ_2. Note that β is positive when θ_2 is leading and negative when θ_1 is lagging.

Anderson *et al.* [29] suggest that under these conditions, the fin segment is subject to time-varying force *K(t)*. The servomotors have to provide torque inputs of $Q_1(t)$ and $Q_2(t)$. If τ is the period of oscillation of the fin segment, let *F* shown in Figure 5.1 be the time-averaged value of *K(t)*, and *P* the average input power per cycle:

$$F = \frac{1}{\tau}\int_0^{\tau} K(t)dt\,, \tag{5.5}$$

$$P(t) = \frac{1}{\tau}\left(\int_0^{\tau} Q_1(t)\frac{d\theta_1}{dt}(t)dt + \int_0^{\tau} Q_2(t)\frac{d\theta_2}{dt}(t)dt\right). \tag{5.6}$$

The time-average useful force along *x*-axis, thrust *T*, is given by:

$$T = \frac{1}{\tau}\int_0^{\tau} K(t)\sin\phi(t)dt\,. \tag{5.7}$$

Collectively, for *n* number of segments, *T* assumes greater value, which is theoretically *nT*. In this case any hydrodynamic interaction is ignored as propulsive waves propagate along the fins. The propulsive efficiency, η, is defined to be the ratio of useful power over input power as:

$$\eta = \frac{TV}{P}\,. \tag{5.8}$$

5.2 Experimental Studies on Knifefish Robot

Several experiments were carried out on the designed undulating fin by using the constructed robots, knifefish robot and cuttlefish robot, as shown in Chapter 3. The studies were aimed at obtaining the effect of various swimming modes of the undulating fin. The experiments were performed in an indoor (laboratory) water tank and in a diving pool, a real environment in which water current was present.

5.2.1 Setup and Procedure of Laboratory Experiment

Experiments were carried out with the following equipment:

- A water tank of 240 cm by 80 cm, and water depth of 70 cm.
- A biomimetic underwater robot swimming by anal fin.
- A video camera with image capture-ability of 25 frames per second (frame/s).
- A black reference point was place in the middle of the robot to be captured by the video camera.
- Two fixed black reference points between which the camera was to capture the motion of the robot. All black reference points are required for image processing. The reference points and the video camera were at the same level from the ground, i.e. 1 m. Detailed setup positions are shown in Figure 5.2(b).

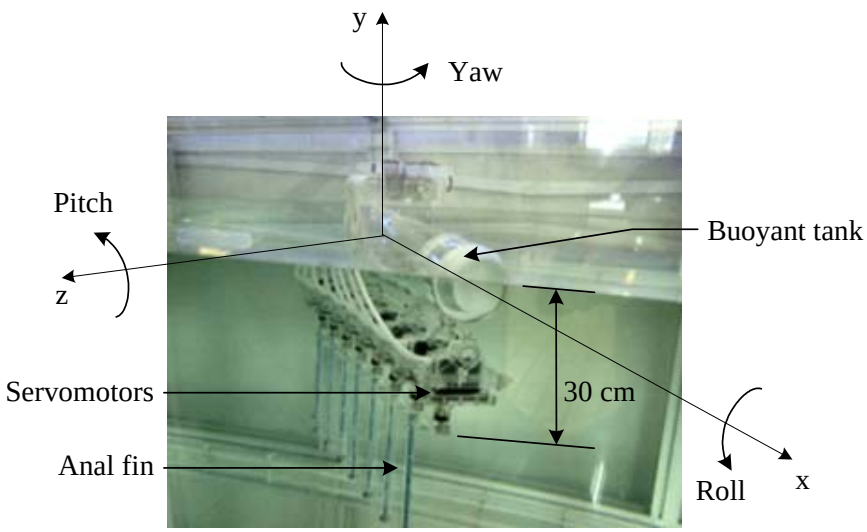

(a)

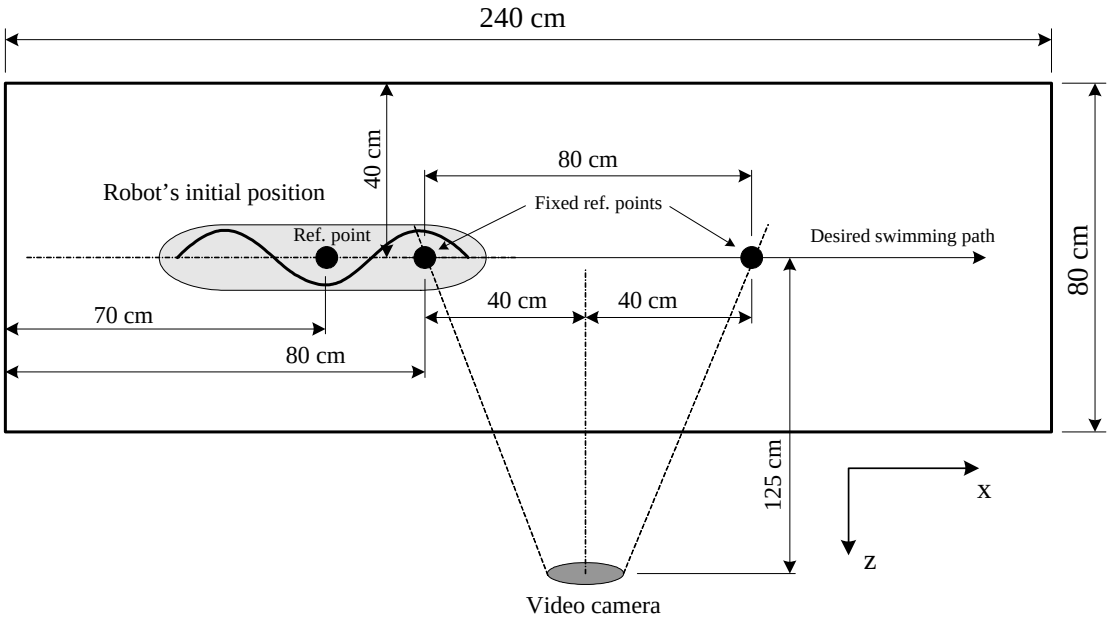

(b)

Figure 5.2. (a) Biomimetic robot swimming by anal fin used in experiments, and its fin was submerged 25 cm underwater. (b) Top View of experimental setup consisting of 240 cm by 80 cm water tank, and water depth of 70 cm, and a video camera.

Table 5.1. Outline of knifefish robot specifications.

Biomimetic knifefish robot		Undulating fin	
Mass	6.2 kg	Mass	3 kg
Length	80 cm	Length	63 cm
Height	56 cm	Material	Acrylic
Width	11 cm	Width	20 cm
Actuator	8 servomotors, Futaba S3801	Peak-to peak amplitude	10 cm
Power source	7.5 V, 3000 mAh NiMH battery	Controller	4 parallel processing Basic Stamps
		Fin segments	7 (8 servomotors)

The biomimetic knifefish robot was powered by 7.5 V *Nickel Metal Hydride* (NiMH) batteries of 3000 mAh. The undulating fin was controlled by four basic stamps arranged in parallel processing. The program loaded in the microcontroller was the same as that described in Chapter 4. However, this controller only controlled 8 servomotors. Detailed program and circuitry of the knifefish robot is explained in Appendix B. The amplitude envelope of the undulating fin was set in the program to be 10 cm, and the tail beat frequency 8/9 Hz. Constant amplitude envelope of 10 cm is equivalent to:

$$g_1 = g_2 = g_3 = ... = g_n = 30°,$$

which is described in Chapter 4. Using the present mechanical system, it is recommended that future experiments do not exceed 1 Hz tail beat frequency as the servomotors may overheat and cause short circuit. Overall specifications of the robot and undulating fin are outlined in Table 5.1.

Having set all the equipment at their positions, shown in Figure 5.2(b), the following procedure was performed during the experiments:

- The undulating fin was set at the desired phase difference β.
- The biomimetic robot was positioned and aligned along the desired swimming at its initial position, as shown in Figure 5.2(b).
- Three-minute waiting time was required for the water to stabilize.
- The undulating fin was run at 8/9 Hz tail beat frequency.
- Video camera captured the motion robot at 25 frames per second. The two fixed black points and the black point on the robot were the main target. Stop capture when the robot has passed the second reference point.
- Repeat experiment for other β.

5.2.2 Results and Discussion

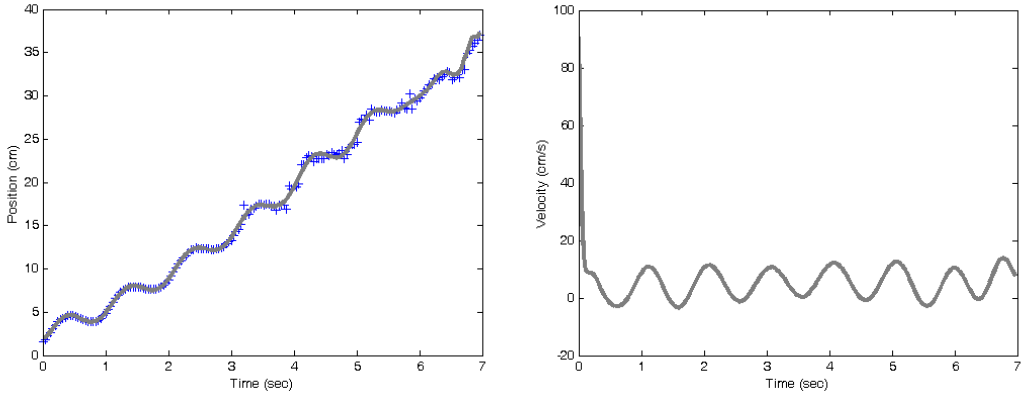

(a) (b)

Figure 5.3. (a) Position curve and (b) velocity curve of biomimetic robot when $\beta = 20°$.

The motion of the robot captured by the video camera was put into many images such that the positions of the robot could be obtained based on the three black reference points. The images were processed using MATLAB, and every image was binarized into black and white such that only the three black reference points were apparent. The position curve of the robot was then plotted with respect to time, as shown in Figure 5.3(a). A curve was fitted to the points on the position curve, and its equation was differentiated to obtain the velocity curve in Figure 5.3(b). Overall observation made during the experiments is presented in Table 5.2

Table 5.2. Experimental observation performed on knifefish robot with constant amplitude envelope of 10 cm and tail beat frequency of 8/9 Hz.

Exp. no.	β	N ($n_f = 7$)	C (Amp)	V (cm.s^{-1})	Observation
1	20°	7/18	1.85	5	• Severe roll oscillations accompanied by yaw oscillations • No pitch • Overall straight swimming path
2	30°	7/12	1.95	10	• Roll oscillations accompanied by yaw oscillations, however lesser than previous • No pitch • Overall straight swimming path
3	40°	7/9	2.1	15	• Roll oscillations accompanied by yaw, however lesser than previous oscillations • No pitch • Overall straight swimming path
4	50°	5/6	2.1	20	• No apparent roll and yaw • Velocity varied with time • Straight swimming path
5	60°	7/6	2	20	• No apparent roll and yaw • Straight swimming path • Smooth forward motion
6	70°	49/36	1.8	18	• No apparent roll and yaw • Straight swimming path • Forward motion smoother than previous
7	80°	14/9	1.8	15	• No roll and yaw • Straight swimming path • Very smooth forward motion
8	90°	7/4	1.8	12	• No roll and yaw • Straight swimming path • Very smooth forward motion

Legend	Description
β	Phase difference between consecutive servomotors (see Chapter 4)
N	Number of waves present in undulations (Equation 5.9)
C	Current (measured by multimeter)
V	Time-average velocity (obtained from experiment)
Roll	Rotation about *x*-axis (defined in Figure 5.2(a))
Yaw	Rotation about *y*-axis (defined in Figure 5.2(a))
Pitch	Rotation about *z*-axis (defined in Figure 5.2(a))

An undulating fin is normally characterized by the number of waves *N* present when the fin is undulating, which is related to β by:

$$N = \frac{\beta n_f}{360°}, \tag{5.9}$$

where n_f is the number of fin segments.

5.2.2.1 Periodic Velocity Variations in Experiments 1, 2, 3, and 4 (β = 20°, 30°, 40°, and 50°)

Direct observations by eye during Experiments 1, 2, and 3 in which less than one wave was present, showed periodic velocity variation accompanied by roll and yaw oscillations. The apparent slow speed of the robot in experiments 2 and 3 was not caused by yaw and roll. Roll and yaw were caused by the extra energy which was not transformed into forward motion of the robot. It can be described by the following equation:

$$\text{Input energy} = \text{Energy}_{\text{forward}} + \text{Energy}_{\text{roll and yaw}}. \tag{5.10}$$

Severe yaw oscillations in Experiment 2 causes the velocity curve in Figure 5.4(a) to show negative value. This however does not mean that the robot is moving backward when its velocity is shown negative. Pitch was observed only when the robot is accelerating or decelerating because the robot's center of gravity was located below it center of buoyancy. No pitch when the robot was moving forward, either at constant or varying velocity.

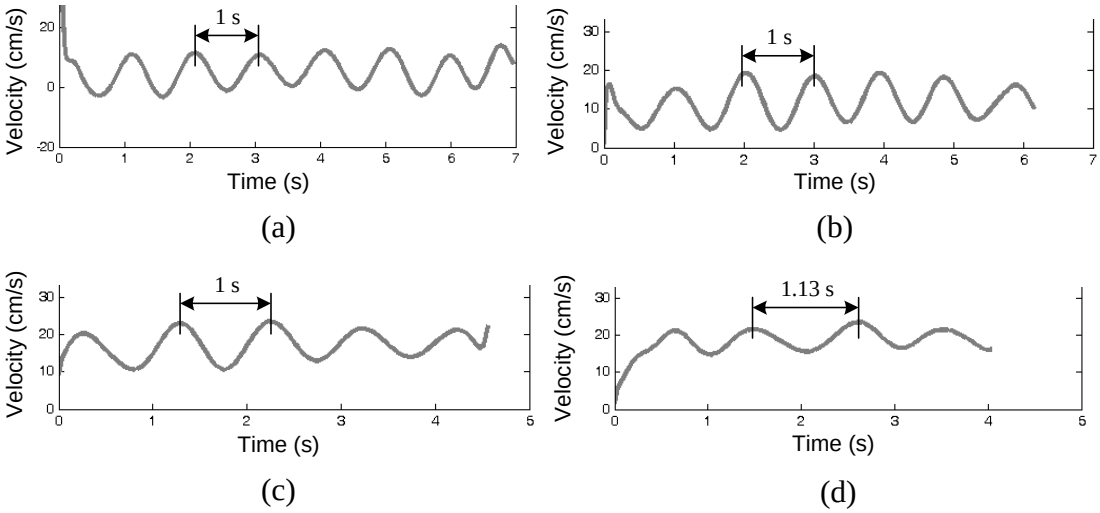

Figure 5.4. Velocity curves of various swimming modes for $N < 1$: (a) $\beta = 20°$, (b) $\beta = 30°$, (c) $\beta = 40°$, (d) $\beta = 50°$. The patterns display periodic variations.

The periodic velocity gain and loss was not apparent in Experiment 4 ($\beta = 50°$). However, further analysis into the velocity curve obtained from experiment 4, shown in Figure 5.4(d), reveals the periodic pattern. Another note-worthy observation of Figure 5.4 is that the pattern repeats itself at a frequency near that of the tail beat, which is 8/9 Hz.

5.2.2.2 Camera Sampling Rate

An important factor that must be taken into consideration when capturing an object moving at a certain frequency is the capture rate or sampling frequency. In the experiments, a video camera with sampling frequency of 25 frames per second was used to capture the robot's motion, which had one frequency component of 8/9 Hz.

According to Nyquist [30] sampling theorem, the sampling frequency must at least be twice the highest signal frequency so that signal can be reconstructed correctly, which can be expressed as follows:

$$f_{sampling} \geq 2 f_{signal} . \tag{5.11}$$

It can be concluded therefore that the camera used in the experiment was adequate to sample the robot's motion for the following reason:

$$25\,\text{Hz} > 2 \times (8/9)\,\text{Hz}.$$

Camera with higher frame rate may be used to proof that there was no aliasing in the data sampling [30].

5.2.2.3 Constant Velocity in Experiments 5, 6, 7, and 8 (β = 60°, 70°, 80°, and 90°)

Roll and yaw oscillations were not apparent by direct observations in experiments 5, 6, 7, and 8. The velocity curves obtained from these experiments reveals roll and yaw were completely absent when the robot is moving forward. Their absence seems to confirm the analysis made by Sfakiotakis, Lane, and Davies [21], and Lindsey [22] stating that at least one wave is present when a fish is swimming. Figure 5.5 shows constant velocity curves obtain from experiments 5, 6, 7, and 8. Experiments 5 and 6 show small oscillations when the robot was gaining speed from rest. Relatively constant velocity was observed after 1 second.

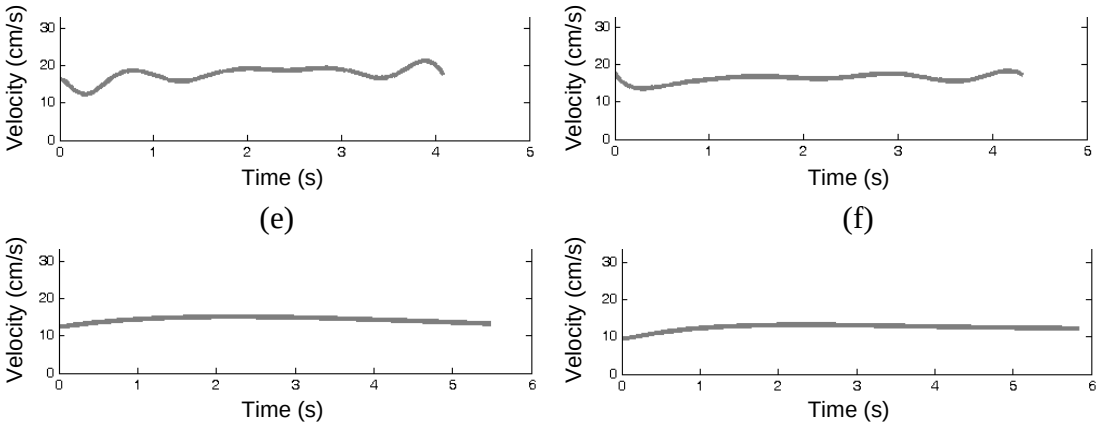

Figure 5.5. Velocity curves when N >1: (a) β = 60°, (b) β = 70°, (c) β = 80°, (d) β = 90°. Constant velocity was observed in these experiments.

In conclusion, constant velocity and the absence of roll and yaw are always desirable since the robot's swimming path can be fully controlled. Experiments 5, 6, 7, and 8 also showed that the robot could move in a straight line when more than one wave ($N > 1$) was present in undulations. However, the number of waves does not seem proportional to the increase of velocity, as shown in Figure 5.6. In the white area ($N > 1$), the velocity is declining as more waves were present in undulations.

Note that in the absence of acceleration, the robot is moving forward at constant velocity and the thrust is equal to the drag force acting against the robot. At constant velocity, the thrust force is therefore:

$$F_{drag} = F_{thrust} = \frac{1}{2} C_d \rho A V^2, \tag{5.12}$$

where C_d is the drag coefficient of the robot, ρ is the water density, A is the area of the robot the contributes to the drag, and V is the robot's velocity [31]. Equation (5.12) signifies that higher force F_{thrust} is required at higher velocity V.

For the present undulating fin swimming with constant amplitude envelope of 10 cm and fin length of 63 cm, the most efficient swimming method is found at β = 60°, which has the highest recorded velocity of 20 cm/s. Note that β = 60° corresponds to the number of waves of 7/6, as given in Table 5.2.

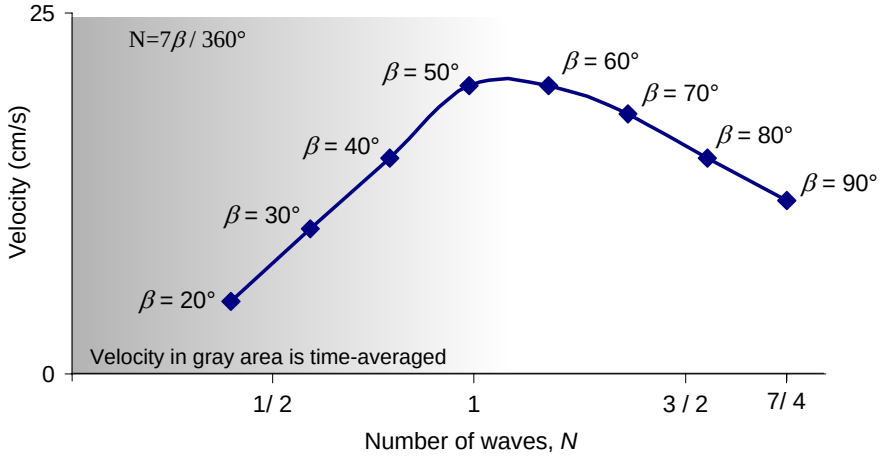

Figure 5.6. Velocity plot of 63-cm fin obtained from water tank experiment. Due to the oscillatory nature of velocity for β less than 60°, the velocity in the gray area is plotted based its time-averaged value (α = 8/9 Hz).

The gray area as shown in Figure 5.6, in which periodic velocity variations are observed, are not of interest as it only contributes to inefficient swimming and inconsistent with nature [21, 22]. Note that darker area suggests more apparent periodic velocity variation, and roll and yaw oscillations. Future experiments should focus on how to obtain the force of the constructed undulating fin by using more that one wave in the undulations.

5.2.3 Diving Pool Experiment of Knifefish

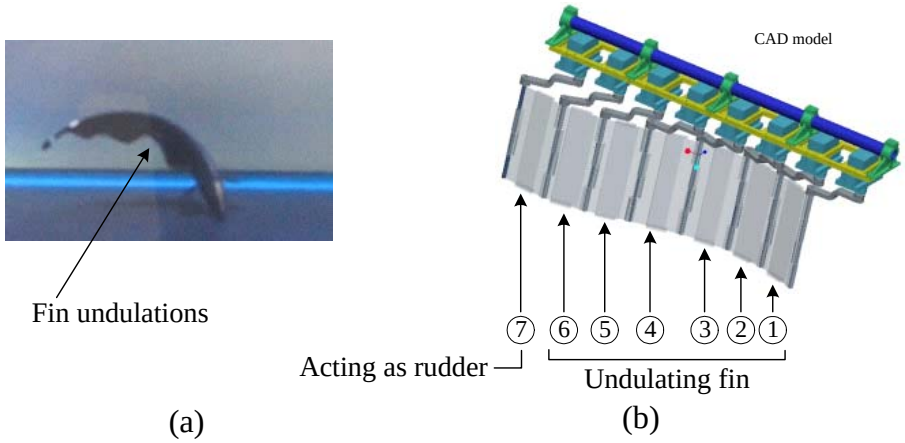

Figure 5.7. Maneuvering technique of: (a) A real knifefish by bending its body, and (b) the knifefish robot by using fin segment 7 as rudder to turn.

Having done laboratory experiments, the robot was deployed at NTU diving pool, which may simulate real situation in which the robot has to encounter water current. The water in the diving pool was constantly circulating for filtering, which is a requirement for a pool. The deployment was done by remote controlling the robot from the side of the pool as shown in Figure 5.8(a). The fin of the robot was undulating at 8/9 Hz.

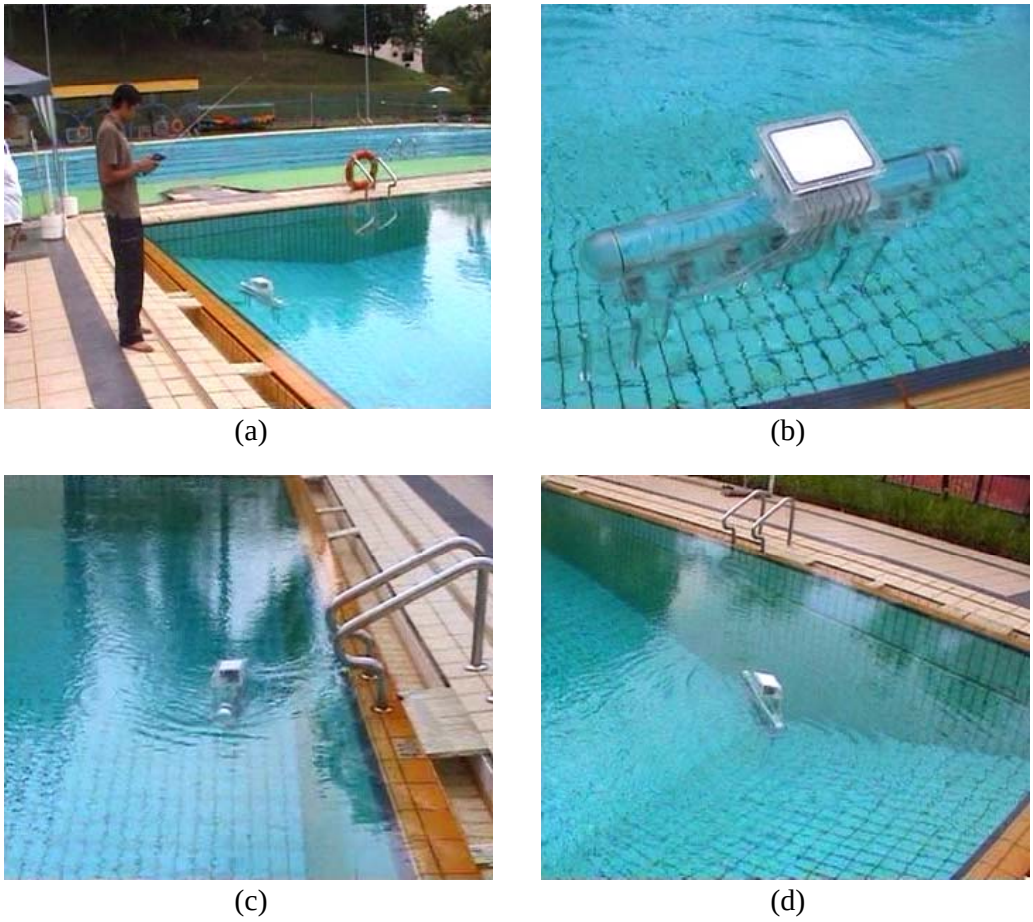

(a) (b)

(c) (d)

Figure 5.8. Diving pool experiment of robot swimming by undulating fin: (a) the robot was remote-controlled, (b) close-up view of the robot, (c) the robot swam parallel to the wall of the pool, (d) and it made a turn by using rudder (fin segment 7).

Unlike real fish whose body is bent for turning, as shown in Figure 5.7(a), the body of the constructed knifefish robot was stiff and remained straight while turning. Therefore, fin segment 7 (or tail), as shown in Figure 5.7(b), was used as a rudder for turning. Detailed control of the knifefish robot is provided in Appendix B.

Some degree of success was achieved in the experiment. In the vicinity of the wall of the pool, away from center of water current, the robot was able to swim in a straight line and turn a corner as shown in Figures 5.8(c) and 5.8(d), respectively. The mechanical system of the robot was working well and no leakage was found. However, the robot was not able to pass through strong water current and often it was carried away.

5.3 Experimental Studies on Cuttlefish Robot

Further experimental studies were performed on a pair of undulating fins attached to a buoyant tank, which allows the undulating fin to move freely during experiment. The assembly of the undulating fins mimicked the swimming method of a cuttlefish, and hence the name of the cuttlefish robot. Experiments on this robot were performed at NTU diving pool as shown in Figure 5.9. The environment was characterized by disturbance created by water current. The diving pool experiments were aimed at collecting data on the velocity of the robot and observing the robot's performance in coping with water current.

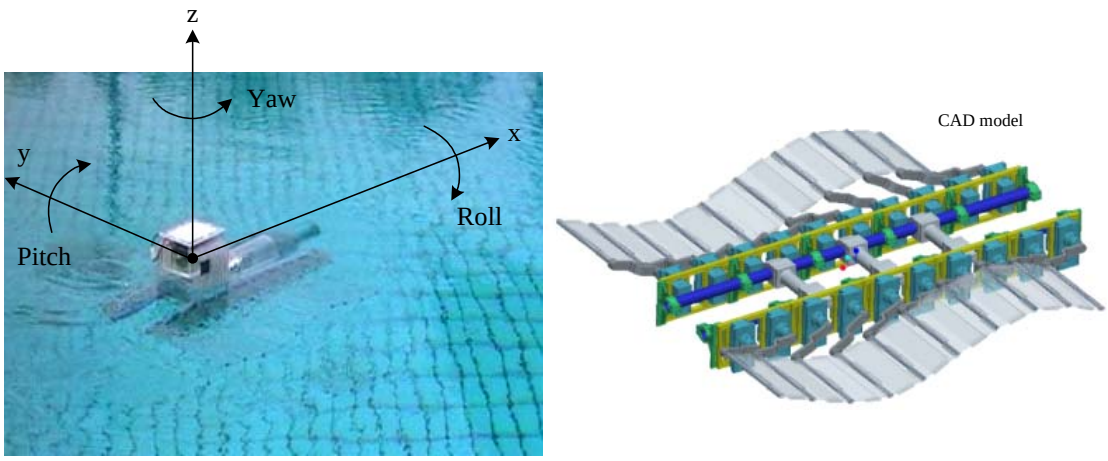

Figure 5.9. Cuttlefish robot was swimming to the middle of the pool where water current was strong.

Cuttlefish makes use of its lateral fins for low speed locomotion and hovering [23]. The lateral fins of the cuttlefish acts like a track vehicle. By modulating the speed of its lateral fins, a cuttlefish can perform turning at a certain radius and on-the-spot yaw. The fins of the cuttlefish robot act in the same manner as the fins of the real cuttlefish. The independent control of each fin, as described in Chapter 4, allows the fins to move in different speeds and different directions, which can accommodate on-the-spot turning or yaw. Note that the knifefish robot made a turn by using a rudder, which is the fin segment 7 as shown in Figure 5.7. The mechanical components worked well and no leakage was found. It was observed that the cuttlefish robot could cope with water current better than the knifefish robot.

Table 5.3. Outline of cuttlefish robot specifications.

Biomimetic cuttlefish robot		One undulating fin module	
Mass	12 kg	Mass	4 kg
Length	90 cm	Length	90 cm
Height	40 cm	Material	Acrylic
Width	85 cm	Width	20 cm
Actuator	20 servomotors, Futaba S3801	Peak-to peak amplitude	10 cm
Power source	7.5 V, 3000 mAh NiMH battery	Controller	6 parallel processing Basic Stamps
		Fin segments	9 (10 servomotors)

Each module of undulating fin consisted of ten servomotors, which has the same specification as those used in the knifefish robot. Overall specifications of the cuttlefish robot are outlined in Table 5.3. The fin was undulating at 8/9 Hz and at constant amplitude envelope of 10 cm.

Due to the disturbance created by the water current, often the robot could not move in a straight line. In this situation, the method used in obtaining the velocity of the knifefish in Section 5.2.1 could not apply. Therefore, the velocity of the robot is measured based on the distance it traveled and the time elapsed to travel that distance. In these experiments, the relationship between phase difference β with respect to the velocity V was obtained.

Table 5.4 summarizes parameters used in the experiments, and Figure 5.10 depicts the relationship between the number of waves N and the velocity V of the robot. The plot in Figure 5.10 is consistent with the plot in Figure 5.6, in which the velocity V of the robot decreased as the number of waves N of the fin increased for $N > 1$. The maximum velocity of the robot was 20 cm/s at $\beta = 50°$, which is equivalent to $N = 5/4$.

The region of $N > 1$ is of the main interest because of the absence of periodic variations and consistency with nature [21, 22]. The experiments were performed only in the region of $N > 1$ due to the constraint of battery capacity, which could power the robot only for thirty minutes. Future experiments and research on the undulating fin described in this thesis may investigate the region of $N \leq 1$, and the relationships of other parameters with the velocity of the robot.

Table 5.4. Experimental observation performed on cuttlefish robot with constant amplitude envelope of 10 cm and tail beat frequency of 8/9 Hz.

Exp. no.	β	$N = 9\beta/360°$	V (cm/s)
1	50°	5/4	20
2	60°	3/2	16
3	70°	7/4	15
4	80°	2	12.5
5	90°	9/4	12

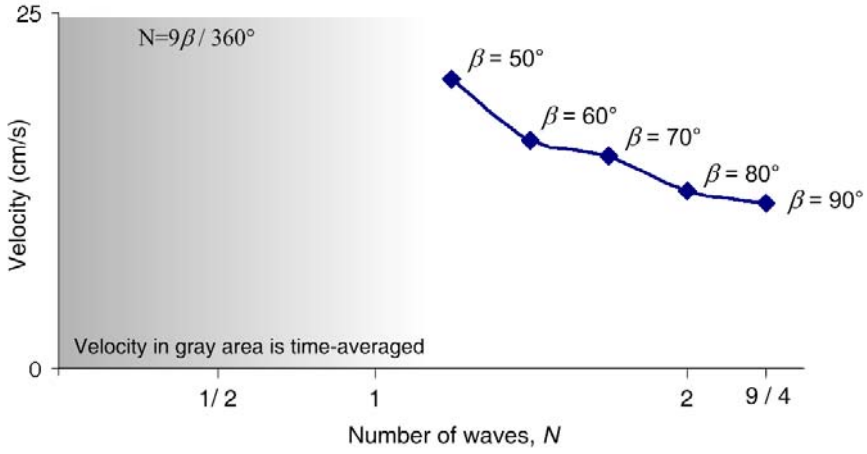

Figure 5.10. Velocity plot of 81-cm lateral fin for $N > 1$.

Chapter Six
Conclusion and Recommendations

6.1 Conclusion

This research project was pursued with an objective of analyzing the performance of an undulating fin. An unconventional and modular undulating fin has been designed and constructed. It consists of several fin segments, whose number can be varied depending on application, and each fin segment is made of two-degree-of-freedom slider mechanism. The undulating fin was then integrated with a buoyant tank to give it the shape of a fish swimming with a long-based anal fin, which is a black ghost knifefish. In the course of the research, the design of the undulating fin was extended to mimic a cuttlefish swimming by undulations of its paired lateral fins. Two undulating fins were therefore manufactured to mimic the cuttlefish. At present, control system for the undulating fin has been developed, and it can accommodate both single and paired undulating fin. The control architecture made use of Basic Stamp microcontrollers, although limited memory space, were arranged in parallel processing in order to send signal every 25 milliseconds to maximum 28 servomotors. A clock was used to synchronize all processes. The control architecture can be easily extended to accommodate more actuators.

Several experiments were conducted in a laboratory and in a diving pool. The robots in Figure 6.1 were used for the experiments. The experiments were conducted to analyze the behavior of the robot when swimming with various numbers of undulatory waves. The fin was undulating at 8/9 Hz in these experimental studies. Other undulation frequency (α) can be specified for similar experiments.

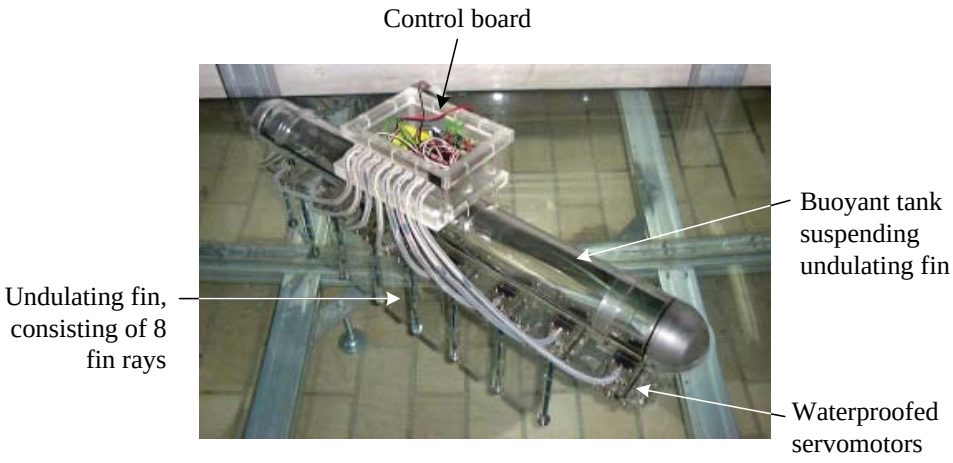

(a)

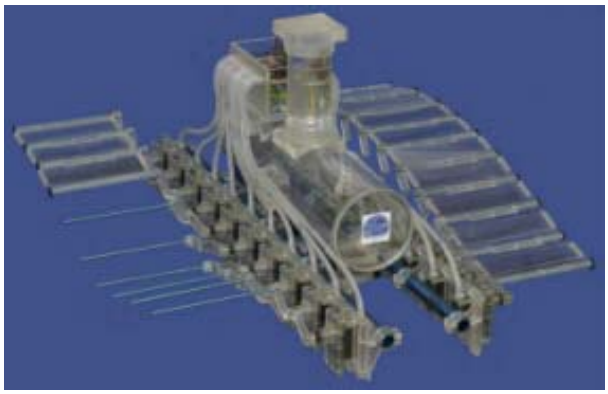

(b)

Figure 6.1. Biomimetic robots used for experimental studies: (a) knifefish robot, (b) cuttlefish robot.

Analysis into velocity curves obtained from the experiments on the knifefish robot reveals periodic pattern, which has almost the same frequency as that of tail beat. This was proven by several experiments by changing the number of waves. The experiments have also proved that at least one wave must be present for stable swimming [21], i.e. constant velocity, which is in conformity with anguilliform swimming method. Yaw oscillations can be observed in sharks swimming behavior, since less then one wave is present in its body undulations [22]. Based on the experiments on the knifefish and cuttlefish robots, the velocity of the robots however was not proportional to the addition of undulatory waves. Experiments revealed that the highest velocity was produced when undulatory waves was slightly more than one.

6.2 Recommendations

6.2.1 Future Experiments

At present, the exact amount of thrust has not been measured, and also the efficiency of the robot. Future research may look into steady swimming thrust measurement so that efficiency of the robot can be obtained and further changes can be made for improvement.

The performance of the undulating fin has not yet been formalized. The results obtained in this research work only serves as preliminary findings. More experiments are required in order to establish the relationships of various fin parameters such as phase difference, robot's velocity, tail beat frequency, fin length, and amplitude envelope. Note that the present control system is open loop. By having established the parametric relationships, the closed-loop control system can be implemented to test the relationships.

6.2.2 Undulating Fin with Minimum Actuators

The undulating fin developed for this research was built primarily for experiment purposes and for complete modeling of its natural counterpart. Undulating-finned fish has capability to change its fin wave parameters as it swims. It is the main reason why the undulating fin prototype described in this thesis has ten servomotors. It is however not necessary to have so many servomotors when the undulating fin is to be deployed without changing its wave parameters. Therefore, the fin segments described in Chapter 3 might be connected by linkages such that one main motor is sufficient to undulate the fin. The linkages are to be built to effectuate undulations based on optimum values of wave parameters, which are acquired from experiment, to ensure efficient deployment. The proposed development is called single-motor-multi-joint assembly [32].

6.2.3 Body of Cuttlefish or Knifefish Robot

If we ever noticed a fish swimming in a pond or in an aquarium and realized that they swim very gracefully, and when they are not moving they seem to put no effort to

maintain their position in still water; they are in harmony with their surroundings. The fish is able to maintain its depth in water, being weightless, without the help of its fin. An organ known as swim bladder [33] allows the fish to quickly adjust its density relative to its surroundings by changing the volume of the bladder. In an attempt to imitate nature, an American ship maker David Bushnell in 1776 made a human-powered submersible vessel. In order to submerge, the vessel was purposely flooded with water until it was heavy enough. A hand pump was used to remove the water from so that the vessel could surface. It then laid foundation for modern submarines. Present submarines are using ballast tanks, which are tanks flooded with water to enable the submarine to dive, surface, and maintain depth underwater. Some underwater robots employ piston mechanisms to model ballast of a submarine. Other method in controlling depth of a vessel is by using propeller(s), which is widely used in ROVs and AUVs. The disadvantage of this system is that it requires more power than ballast system since the propeller(s) must constantly rotate in order to maintain depth. Ballast system is therefore more preferred in robotics application since it requires less power than propeller system in maintain depth underwater, thus allowing longer deployment time.

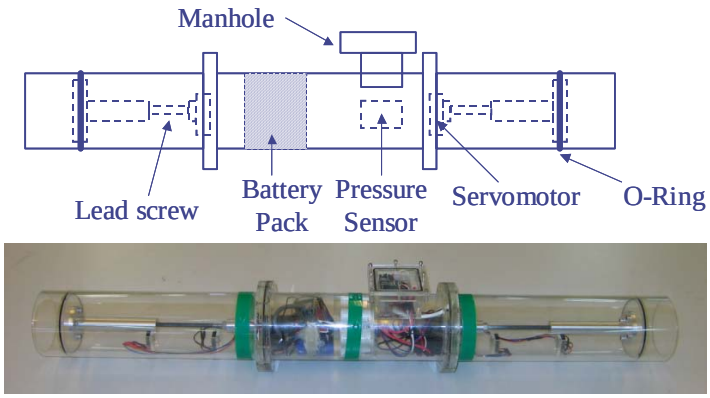

Figure 6.2. Two-piston variable density chamber.

Current development of the undulating fin described in this thesis has not reached a stage of ready deployment. A customized control board and algorithm have been developed only for the undulating fin. In order to produce a fully deployable undulating-fined biorobots, a ballast tank is recommended to be attached to the present undulating fin. A two-piston variable density chamber [34], as shown in Figure 6.2, was designed and constructed in NTU under Dr. F.M.J. Nickols' supervision. It has been successfully tested. The chamber can be attached directly to

the present undulating fin or used as a guide to designing a new variable density chamber.

6.3 Future Research

6.3.1 Development of Energy Efficient Oscillating Wing/Fin

Every living creature that can move, in the air, on the land, or in the water, possesses a locomotion system that either oscillates or undulates. The way humans walk, for instance, can be likened to an oscillating pendulum. Fish in the water are swimming by flapping their tail back and forth, which is similar to oscillation. Some other fish such as needlefish, knifefish, and cuttlefish swim by body or fin undulation. Birds are flying in the air by flapping their wing rhythmically according to a certain pattern, which may be called oscillation.

Many species of birds migrate very long distance for breeding or avoiding adverse climate condition. Alaskan bar-tailed godwits, for instance, are known to have the longest non-stop migration flight of 6800 miles [35]. Many types of fishes also migrate on regular basis, raging from daily to annual, with distances ranging from few meters to thousands of kilometers. The purpose of migration usually relates to either feeding or breeding, although in some other cases the reason is still unknown.

Studies conducted by Johnsen and Kier [36] reveal one important factor that could make such long distance migration possible. Their studies suggest possibility of tissue fibers in the fin of cuttlefish storing elastic energy during fin bending, thus allowing the fin to function as a harmonic oscillator and thereby increasing the efficiency of the fins during locomotion. The same concept may also apply to the mechanical system of bird's wings and human legs, which makes them efficient oscillators.

6.3.2 Artificial Muscle Undulating-Finned Robot

The future of biomimetic application relies on the advanced development of actuators. Emerging biologically inspired materials such as shape memory alloy (SMA), electro-active polymer (EAP), and shape-memory polymer (SMP) suggest avenues worth

pursuing which then may replace present motor-based actuators, such as servomotors. EAP has a potential in modeling the fish muscles, including undulating fins [37-39].

6.3.3 Other Variants of Undulating-Finned Biorobots

In this research two variants of undulating-finned biorobots were developed. They were cuttlefish robot with a pair of undulating lateral fins, and a knifefish robot with a long anal fin. Those two robots are inherently stable because its center of buoyancy is located above its center of gravity. Using the fin module developed in this research, other variants of undulating-finned biorobots can be constructed. An upside-down equivalent of knifefish as shown in Figure 3.2, which is a fish swimming with dorsal fin such as bowfin, may be considered.

References

[1] S. Vogel, "Cat's Paws and Catapults", *W.W Norton*, New York, 1998.

[2] F. E. Fish, "Limits of Nature and Advances of Technology: What Does Biomimetics Have to Offer?", in *Proc. of 1st Int. Sym. on Aqua Bio-Mechanisms*, N. Kato and Y. Suzuki, Eds., Tokai University Pacific Center, 3-12, Hawaii, 2000.

[3] Pipe Inspection Robot, http://www.cityu.edu.hk/applied_research/electronics/FSE_EE_RobinBradbeer_02.html, June 2005.

[4] Coelacanth Robotic Fish of Mitsubishi Heavy Industry, http://www.mhi.co.jp/enews/e_0898.html, June 2005.

[5] Decompression Sickness (Bends), http://science.howstuffworks.com/question101.htm, June 2005.

[6] Underwater Robot for Mine Defense, http://www.publictechnology.net/modules.php?op=modload&name=News&file=article&sid=2989, June 2005.

[7] C. M. Breder, "The Locomotion of Fishes", *Zoologica* vol. 4, 159-297, 1926.

[8] The American Heritage Dictionary of the English Language, 4th ed., *Houghton Mifflin Company*, 2000.

[9] Robot history, http://prime.jsc.nasa.gov/ROV/history.html, April 2005.

[10] M. E. Rosheim, "Robot Evolution: The Development of Anthrobotics", *John Wiley & Sons Inc.*, Canada, 1994.

[11] MIT Tuna Robot, http://web.mit.edu/towtank/www/Tuna/Tuna1/tuna1.html, April 2005.

[12] R. Mason and J. W. Burdick, "Construction and Modeling of a Carangiform Robotic Fish", in *Proc. of the Int. Conf. Experimental Robotics*, Sydney, Australia, 1999.

[13] R. Mason and J. W. Burdick, “Experiments in Carangiform Robotic Fish Locomotion”, in *Proc. of the IEEE Int. Conf. Robotics and Automation*, San Francisco, 2000.

[14] Essex Robot Fish, http://cswww.essex.ac.uk/Research/roboticfish, March 2005.

[15] Robotic Fish of Beijing University of Aeronautics and Astronautics (BUAA), http://english.people.com.cn/200412/07/eng20041207_166401.html, June 2005.

[16] Lamprey robot, www.neurotechnology.neu.edu, April 2005.

[17] R. W. Blake, “Swimming in electric eels and knifefishes,” *Can. J. Zool.*, vol. 61, pp. 1432-1441, 1983.

[18] M. A. MacIver, E. Fontaine, and J. W. Burdick, “Designing Future Underwater Vehicles: Principles and Mechanism of a Weakly Electric Fish”, *IEEE J. Oceanic Eng.*, vol. 29, 651-659, 2004.

[19] FLAPS and fish swimming basics, http://www.ece.eps.hw.ac.uk/Research/oceans/projects/flaps/describe.htm, May 2005.

[20] M. Sfakiotakis, D. M. Lane, and B. C. Davies, “An experimental undulating-fin device using the parallel bellows actuator,” in *Proc. IEEE Int. Conf. Robotics Automation*, Seoul, 2001.

[21] M. Sfakiotakis, D. M. Lane, and J. B. C. Davies, “Review of fish swimming modes for aquatic locomotion,” *IEEE J. Oceanic Eng.*, vol. 24, pp. 237-252, 1999.

[22] C. C. Lindsey, ”Form, function and locomotory habits in fish,” in *Fish Physiology Vol. VII Locomotion*, W. S. Hoar and D. J. Randall, Eds. New York: Academic, pp. 1-100, 1978.

[23] W.M. Kier and J.T. Thompson, “Muscle Arrangement, Function and Specialization in Recent Coleoids”, in *Proc. Coleoid Caphalopods through Time*, Berlin, Sept. 2002.

[24] P.W. Webb, “Maneuverability – General Issues”, *IEEE J. Oceanic Eng.*, vol. 29, 547-555, 2004.

[25] C. E. Wilson and J. P. Sadler, “Kinematics and Dynamics of Machinery”, 2nd ed., 1-20, New York: Harper Collins, 1993.

[26] M.J. Lighthill, “Large-amplitude elongated-body theory of fish locomotion”, *Proc. R. Soc. Lond. A* vol. 179, 125-138, 1971.

[27] F. E. Fish *et al.*, “Conceptual Design for the Construction of a Biorobotic AUV Based on Biological Hydrodynamics”, *in Proc. of the 13th int. Sym. of Unmanned Untethered Submersible Technology*, New Hampshire, 2003.

[28] Basic Stamp documentation, http://www.parallax.com, April 2005.

[29] J. M. Anderson, K. Streitlien, D.S. Barrett, and M.S. Triantafyllou, “Oscillating foils of high propulsive efficiency”, *J. Fluid Mech.* vol. 360, 41-72, 1998.

[30] Nyquist sampling theorem, http://mathworld.wolfram.com/NyquistFrequency.html, May 2005.

[31] M. C. Potter and D. C. Wiggert, “Mechanics of Fluids”, 2nd ed., Upper Saddle River, NJ: Prentice-Hall, 1997.

[32] J. Liu, I. Dukes, and H. Hu, “Novel Mechatronics Design for a Robotic Fish,” submitted to *int. IEEE Conf. IROS*, 2005.

[33] G. S. Helfman, B. B. Collette, and D. E. Facey, “The Diversity of Fishes,” *Blackwell Science*.

[34] T. S. Indrawati, “Design and Control Implementation of Two-Piston Robotic Submarine”, *Final Year Project*, Nanyang Technological university, 2003.

[35] Bird migration, http://en.wikipedia.org/wiki/Bird_migration, May 2005.

[36] S. Johnsen and W. M. Kier, “Intramuscular Crossed Connective Tissue Fibers: Skeletal Support in the Lateral Fins of Squid and Cuttlefish (Mollusca: Caphalopoda),” *J. Zool. Lond.* vol. 231, 311-338, 1993.

[37] J. W. Paquette and K. J. Kim, “Ionomeric Electroactive Polymer Artificial Muscle for Naval Applications,” *IEEE J. Oceanic Eng.*, vol. 29, 729-737, 2004.

[38] A. Punning, M. Anton, M. Kruusmaa, and A. Aabloo, “A Biologically Inspired Ray-like Underwater Robot with Electroactive Polymer Pectoral Fins,” in *Proc. of the Int. IEEE Conf. Mechatronics and Robotics 2004 (MechRob'04)*, vol. 2, 241 – 245, Aachen, 13 - 15 Sept., 2004.

[39] S. Guo, T. Fukuda, and K. Asaka, “A New Type of Fish-like Underwater Microrobot”, *IEEE/ASME Trans. on Mechatronics*, vol. 8, Issue 1, 136-141, 2003.

Appendix A

Robot Manual

Appendix A
Robot Manual

A.1 Mechanical Structure

Mass: 6.2 kg
Number of fin segments: 7
Number of Actuators: 8 Futaba Servomotors S3801
Structural material: Acrylic (1200 kg/m^3)

The robot was constructed mainly for experiment purpose. However on board compartments are waterproofed and it can withstand 10-meter water depth. The robot is a biomimetic of a black ghost knifefish, which is swimming by undulations of its anal fin. It is however currently not equipped with a variable buoyancy chamber, which allows it to dive and surface. Buoyant tank is used to suspend the robot floating, while the undulating fin is submerged 30 cm below water surface. The buoyant tank has been redesigned with rounded ends, in order to minimize drag while swimming. The robot is completely stable since its *center of gravity* (CG) lies below its *center of buoyancy* (CB). Note that buoyant force (F_B) is always pointing upward and weight of the object (W) is always pointing downward. One main criterion for stability is that the two forces, F_B and W, must act collinearly. With this hypothesis, there are two positions in which a submerged body may assume stability:

1. CG is located above CB and the forces are acting collinearly. This is the situation of inverted pendulum. Appropriate control system must be implemented to handle disturbances. This situation is however not naturally stable simply because they are not found in nature. Slight disturbance to the body will cause instability and thus the body moves to its naturally stable orientation as in Figure A1(b).
2. CG is located below CB and the two forces are acting collinearly. This is natural stability. Any disturbance to the body will create moment arm *r* between CB and CG as in Figure A1(a), which tends move the body back to its naturally stable position as in Figure A1(b).

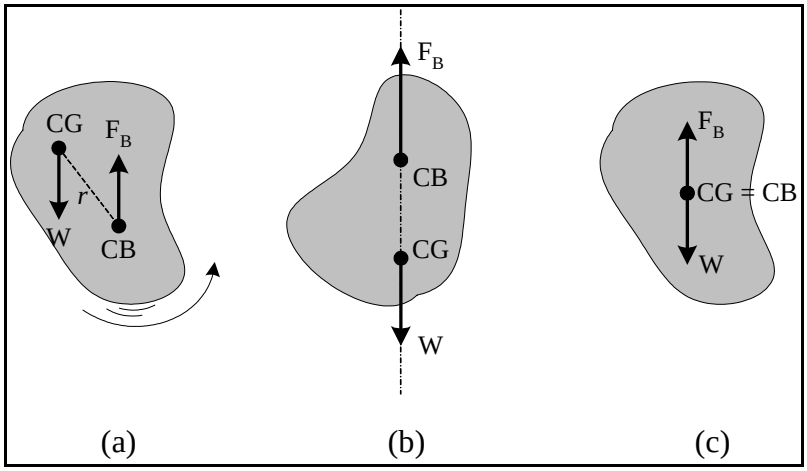

Figure A1. Stability of submerged body: (a) unstable, CB is below CG, (b) stable, CB is above CG and forces are acting collinearly, (c) neutral, CG = CB and forces are acting collinearly.

Object's density also plays role in its stability. Neutral stability in Figure A1(c) can only be met when the object is made of uniform density distribution and it must have the same density as its surrounding medium. Most of robotics systems are made of composite materials and thus nonuniform density distribution. Normally robot is recommended to be naturally stable. However, in other application such as fighter planes, stability is rendered by rigorous control.

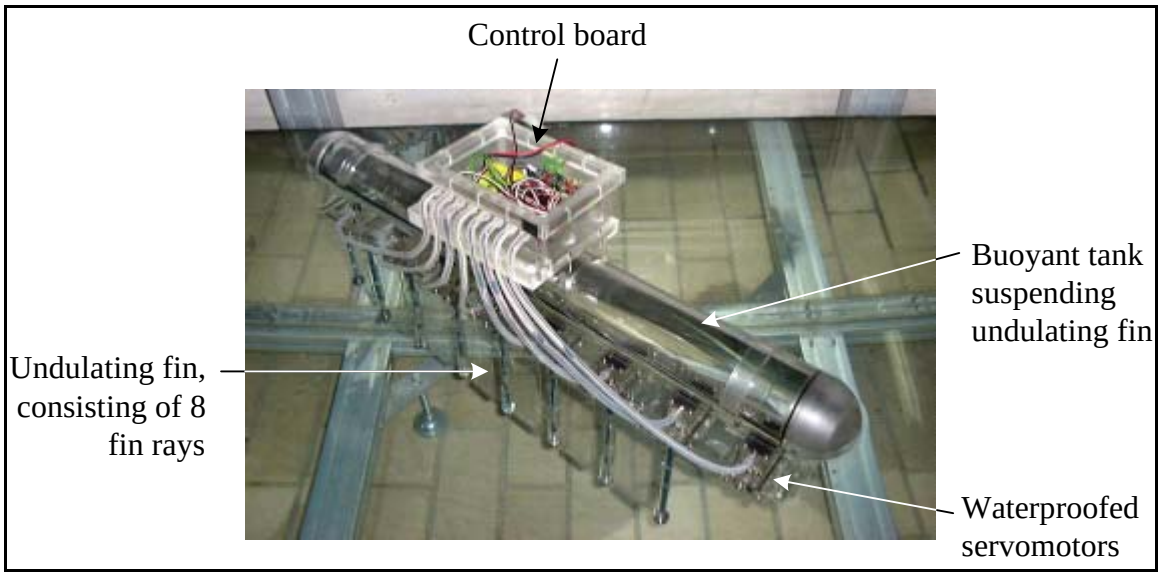

Figure A2. Biomimetic robot used for experiments.

The propulsion system of the robot is an undulating fin with variable amplitude, wavelength, and undulation frequency. These three variables are based on the generalized theory developed in Chapter 4. Their values can be changed in the control program. Other parameters of the undulating fin include fin length and fin width. They are associated with mechanical structure, which means changing these parameters requires changing the mechanical components.

The undulating fin consists of 8 fin rays, therefore 7 fin segments, which accommodate maximum 1.75 wavelength, when consecutives servomotors are positioned at 90° phase difference. Consult Chapter 4 for detailed explanation of parameters designation.

Electronics used to control the robot in Figure A2 is similar to that explained in Chapter 4. However, four microcontrollers used for control instead of six. Four-channel RF receiver is also used in place of potentiometers. Communication lines consist of data bus and flag bus. Their explanation can be found in Basic Stamp manual. Two different microcontrollers are used in the control electronics. They are BS2p and BS2sx. Any Basic Stamp 2 microcontroller can used in the control electronics.

Each RF channel consists of three output pins: ground, supply voltage and signal. Normally the three pins are used to drive a servomotor. For our purpose, only the signal pin is connected to a corresponding pin of BS2p(3). Channel four is an exception. Its signal still pin acts as output. The other two pins however act as input to power the receiver. The power comes from VDD pin, 5 volt regulated voltage, of the BS2p(3).

A.2 Control

A.2.1 Electronic Connections

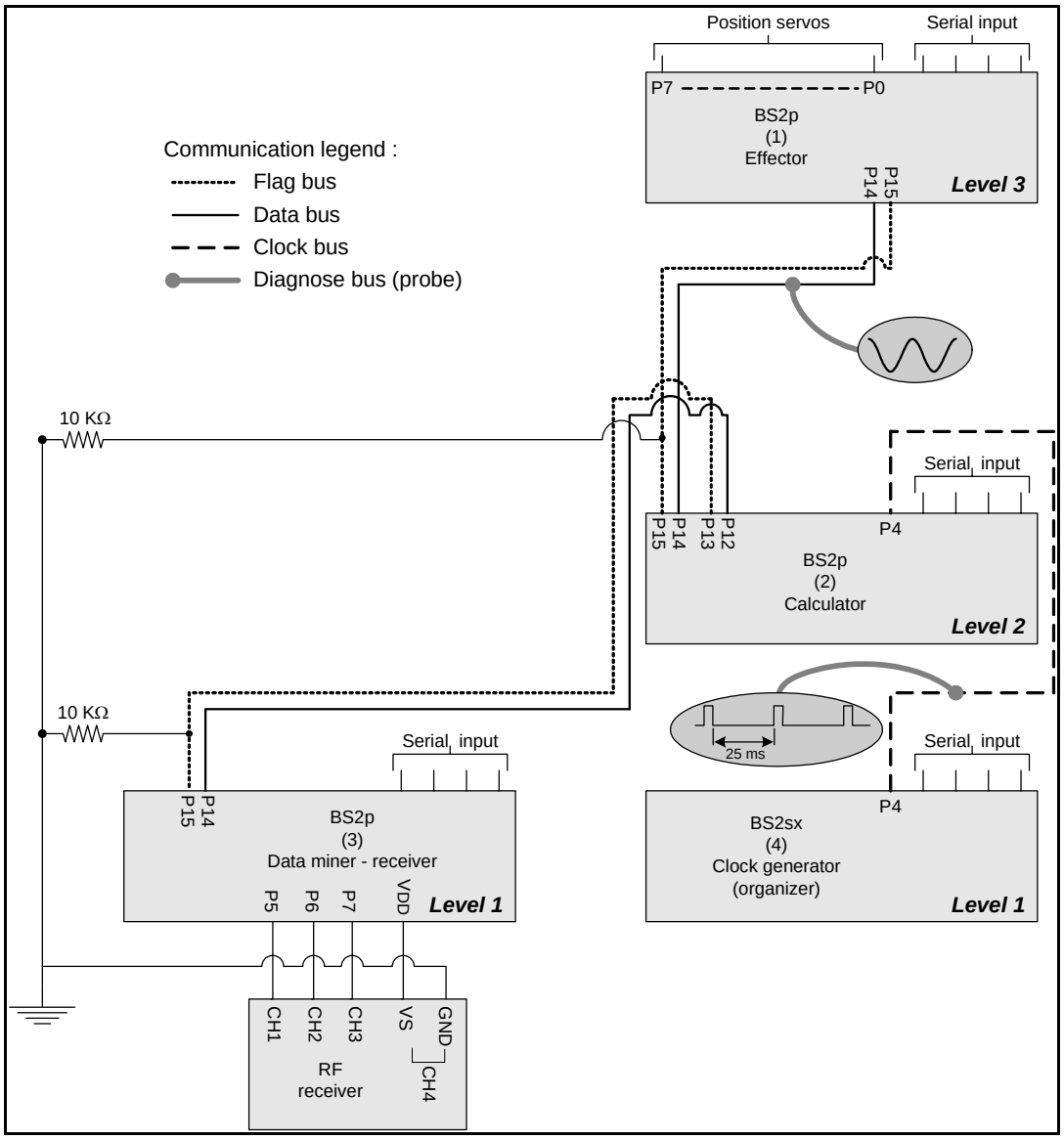

Figure A3. Detail connections of electronics used to control the robot in Figure A2.

A.2.2 Transmitter

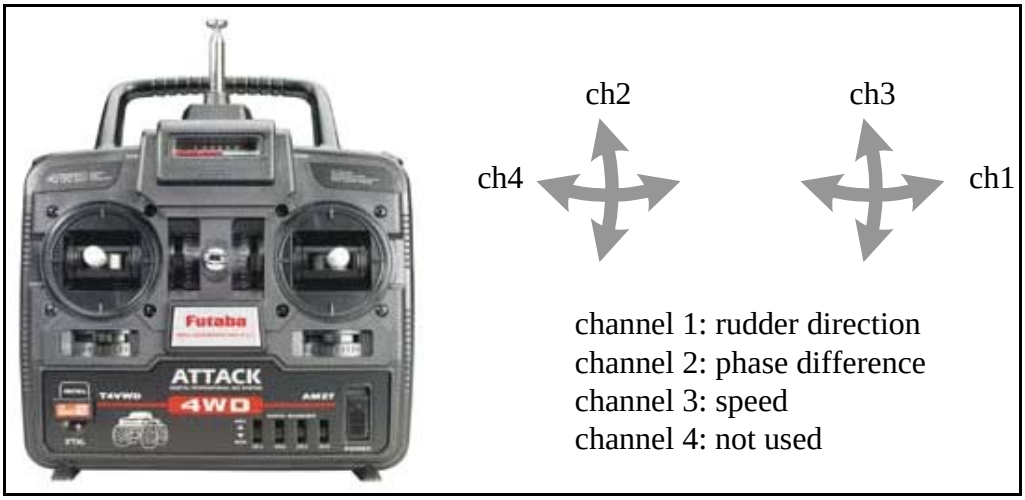

Figure A4. Channel assignment and control handle.

Channel assignment in Figure A4:

- Channel 1 controls rudder direction.
- Channel 2 controls the phase difference (β). It is divided into nine stages from 0 to 9 and β increases from 0° to 90°. 0° is the most upper end of control handle and 90° the most lower end.
- Channel 3 controls the speed of undulation. It is divided into -8/9 Hz, -4/9 Hz, 0, and 4/9 Hz, from the most upper end to the most lower and of the control handle. Negative means backward wave propagation for forward propulsion and vice versa.

A.2.3 Servomotor and Calibration

All the servomotors used as actuators of the present undulating fin are calibrated electronically and mechanically. Take a closer look at the mechanical system of the servomotors and how each is connected to a crank. First of all, the servomotors must be mechanically calibrated, which means the crank attached to each servomotor must at roughly the middle position. This middle position will be called *zero position*, in which all cranks will form a straight line when they are aligned together. Note that the servomotors can only rotate in 180°, they have two mechanical ends (stopper).

The crank must be placed roughly in the middle of the two mechanical ends. This is can seldom be achieved. Second phase of calibration is done electronically to achieve. Mechanical calibration is important to ensure the cranks can oscillate symmetrically with respect to its *zero position*.

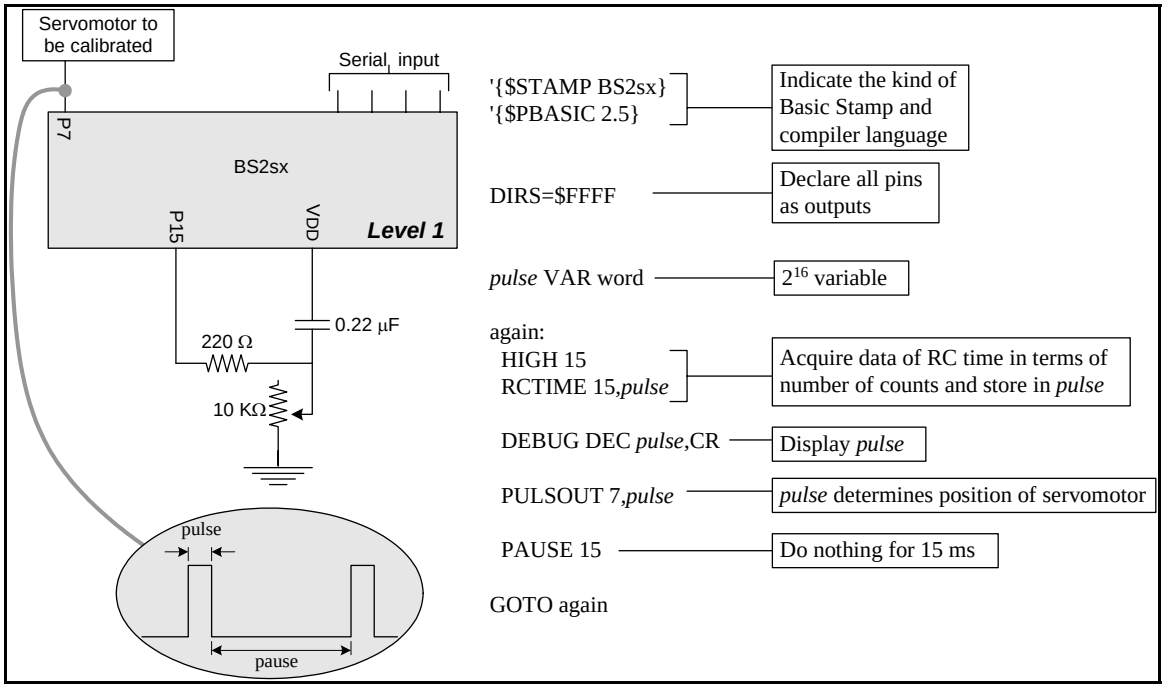

Figure A5. Electronic calibration of servomotors.

Calibration procedure:

- Arrange all servomotors in mechanical structure.
- Do not connect servomotor to Basic Stamp yet.
- Load calibration program to Basic Stamp, and monitor the *pulse*. In order not to damage the servomotor, turn the potentiometer such that the number of counts stored in *pulse* is roughly 1900.
- Connect the servomotor to pin 7, as shown in Figure A5. The crank attached to the servomotor will move accordingly. Turn/adjust the potentiometer such that the all cranks are aligned in a straight line.
- Record the value of *pulse*. Its value will be used in another program.
- Repeat for the next servomotor.

Futaba S3801 is to be drive by PWM (pulse width modulation) signal, while the length of pause remains fixed. Shown in Figure A5 is the expected pulse that can be seen on oscilloscope. The length of the pulse is proportional to the number of counts stored in the variable *pulse* by the following formula:

$$\text{pulse} = 0.8 \times \textit{pulse}\,[\mu\text{s}],$$

where one count is equivalent to 0.8 μs. This only applies to BS2sx. Other Basic Stamps have other specifications. The length of pause in the signal is not the same as PAUSE in the program. Note that processing time must be included. Therefore:

$$\text{pause} = \text{PAUSE} + \text{processing time}\,[\text{ms}].$$

The processing time is seldom calculated. It is normally measured on the oscilloscope. Remember that the servomotors must be driven by a signal having **20 ms – 25 ms** pause. Therefore, adjust the number that follows the PAUSE such that it appears in the oscilloscope the recommended pause length. The unit of PAUSE is in **millisecond**, and PAUSE 15 means do nothing for 15 milliseconds. Detailed programming instructions can be found in the Basic Stamp manual.

A.3 Nickel Metal Hydride Batteries

A battery can be modeled by an ideal voltage source placed in series with a resistor. The resistor is called internal resistance of the battery, and it determines the battery performance in terms of available power when current is drawn from the battery. Figure A6 can be expressed by the following equation:

$$V_{\text{battery}} = V_{\text{ideal}} - IR_{\text{internal}} \qquad \text{(A.1)}$$

$V_{battery}$	Actual battery voltage in use [Volt]
V_{ideal}	Ideal Voltage of the battery with zero internal resistance [Volt]
I	Current drawn from the battery [Amp]
$R_{internal}$	Internal resistance of the battery [Ohm]

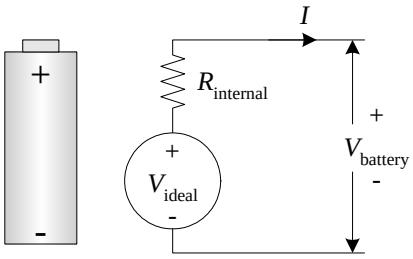

Figure A6. A battery is modeled by an ideal voltage source placed in series with an internal resistor.

Equation (A.1) states that the higher the current drawn from the battery, the lower the actual voltage $V_{battery}$. Therefore, a battery with very low internal resistance is required when high current is to be drawn from the battery. Nickel metal Hydride (NiMH) was a type of battery with very low internal resistance. Note that the internal resistance of the battery is not fixed. It varies with temperature and state of charge. However, internal resistance as low as 260 milliOhms can be expected [NiMH battery, http://www.batteryuniversity.com/partone-22.htm, May 2005.].

Six 1.2-Volt NiMH (Nickel Metal Hydride) batteries in series were used to power eight servomotors, and with a capacity of 3000 mAh (milli-Ampere-hour) the batteries were required to provide constant nominal voltage at 7.2 Volts for the dc motor running at 2 Amps. Note that the battery manufacturer provides an offset voltage such that the six batteries give 7.75 Volts instead of the nominal voltage of 7.2 Volts. The batteries were expected to deliver approximately 2 Amps of current for more or less 90 minutes before they are fully discharged, with an assumption that the battery capacity (C) is linearly related to its discharge time (t) by the current drawn from the battery (I) as expressed by the following equation:

$$C = I\,t \qquad \text{(A.2)}$$

C	Battery capacity [milli-Amp-hour or mAh]
I	Current drawn from the battery [milliAmp]
t	discharge time (hour)

Note that Equation (A.2) is also applicable for charging a battery; I is therefore the charging current and t the charging time.

Appendix B

Control Program

Appendix C

Mechanical Drawings

(All dimensions are in mm and materials are acrylic, unless otherwise specified)

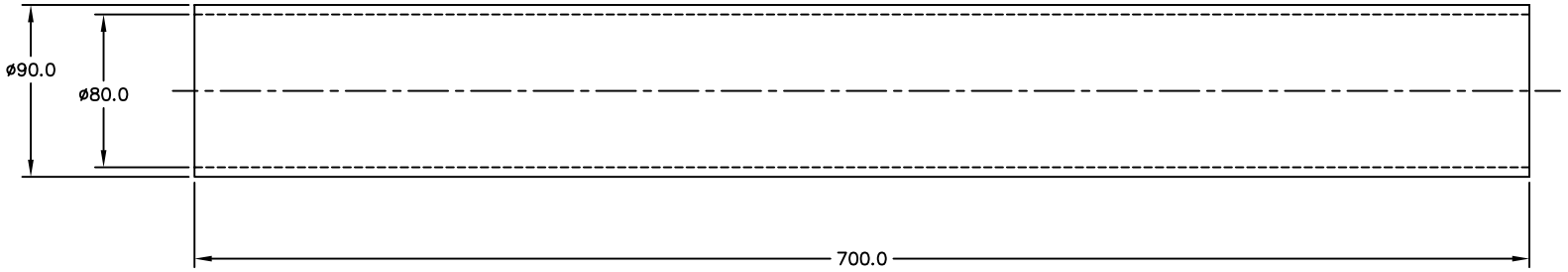

UNLESS OTHERWISE SPECIFIED: ALL DIMENSIONS ARE IN MILLIMETERS. BREAK ALL SHARP EDGES .01 – .03 R OR 45°

	TOLERANCE UNLESS OTHERWISE SPECIFIED	SURFACE TREATMENT	**NAYANG TECHNOLOGICAL UNIVERSITY**
	.X ± .1	AS MACHINED	
	.XX ± .01	MATERIAL	CABLE HOLDER
SHEET 1 OF 1	ANGLES ± 5°	ACRYLIC	

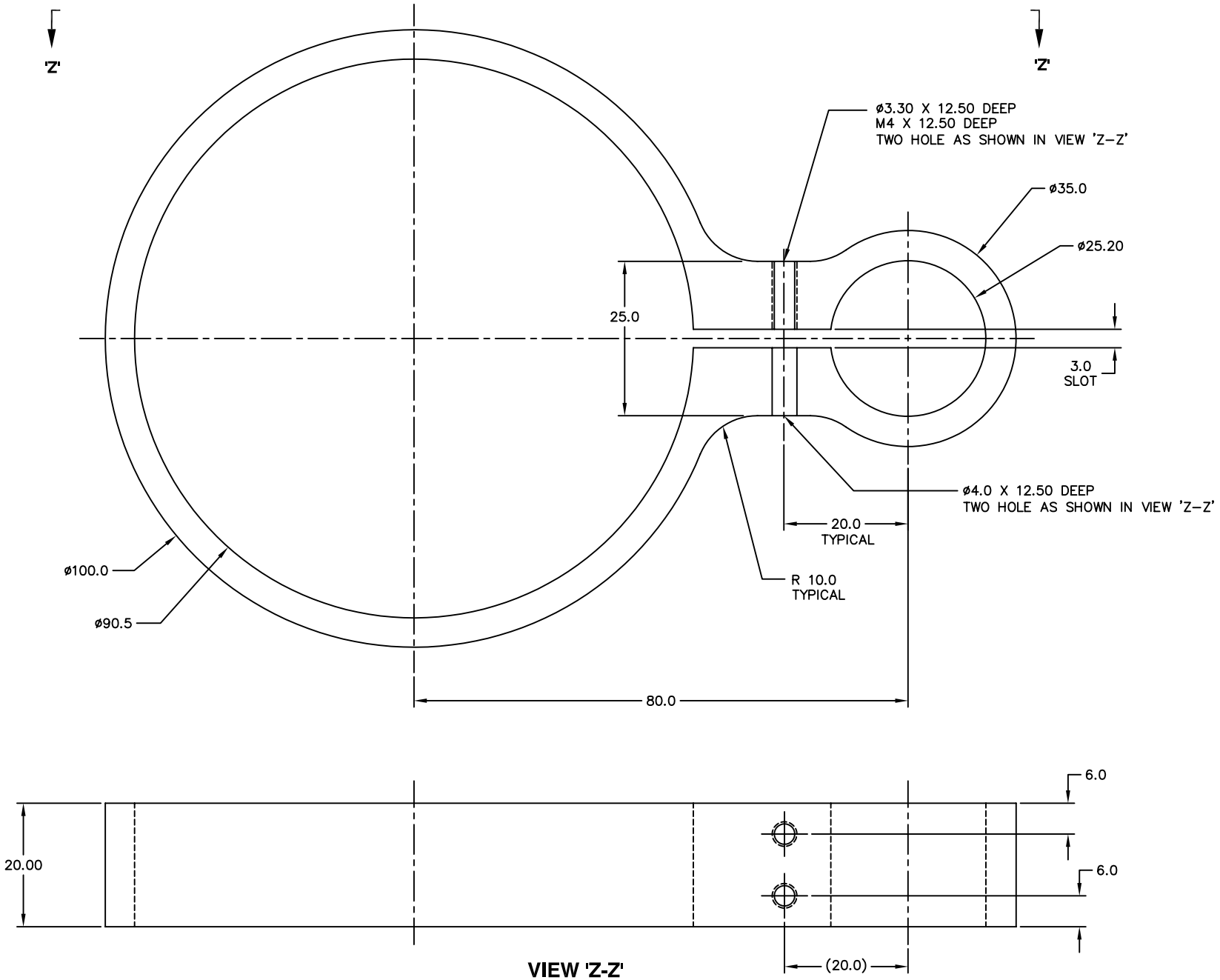

VIEW 'Z-Z'

UNLESS OTHERWISE SPECIFIED: ALL DIMENSIONS ARE IN MILLIMETERS. BREAK ALL SHARP EDGES .01 – .03 R OR 45°

TOLERANCE UNLESS OTHERWISE SPECIFIED .X ± .1 .XX ± .01 ANGLES ± 5°	SURFACE TREATMENT AS MACHINED MATERIAL ACRYLIC	NAYANG TECHNOLOGICAL UNIVERSITY CONNECTOR OF SPINE TO BUOYANT TANK

SHEET 1 OF 1

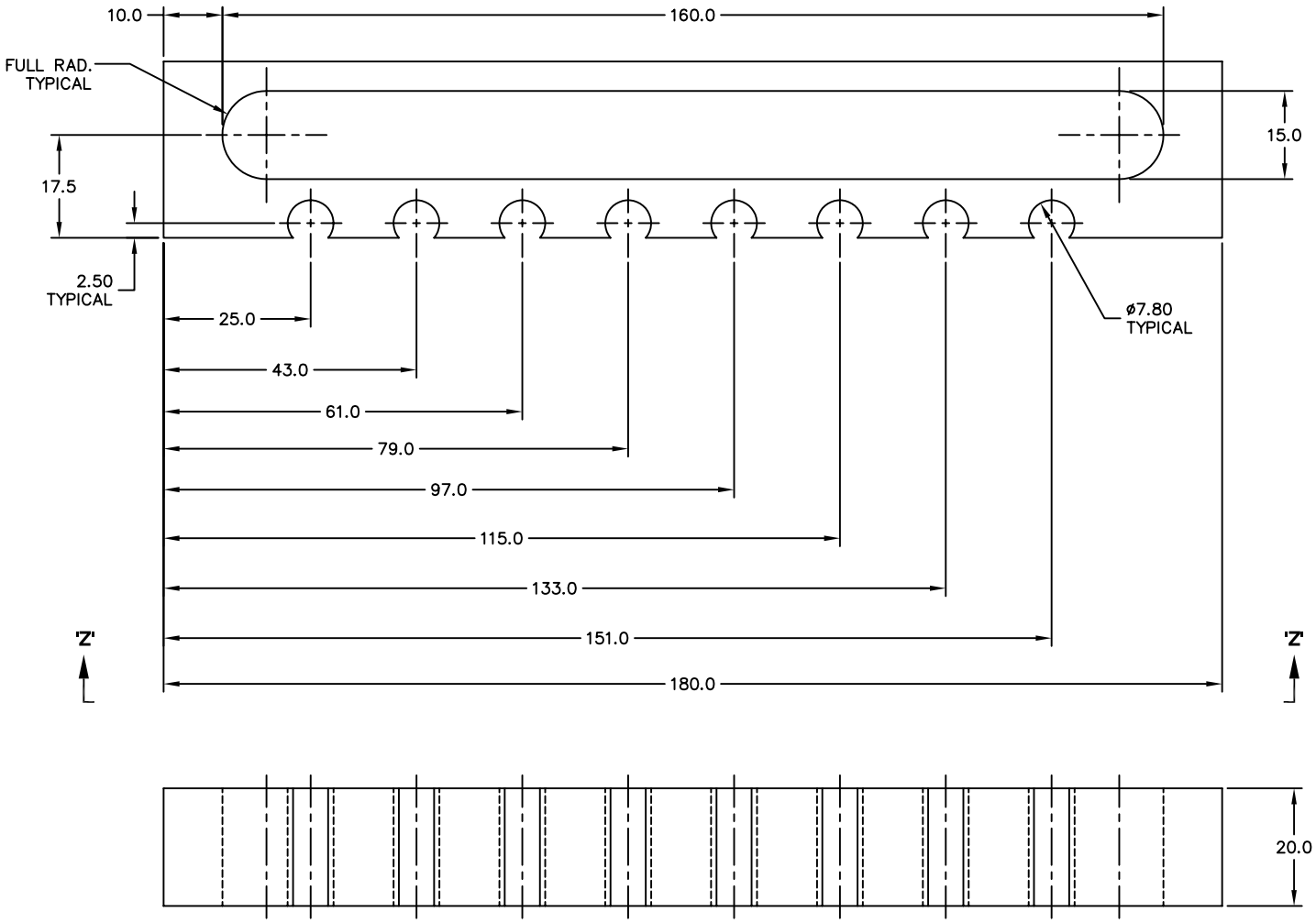

VIEW 'Z-Z'

UNLESS OTHERWISE SPECIFIED: ALL DIMENSIONS ARE IN MILLIMETERS. BREAK ALL SHARP EDGES .01 – .03 R OR 45°

	TOLERANCE UNLESS OTHERWISE SPECIFIED	SURFACE TREATMENT	NAYANG TECHNOLOGICAL UNIVERSITY
	.X ± .1	AS MACHINED	
	.XX ± .01	MATERIAL	CASING COVER
SHEET 1 OF 1	ANGLES ± 5°	ACRYLIC	

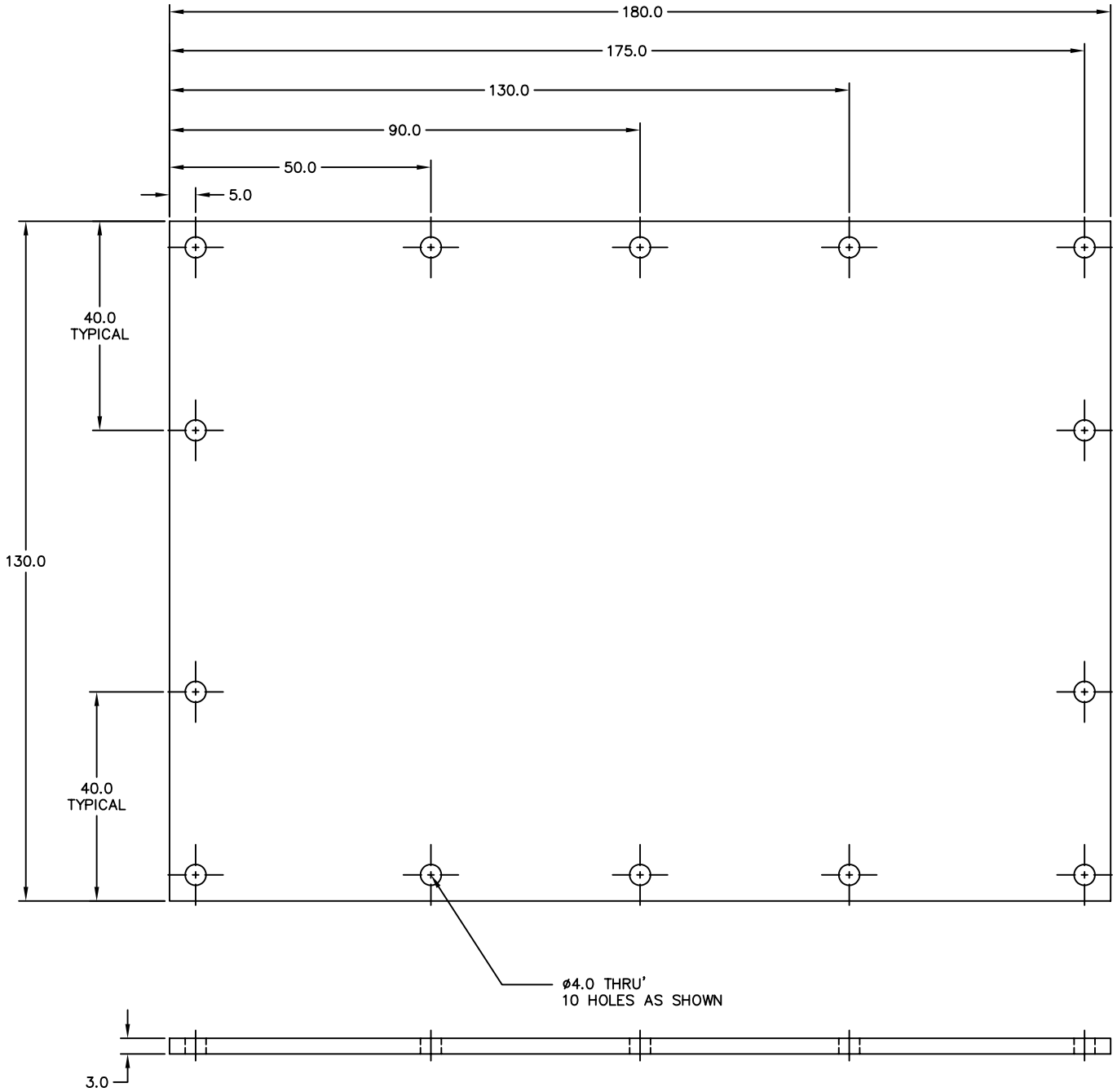

UNLESS OTHERWISE SPECIFIED: ALL DIMENSIONS ARE IN MILLIMETERS. BREAK ALL SHARP EDGES .01 – .03 R OR 45°

TOLERANCE UNLESS OTHERWISE SPECIFIED .X ± .1 .XX ± .01 ANGLES ± 5°	SURFACE TREATMENT AS MACHINED MATERIAL ACRYLIC	NAYANG TECHNOLOGICAL UNIVERSITY CASING COVER

SHEET 1 OF 1

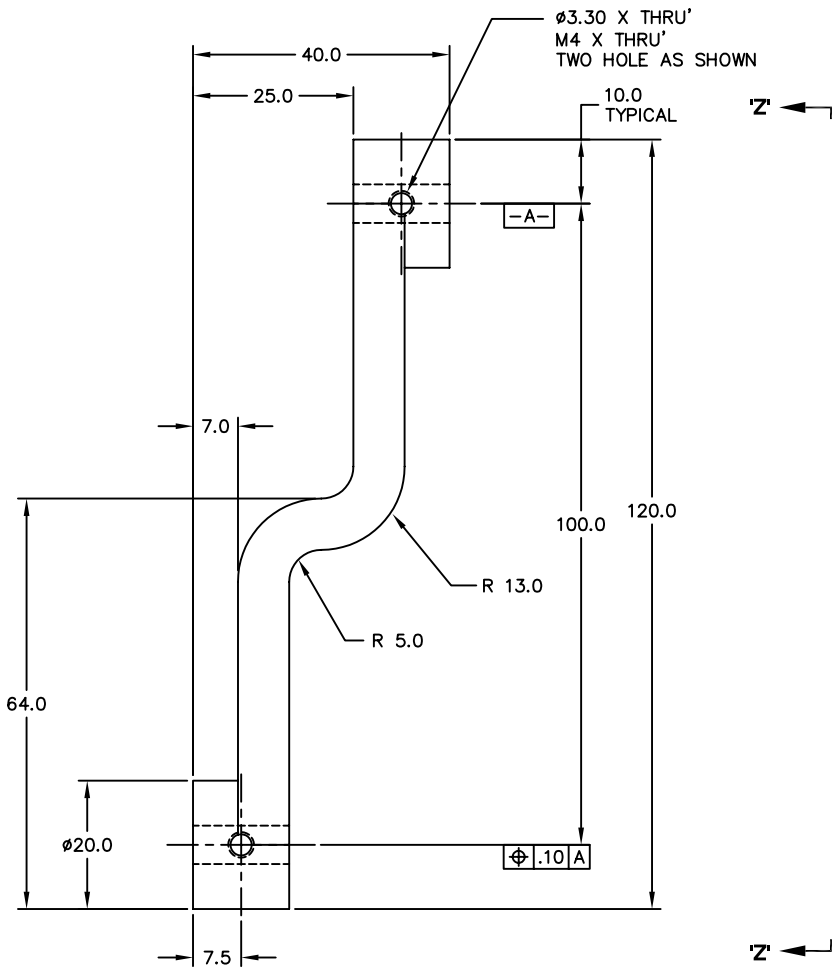

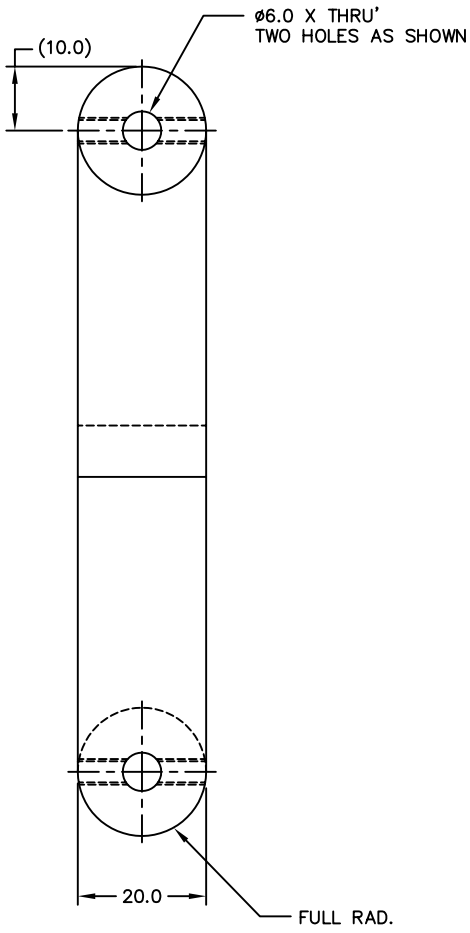

VIEW 'Z-Z'

UNLESS OTHERWISE SPECIFIED: ALL DIMENSIONS ARE IN MILLIMETERS. BREAK ALL SHARP EDGES .01 – .03 R OR 45°

	TOLERANCE UNLESS OTHERWISE SPECIFIED .X ± .1 .XX ± .01 ANGLES ± 5°	SURFACE TREATMENT AS MACHINED MATERIAL ACRYLIC	**NAYANG TECHNOLOGICAL UNIVERSITY** CRANK
SHEET 1 OF 1			

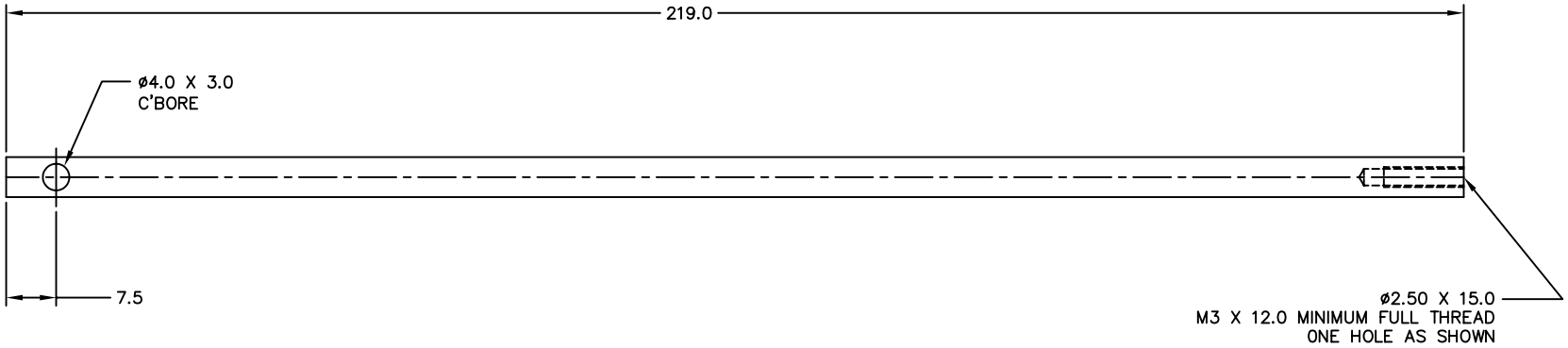

UNLESS OTHERWISE SPECIFIED: ALL DIMENSIONS APE IN MILLIMETERS. BREAK ALL SHARP EDGES .01 – .03 R OR 45°

TOLERANCE UNLESS OTHERWISE SPECIFIED	SURFACE TREATMENT	NAYANG TECHNOLOGICAL UNIVERSITY
.X ± .1	ANODIZED	
.XX ± .01	MATERIAL	FIN RAY
ANGLES ± 1°	ALIMINUM	

SHEET 1 OF 1

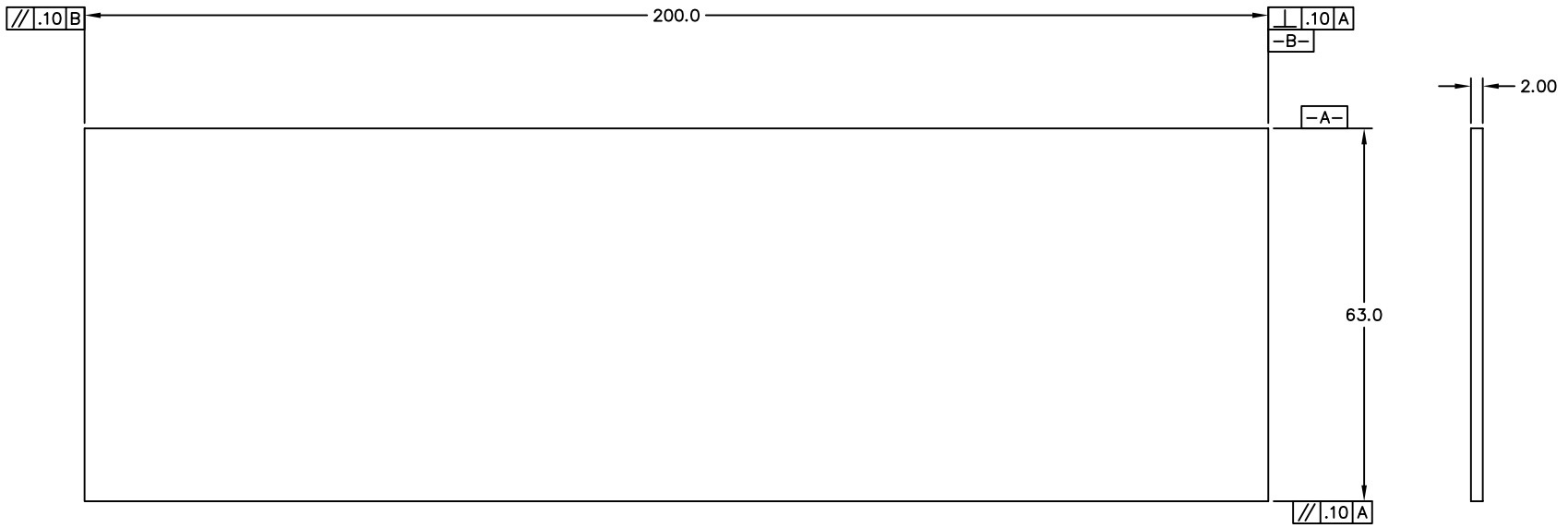

UNLESS OTHERWISE SPECIFIED: ALL DIMENSIONS ARE IN MILLIMETERS. BREAK ALL SHARP EDGES .01 – .03 R OR 45°

TOLERANCE UNLESS OTHERWISE SPECIFIED	SURFACE TREATMENT	NAYANG TECHNOLOGICAL UNIVERSITY
.X ± .1	AS MACHINED	
.XX ± .01	MATERIAL	FIN
ANGLES ± 5°	ACRYLIC	

SHEET 1 OF 1

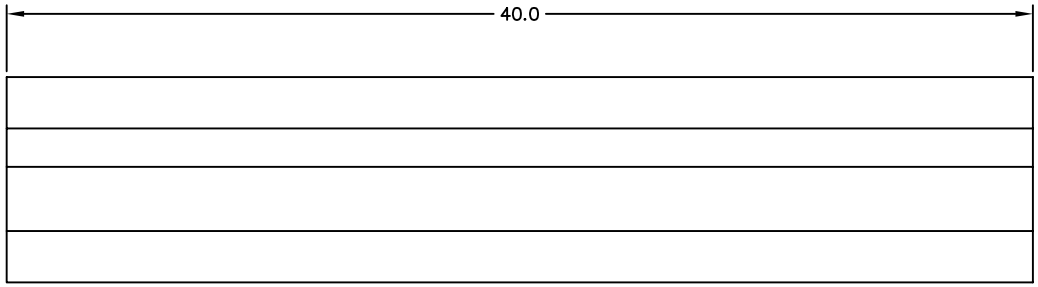

VIEW 'Z-Z'

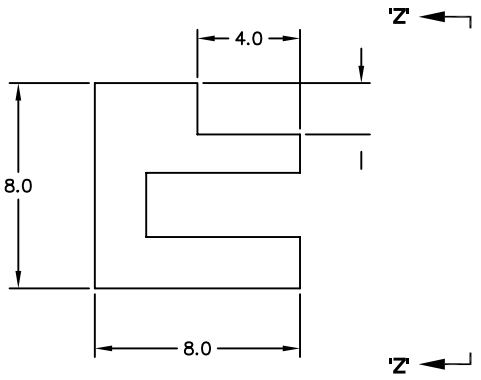

UNLESS OTHERWISE SPECIFIED: ALL DIMENSIONS ARE IN MILLIMETERS. BREAK ALL SHARP EDGES .01 – .03 R OR 45°

	TOLERANCE UNLESS OTHERWISE SPECIFIED	SURFACE TREATMENT	NAYANG TECHNOLOGICAL UNIVERSITY
	.X ± .1	AS MACHINED	
	.XX ± .01	MATERIAL	FIN GUIDE
SHEET 1 OF 1	ANGLES ± 5°	ACRYLIC	

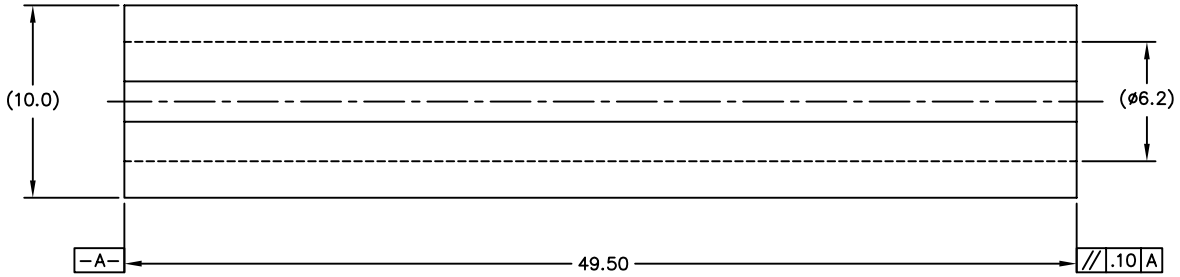

VIEW 'Z-Z'

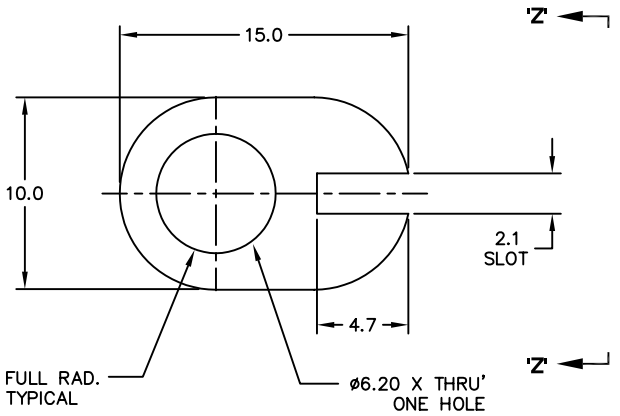

UNLESS OTHERWISE SPECIFIED: ALL DIMENSIONS ARE IN MILLIMETERS. BREAK ALL SHARP EDGES .01 – .03 R OR 45°

TOLERANCE UNLESS OTHERWISE SPECIFIED	SURFACE TREATMENT	**NAYANG TECHNOLOGICAL UNIVERSITY**	
.X ± .1	AS MACHINED		
.XX ± .01	MATERIAL	FIN HOLDER	
SHEET 1 OF 1	ANGLES ± 5°	ACRYLIC	

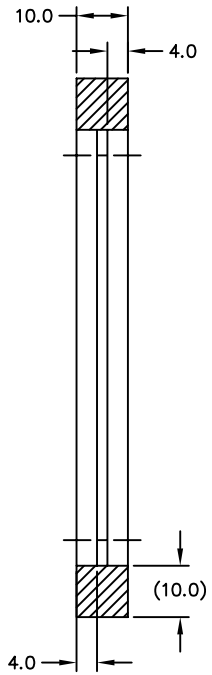

SECTION 'Z-Z'

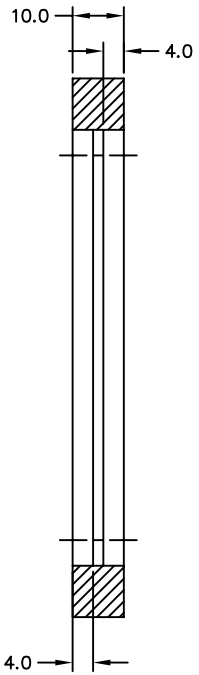

SECTION 'Y-Y'

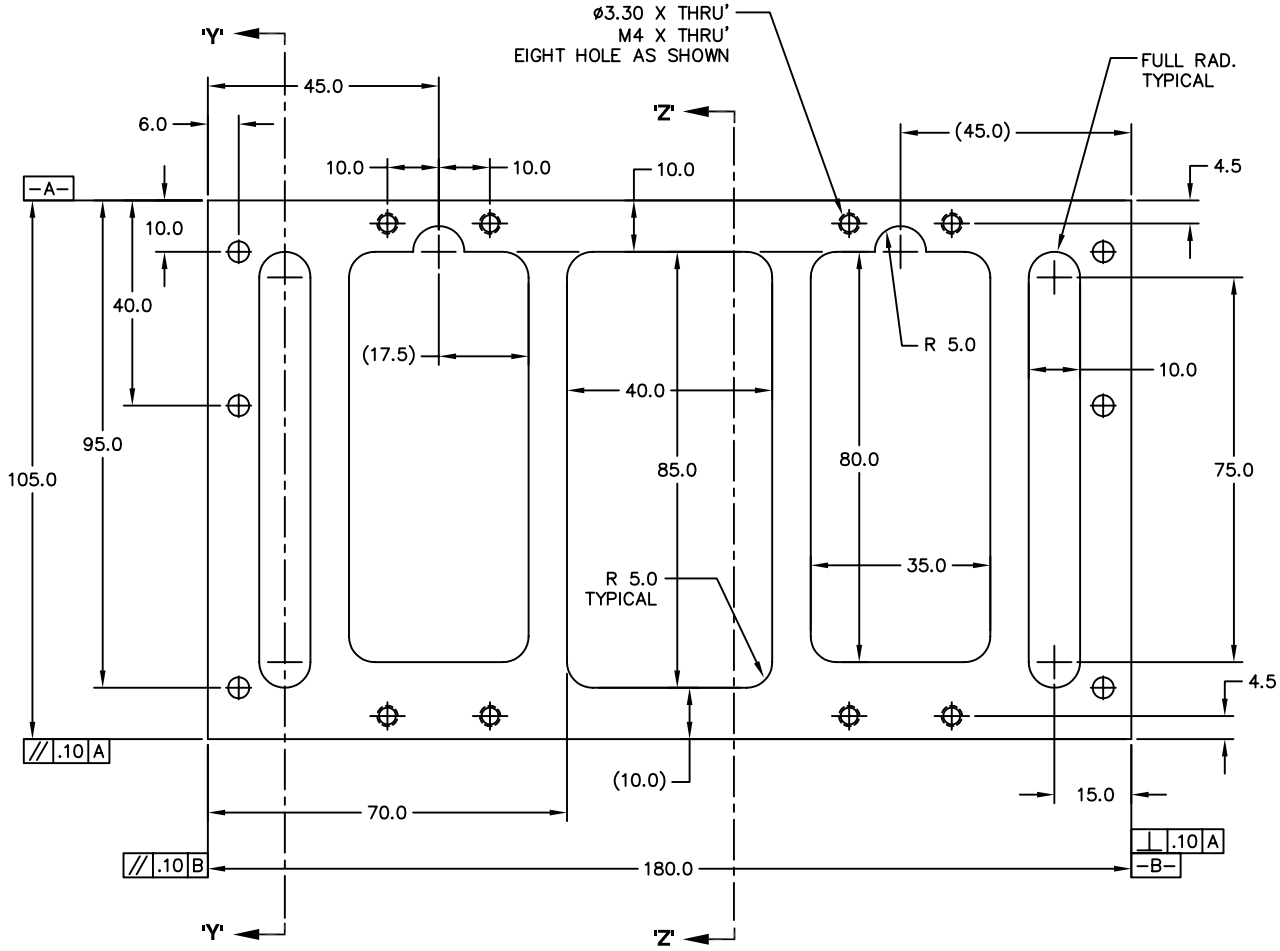

UNLESS OTHERWISE SPECIFIED: ALL DIMENSIONS ARE IN MILLIMETERS. BREAK ALL SHARP EDGES .01 – .03 R OR 45°

TOLERANCE UNLESS OTHERWISE SPECIFIED .X ± .1 .XX ± .01 ANGLES ± 5°	SURFACE TREATMENT AS MACHINED MATERIAL ACRYLIC	NAYANG TECHNOLOGICAL UNIVERSITY GASKET

SHEET 1 OF 1

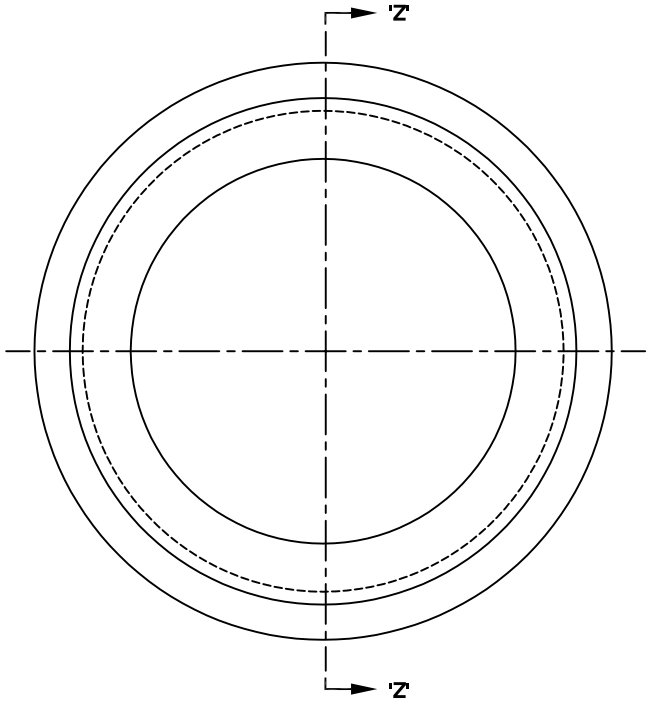

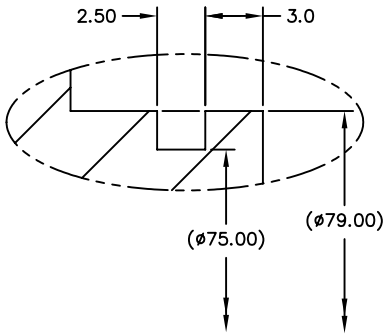

DETAIL 'A'
SCALE 3X
O–RING GROOVE

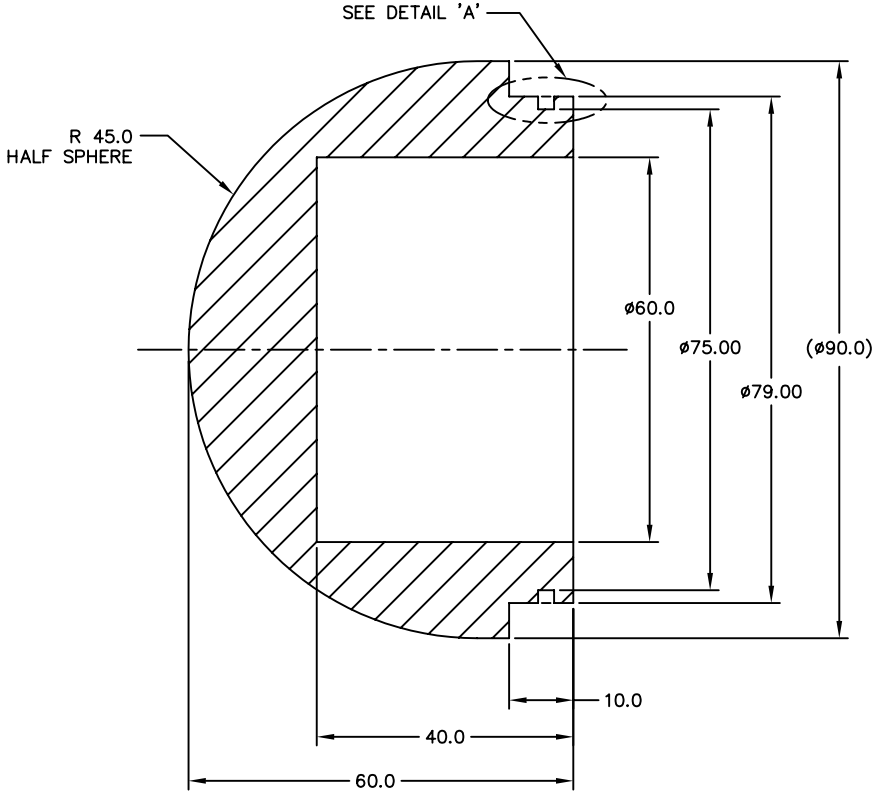

SECTION 'Z-Z'

NOTES:

1. SEALING SURFACE, NO INDENTATION OR DEFECTS ON THESE SURFACES
2. PROTECT THIS CIRCUMFENTIAL AREA WITH HEAVY TAPE AFTER MACHINING.
3. RECOMMENDED O–RING SIZE: ø2.50 MM, 70MM < ID < 75MM.
4. SPLICED O–RING NOT ALLOWED.

UNLESS OTHERWISE SPECIFIED: ALL DIMENSIONS ARE IN MILLIMETERS. BREAK ALL SHARP EDGES .01 – .03 R OR 45°

	TOLERANCE UNLESS OTHERWISE SPECIFIED	SURFACE TREATMENT	NAYANG TECHNOLOGICAL UNIVERSITY
	.X ± .1	AS MACHINED	
	.XX ± .01	MATERIAL	BUOYANT TUBE COVER
SHEET 1 OF 1	ANGLES ± 5°	ACRYLIC	

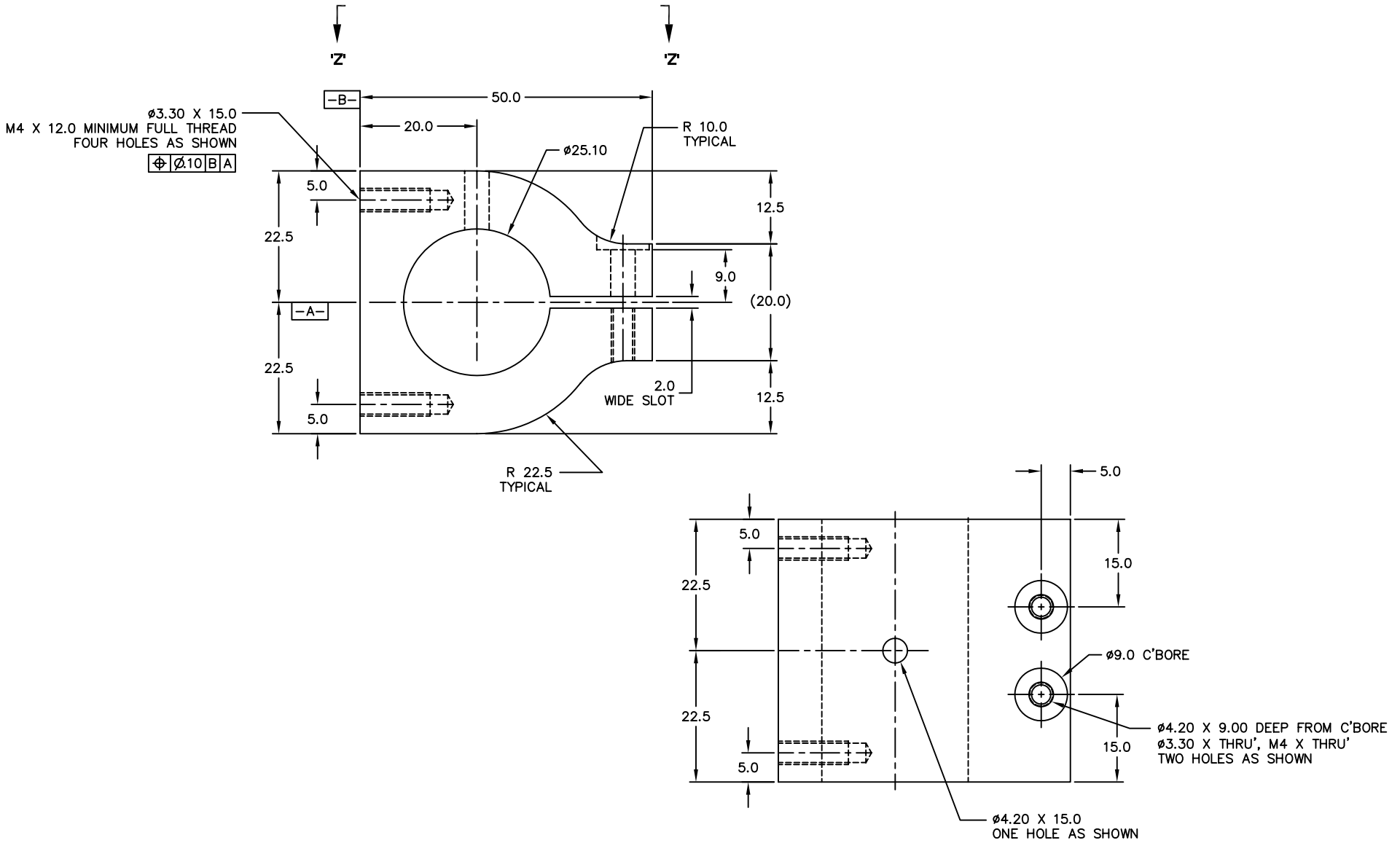

VIEW 'Z-Z'

UNLESS OTHERWISE SPECIFIED: ALL DIMENSIONS ARE IN MILLIMETERS. BREAK ALL SHARP EDGES .01 – .03 R OR 45°

TOLERANCE UNLESS OTHERWISE SPECIFIED .X ± .1 .XX ± .01 ANGLES ± 5°	SURFACE TREATMENT AS MACHINED MATERIAL ACRYLIC	**NAYANG TECHNOLOGICAL UNIVERSITY** SPINE CLAMP F/ SPINE CONNECTOR

SHEET 1 OF 1

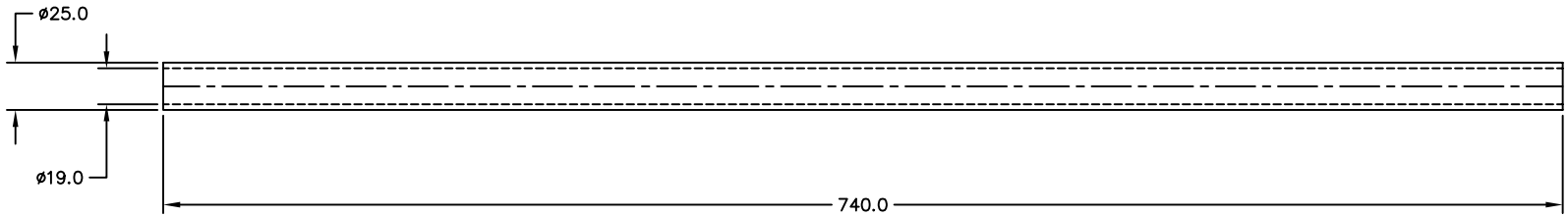

UNLESS OTHERWISE SPECIFIED: ALL DIMENSIONS ARE IN MILLIMETERS. BREAK ALL SHARP EDGES .01 – .03 R OR 45°

	TOLERANCE UNLESS OTHERWISE SPECIFIED	SURFACE TREATMENT	**NAYANG TECHNOLOGICAL UNIVERSITY**
	.X ± .1	ANODIZED	
	.XX ± .01	MATERIAL	SPINE
SHEET 1 OF 1	ANGLES ± 1°	ALIMINUM	

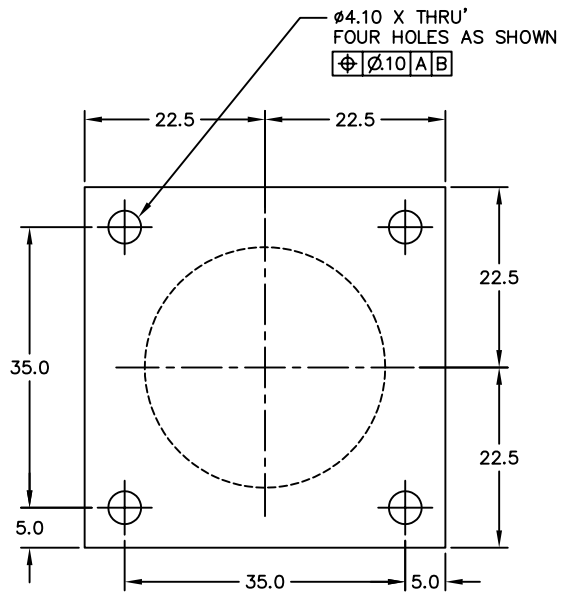

VIEW 'Z-Z'

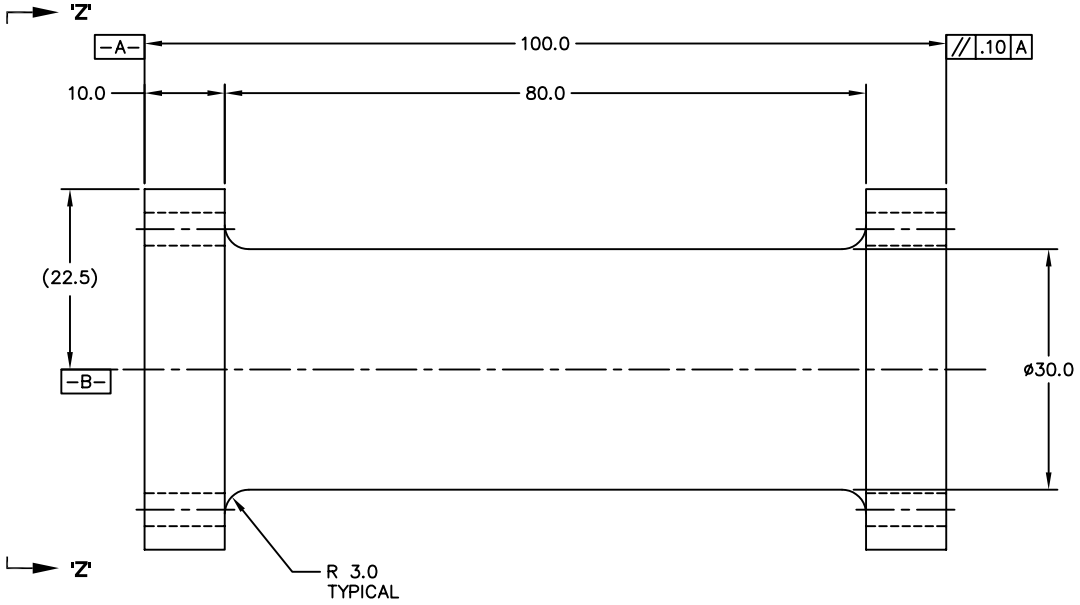

UNLESS OTHERWISE SPECIFIED: ALL DIMENSIONS ARE IN MILLIMETERS. BREAK ALL SHARP EDGES .01 – .03 R OR 45°

	TOLERANCE UNLESS OTHERWISE SPECIFIED	SURFACE TREATMENT	NAYANG TECHNOLOGICAL UNIVERSITY
	.X ± .1	AS MACHINED	
	.XX ± .01	MATERIAL	SPINE CONNECTOR
SHEET 1 OF 1	ANGLES ± 5°	ACRYLIC	

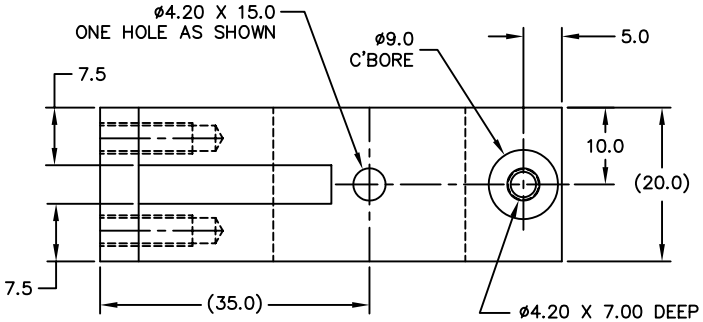

VIEW 'Y-Y'

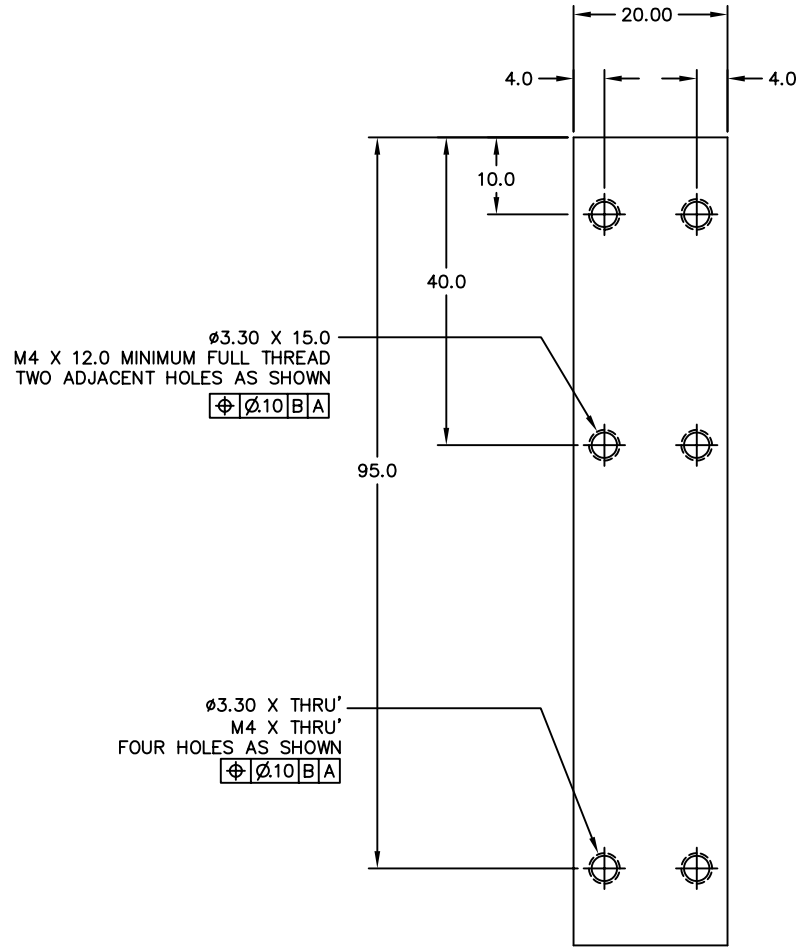

VIEW 'Z-Z'

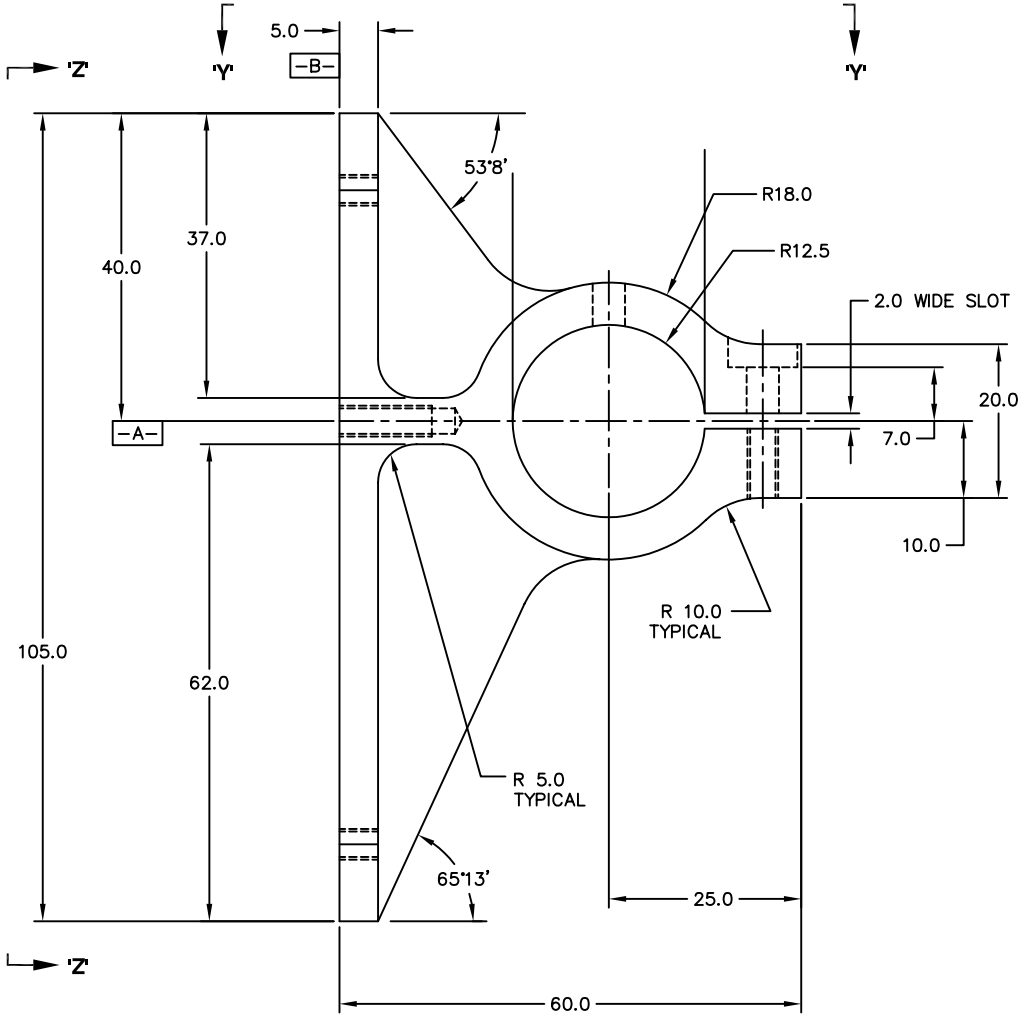

UNLESS OTHERWISE SPECIFIED: ALL DIMENSIONS ARE IN MILLIMETERS. BREAK ALL SHARP EDGES .01 – .03 R OR 45°

TOLERANCE UNLESS OTHERWISE SPECIFIED	SURFACE TREATMENT	NAYANG TECHNOLOGICAL UNIVERSITY	
.X ± .1	AS MACHINED		
.XX ± .01	MATERIAL	GUSSET–TO–SPINE CLAMP	
SHEET 1 OF 1	ANGLES ± 1°	ACRYLIC	

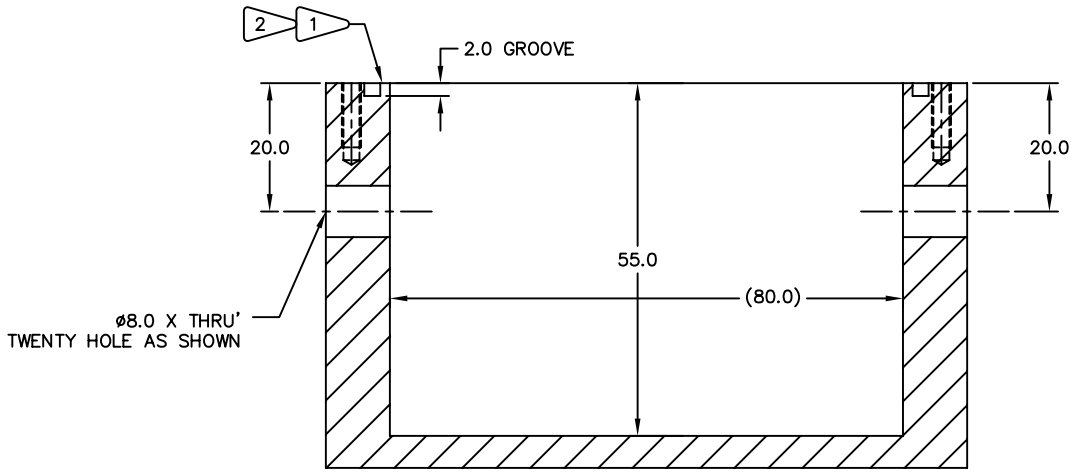

SECTION 'Z-Z'

NOTES:

1. SEALING SURFACE, NO INDENTATION OR DEFECTS ON THESE SURFACES
2. PROTECT THIS CIRCUMFENTIAL AREA WITH HEAVY TAPE AFTER MACHINING.
3. RECOMMENDED O-RING SIZE: ø2.50 MM, 470MM < ID < 480MM.
4. SPLICED O-RING MUST BE WATERPROOF TESTED WITHOUT COMPONETS INSIDE.
5. TO BE ASSEMBLED WITH PCB CASING COVER.

UNLESS OTHERWISE SPECIFIED: ALL DIMENSIONS ARE IN MILLIMETERS. BREAK ALL SHARP EDGES .01 – .03 R OR 45°

	TOLERANCE UNLESS OTHERWISE SPECIFIED	SURFACE TREATMENT	**NAYANG TECHNOLOGICAL UNIVERSITY**
	.X ± .1	AS MACHINED	
	.XX ± .01	MATERIAL	PCB CASING
SHEET 2 OF 2	ANGLES ± 1°	ACRYLIC	

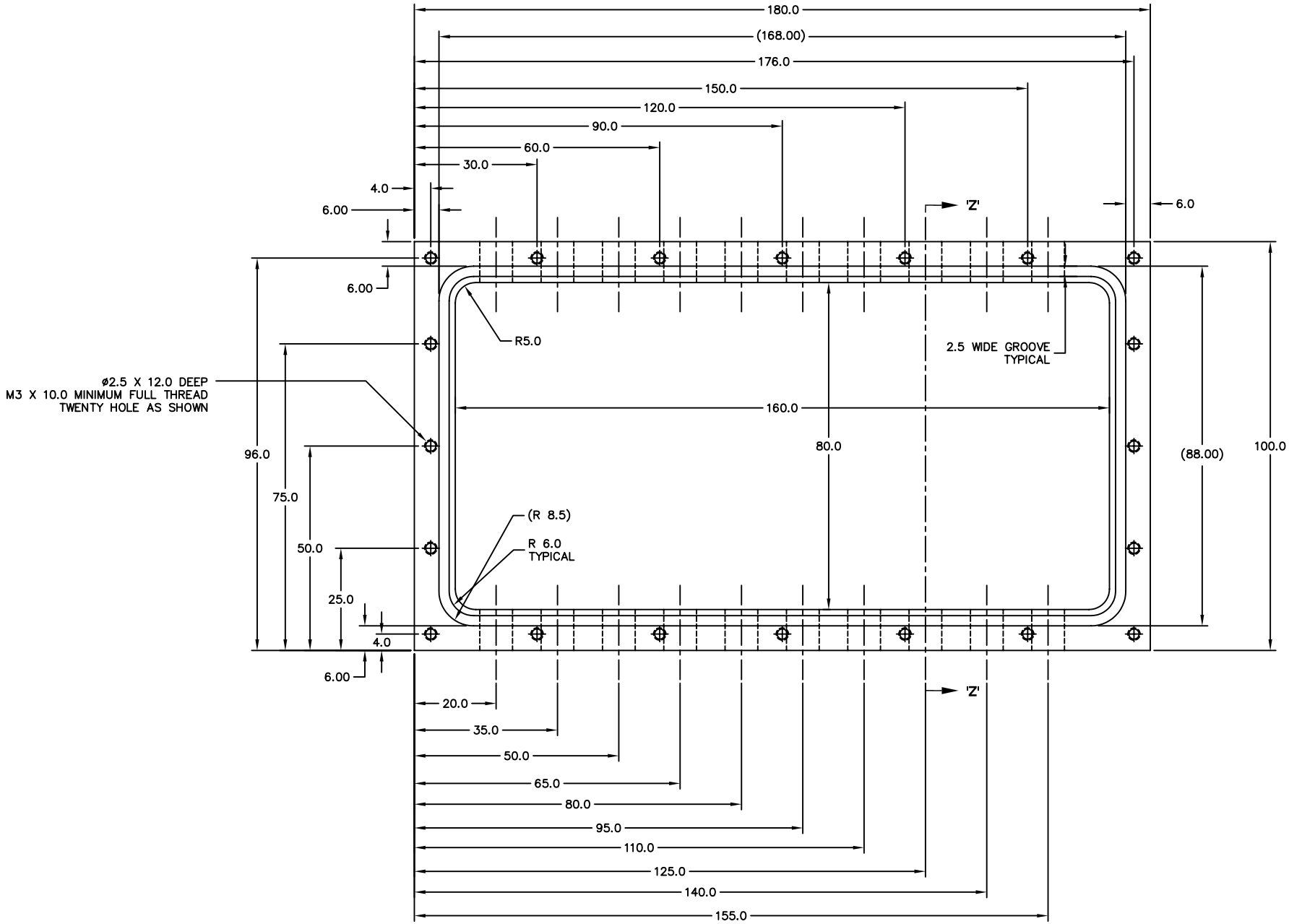

UNLESS OTHERWISE SPECIFIED: ALL DIMENSIONS ARE IN MILLIMETERS. BREAK ALL SHARP EDGES .01 – .03 R OR 45°

TOLERANCE UNLESS OTHERWISE SPECIFIED	SURFACE TREATMENT	NAYANG TECHNOLOGICAL UNIVERSITY
.X ± .1	AS MACHINED	
.XX ± .01	MATERIAL	PCB CASING
SHEET 1 OF 2 — ANGLES ± 1°	ACRYLIC	

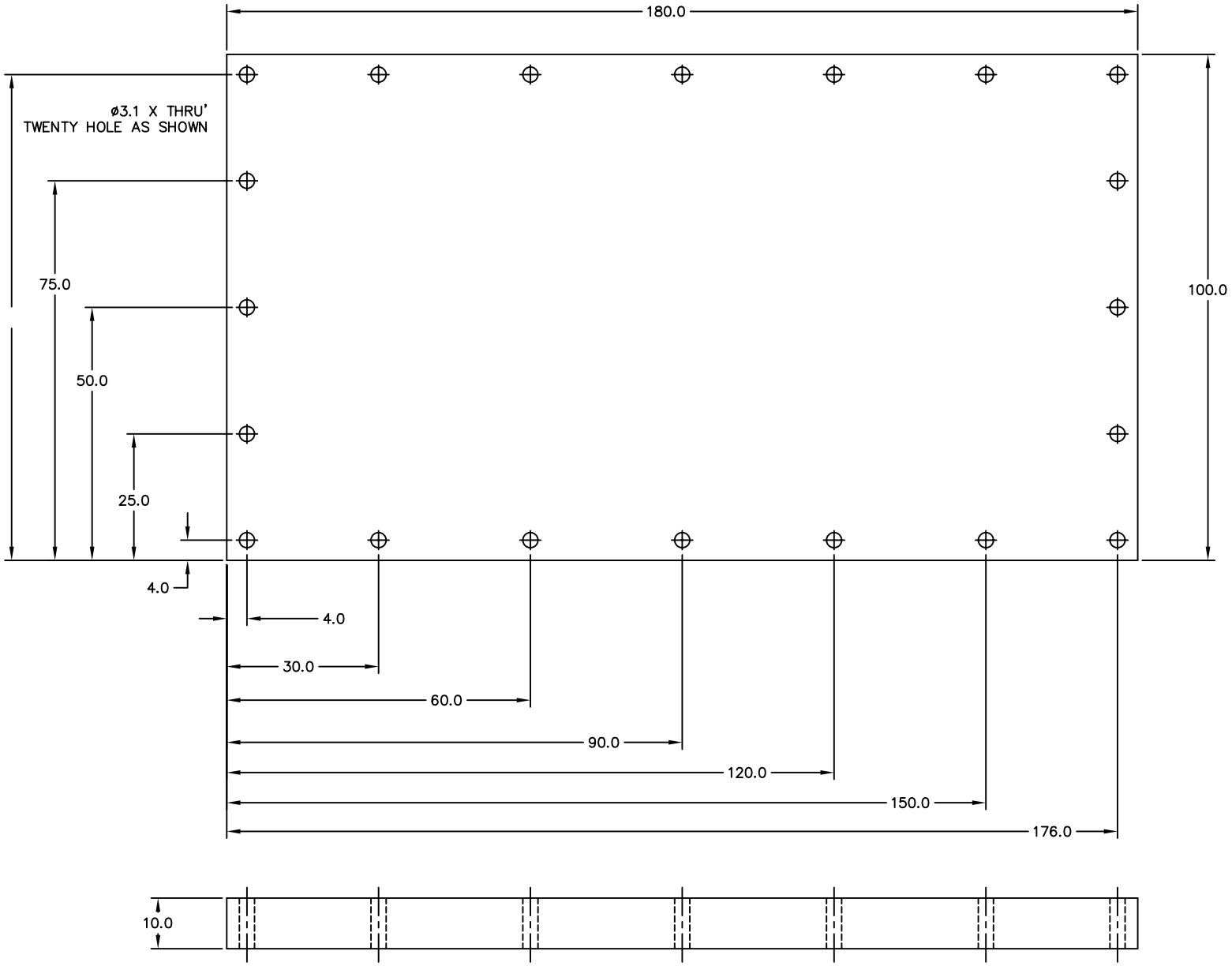

UNLESS OTHERWISE SPECIFIED: ALL DIMENSIONS ARE IN MILLIMETERS. BREAK ALL SHARP EDGES .01 – .03 R OR 45°

TOLERANCE UNLESS OTHERWISE SPECIFIED	SURFACE TREATMENT	**NAYANG TECHNOLOGICAL UNIVERSITY**
.X ± .1	AS MACHINED	
.XX ± .01	MATERIAL	PCB CASING COVER
SHEET 1 OF 1 — ANGLES ± 1°	ACRYLIC	

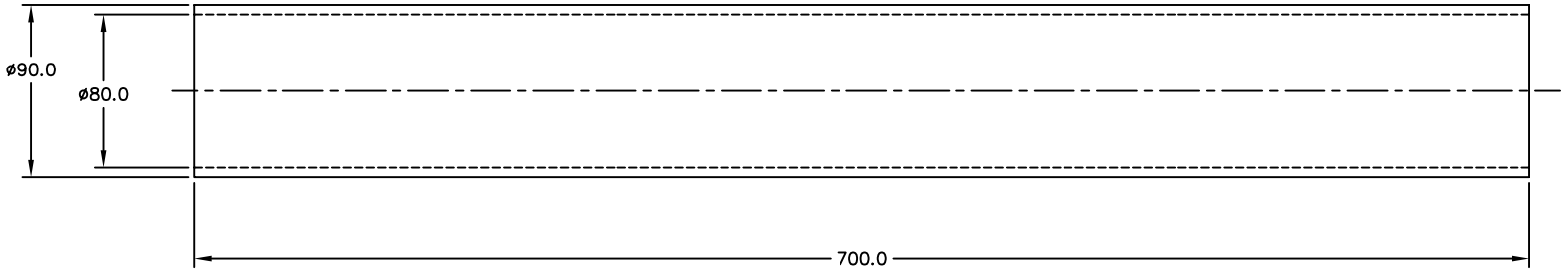

UNLESS OTHERWISE SPECIFIED: ALL DIMENSIONS ARE IN MILLIMETERS. BREAK ALL SHARP EDGES .01 – .03 R OR 45°

	TOLERANCE UNLESS OTHERWISE SPECIFIED	SURFACE TREATMENT	**NAYANG TECHNOLOGICAL UNIVERSITY**
	.X ± .1	AS MACHINED	
	.XX ± .01	MATERIAL	CABLE HOLDER
SHEET 1 OF 1	ANGLES ± 5°	ACRYLIC	

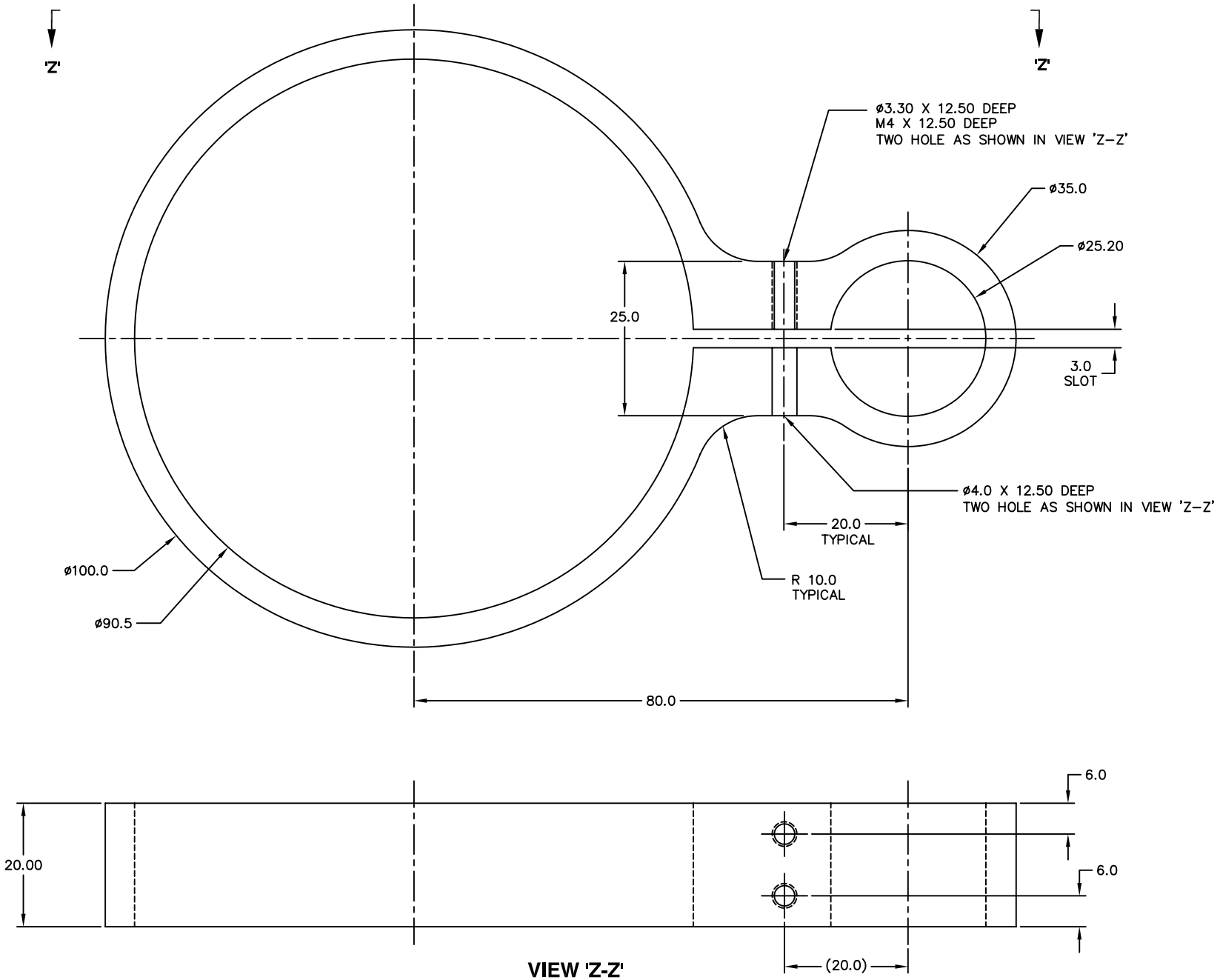

VIEW 'Z-Z'

UNLESS OTHERWISE SPECIFIED: ALL DIMENSIONS ARE IN MILLIMETERS. BREAK ALL SHARP EDGES .01 – .03 R OR 45°

TOLERANCE UNLESS OTHERWISE SPECIFIED .X ± .1 .XX ± .01 ANGLES ± 5°	SURFACE TREATMENT AS MACHINED MATERIAL ACRYLIC	NAYANG TECHNOLOGICAL UNIVERSITY CONNECTOR OF SPINE TO BUOYANT TANK

SHEET 1 OF 1

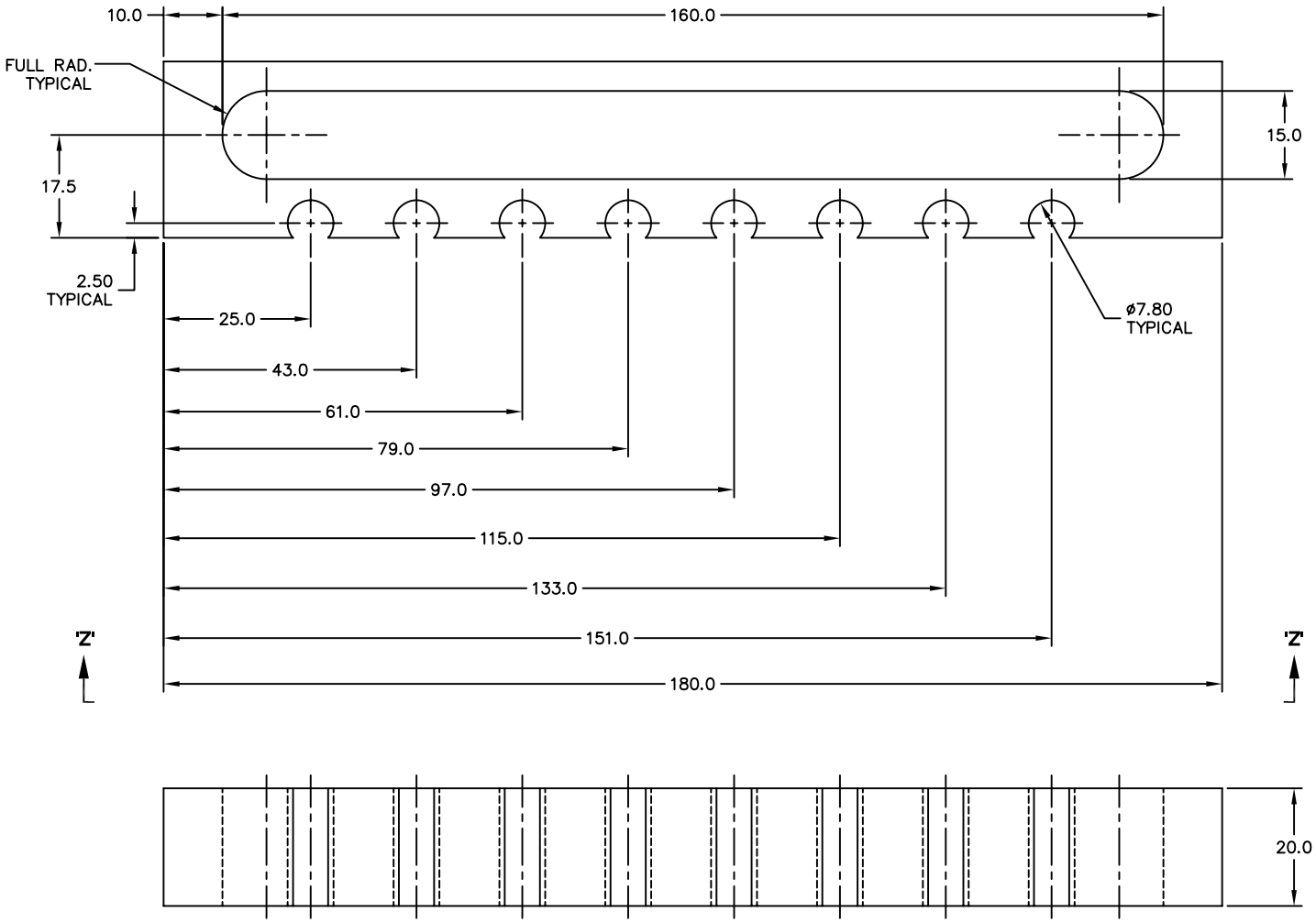

VIEW 'Z-Z'

UNLESS OTHERWISE SPECIFIED: ALL DIMENSIONS ARE IN MILLIMETERS. BREAK ALL SHARP EDGES .01 – .03 R OR 45°

	TOLERANCE UNLESS OTHERWISE SPECIFIED	SURFACE TREATMENT	NAYANG TECHNOLOGICAL UNIVERSITY
	.X ± .1	AS MACHINED	
	.XX ± .01	MATERIAL	CASING COVER
SHEET 1 OF 1	ANGLES ± 5°	ACRYLIC	

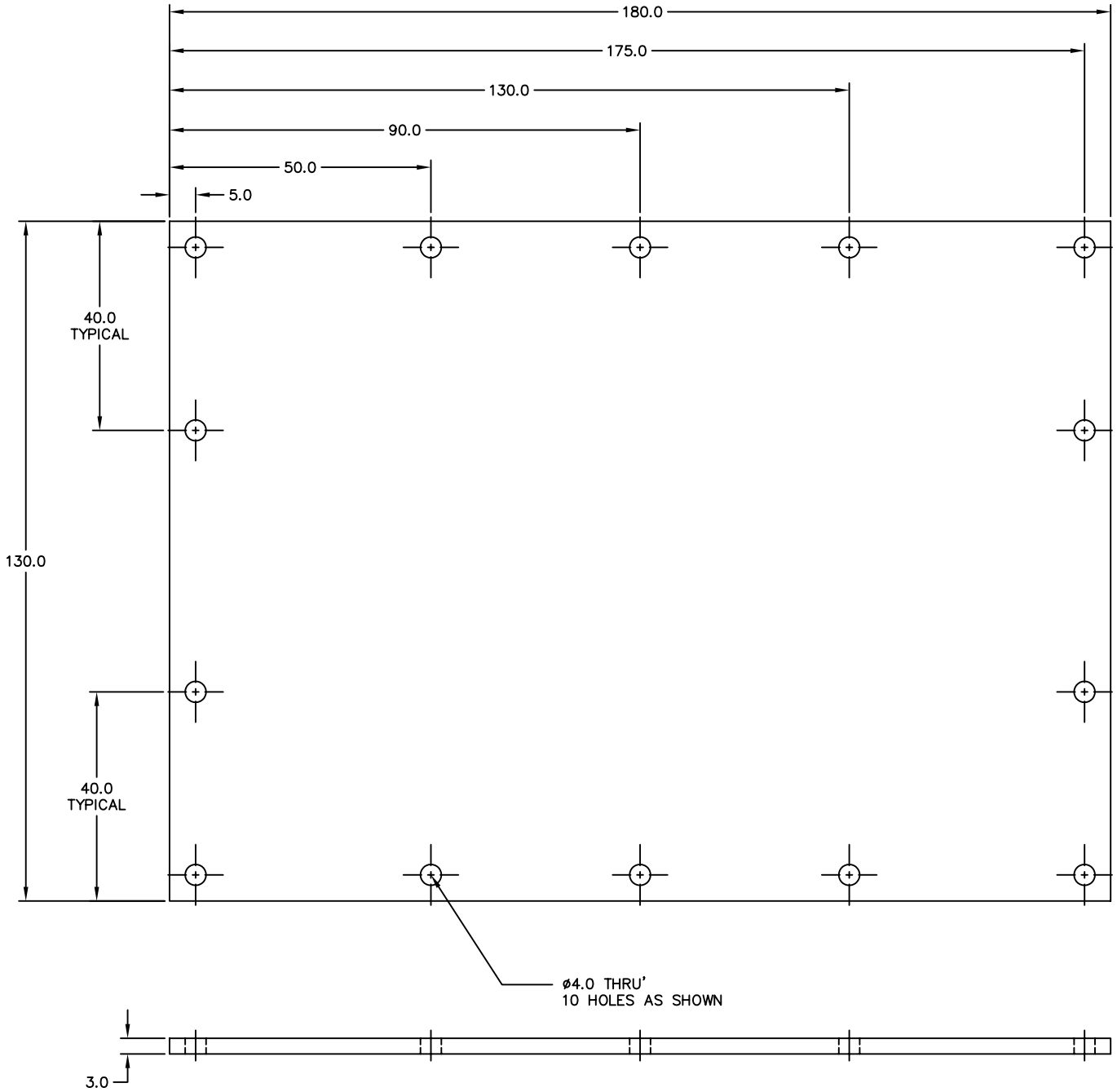

UNLESS OTHERWISE SPECIFIED: ALL DIMENSIONS ARE IN MILLIMETERS. BREAK ALL SHARP EDGES .01 – .03 R OR 45°

TOLERANCE UNLESS OTHERWISE SPECIFIED .X ± .1 .XX ± .01 ANGLES ± 5°	SURFACE TREATMENT AS MACHINED MATERIAL ACRYLIC	NAYANG TECHNOLOGICAL UNIVERSITY CASING COVER

SHEET 1 OF 1

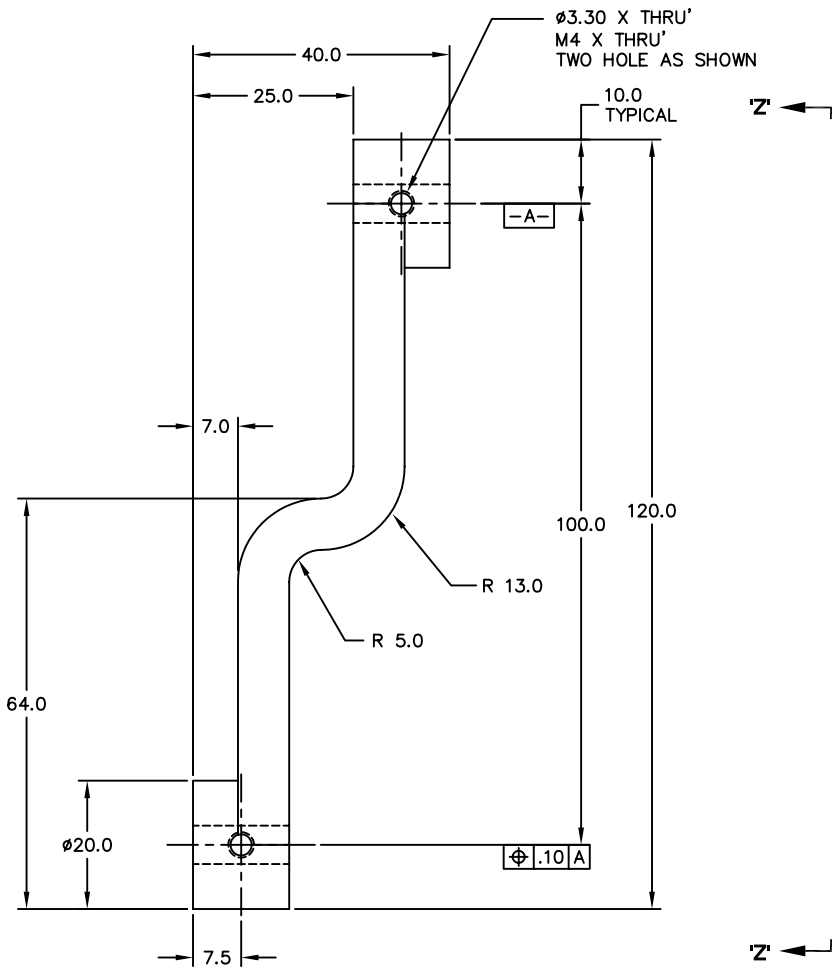

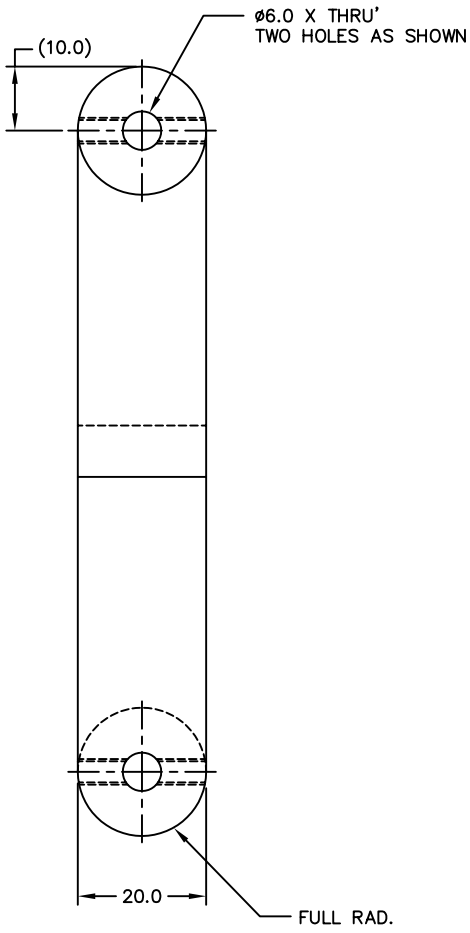

VIEW 'Z-Z'

UNLESS OTHERWISE SPECIFIED: ALL DIMENSIONS ARE IN MILLIMETERS. BREAK ALL SHARP EDGES .01 – .03 R OR 45°

	TOLERANCE UNLESS OTHERWISE SPECIFIED .X ± .1 .XX ± .01 ANGLES ± 5°	SURFACE TREATMENT AS MACHINED MATERIAL ACRYLIC	**NAYANG TECHNOLOGICAL UNIVERSITY** CRANK
SHEET 1 OF 1			

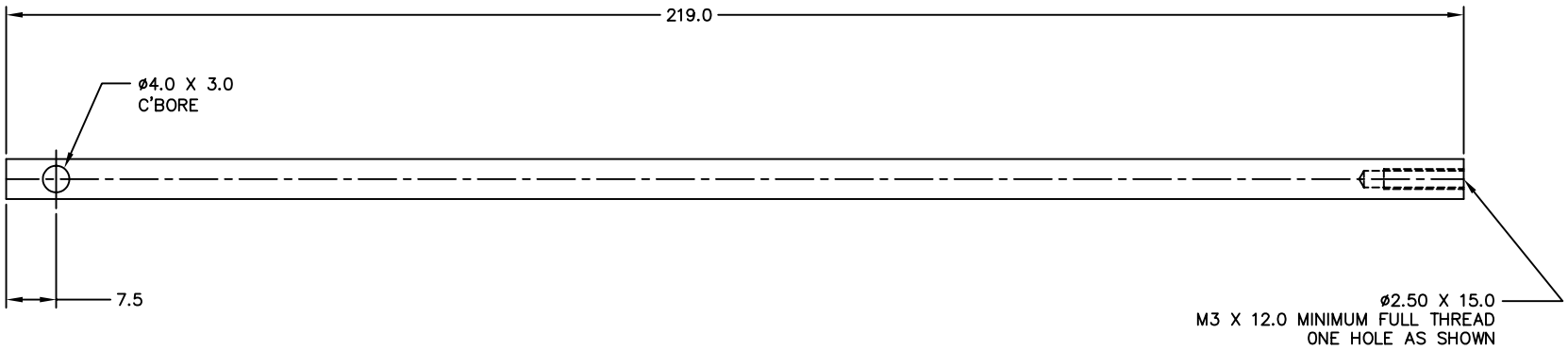

UNLESS OTHERWISE SPECIFIED: ALL DIMENSIONS ARE IN MILLIMETERS. BREAK ALL SHARP EDGES .01 – .03 R OR 45°

TOLERANCE UNLESS OTHERWISE SPECIFIED	SURFACE TREATMENT	NAYANG TECHNOLOGICAL UNIVERSITY
.X ± .1	ANODIZED	
.XX ± .01	MATERIAL	FIN RAY
ANGLES ± 1°	ALIMINUM	

SHEET 1 OF 1

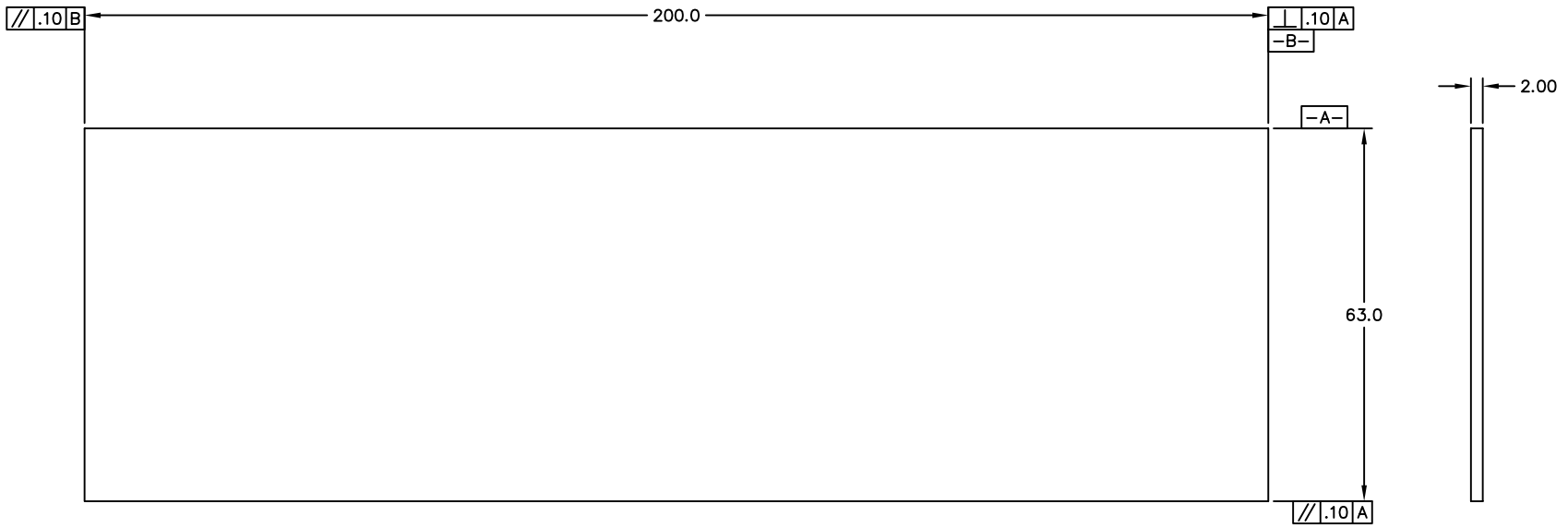

UNLESS OTHERWISE SPECIFIED: ALL DIMENSIONS ARE IN MILLIMETERS. BREAK ALL SHARP EDGES .01 – .03 R OR 45°

TOLERANCE UNLESS OTHERWISE SPECIFIED	SURFACE TREATMENT	NAYANG TECHNOLOGICAL UNIVERSITY
.X ± .1	AS MACHINED	
.XX ± .01	MATERIAL	FIN
ANGLES ± 5°	ACRYLIC	

SHEET 1 OF 1

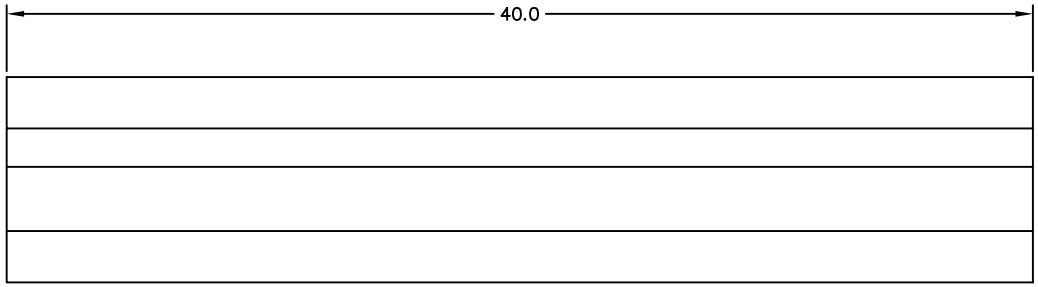

VIEW 'Z-Z'

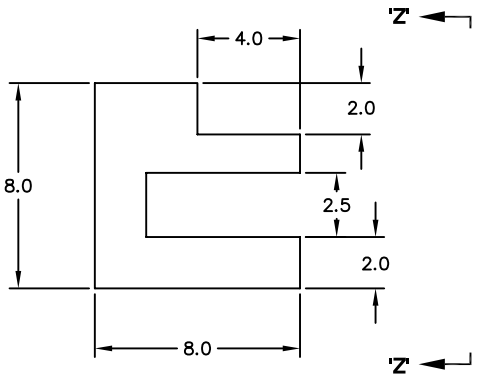

UNLESS OTHERWISE SPECIFIED: ALL DIMENSIONS ARE IN MILLIMETERS. BREAK ALL SHARP EDGES .01 – .03 R OR 45°

	TOLERANCE UNLESS OTHERWISE SPECIFIED	SURFACE TREATMENT	NAYANG TECHNOLOGICAL UNIVERSITY
	.X ± .1	AS MACHINED	
	.XX ± .01	MATERIAL	FIN GUIDE
SHEET 1 OF 1	ANGLES ± 5°	ACRYLIC	

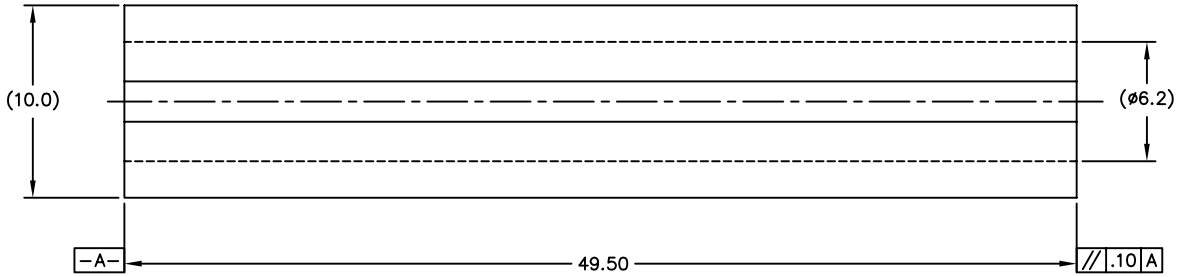

VIEW 'Z-Z'

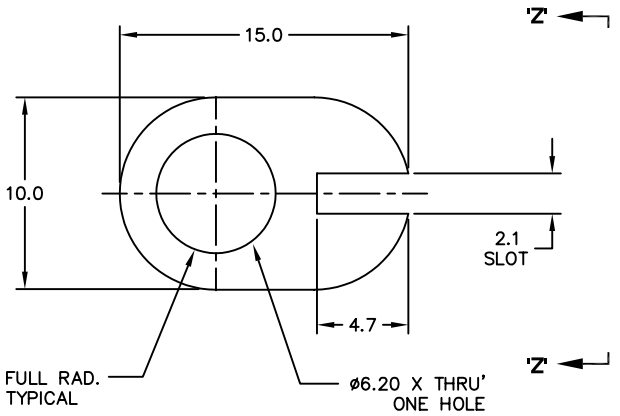

UNLESS OTHERWISE SPECIFIED: ALL DIMENSIONS ARE IN MILLIMETERS. BREAK ALL SHARP EDGES .01 – .03 R OR 45°

TOLERANCE UNLESS OTHERWISE SPECIFIED	SURFACE TREATMENT	**NAYANG TECHNOLOGICAL UNIVERSITY**	
.X ± .1	AS MACHINED		
.XX ± .01	MATERIAL	FIN HOLDER	
SHEET 1 OF 1	ANGLES ± 5°	ACRYLIC	

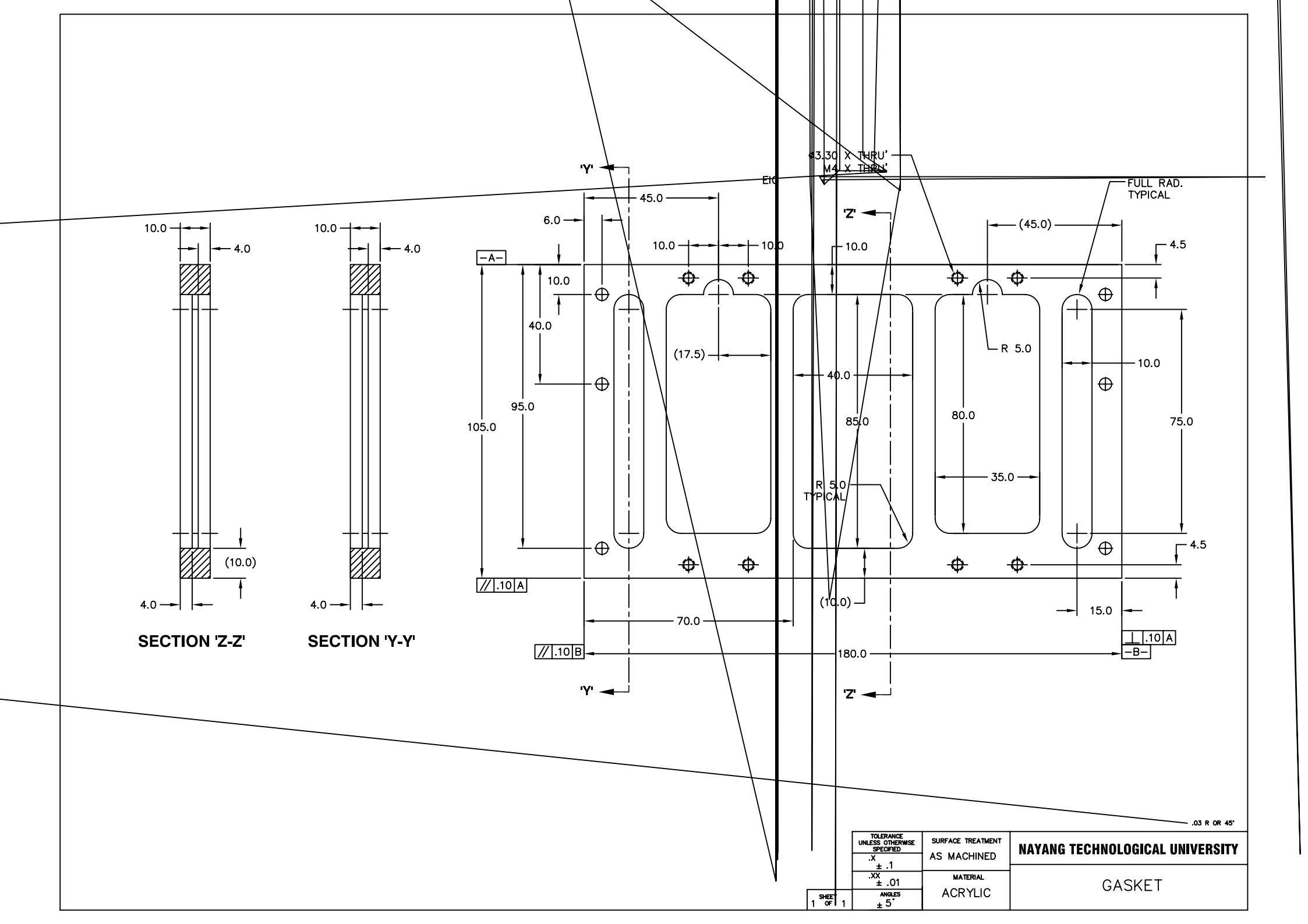

TOLERANCE UNLESS OTHERWISE SPECIFIED .X ± .1 .XX ± .01 ANGLES ± 5°	SURFACE TREATMENT AS MACHINED MATERIAL ACRYLIC	NAYANG TECHNOLOGICAL UNIVERSITY GASKET

SHEET 1 OF 1

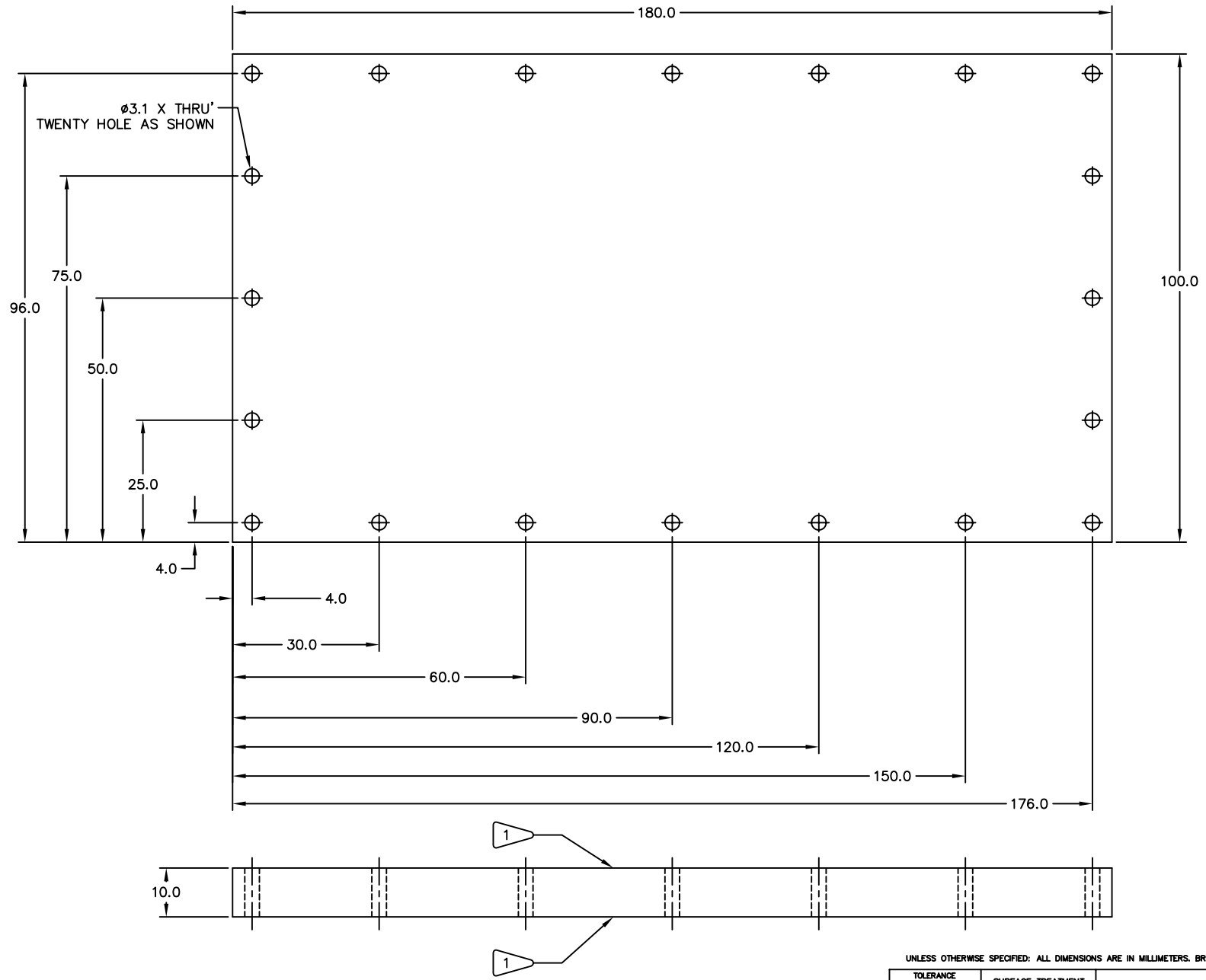

NOTES:

1. SEALING SURFACE, NO INDENTATION OR DEFECTS ON THESE SURFACES

UNLESS OTHERWISE SPECIFIED: ALL DIMENSIONS ARE IN MILLIMETERS. BREAK ALL SHARP EDGES .01 – .03 R OR 45°

TOLERANCE UNLESS OTHERWISE SPECIFIED .X ± .1 .XX ± .01 ANGLES ± 1°	SURFACE TREATMENT AS MACHINED MATERIAL ACRYLIC	NAYANG TECHNOLOGICAL UNIVERSITY PCB CASING COVER

SHEET 1 OF 1

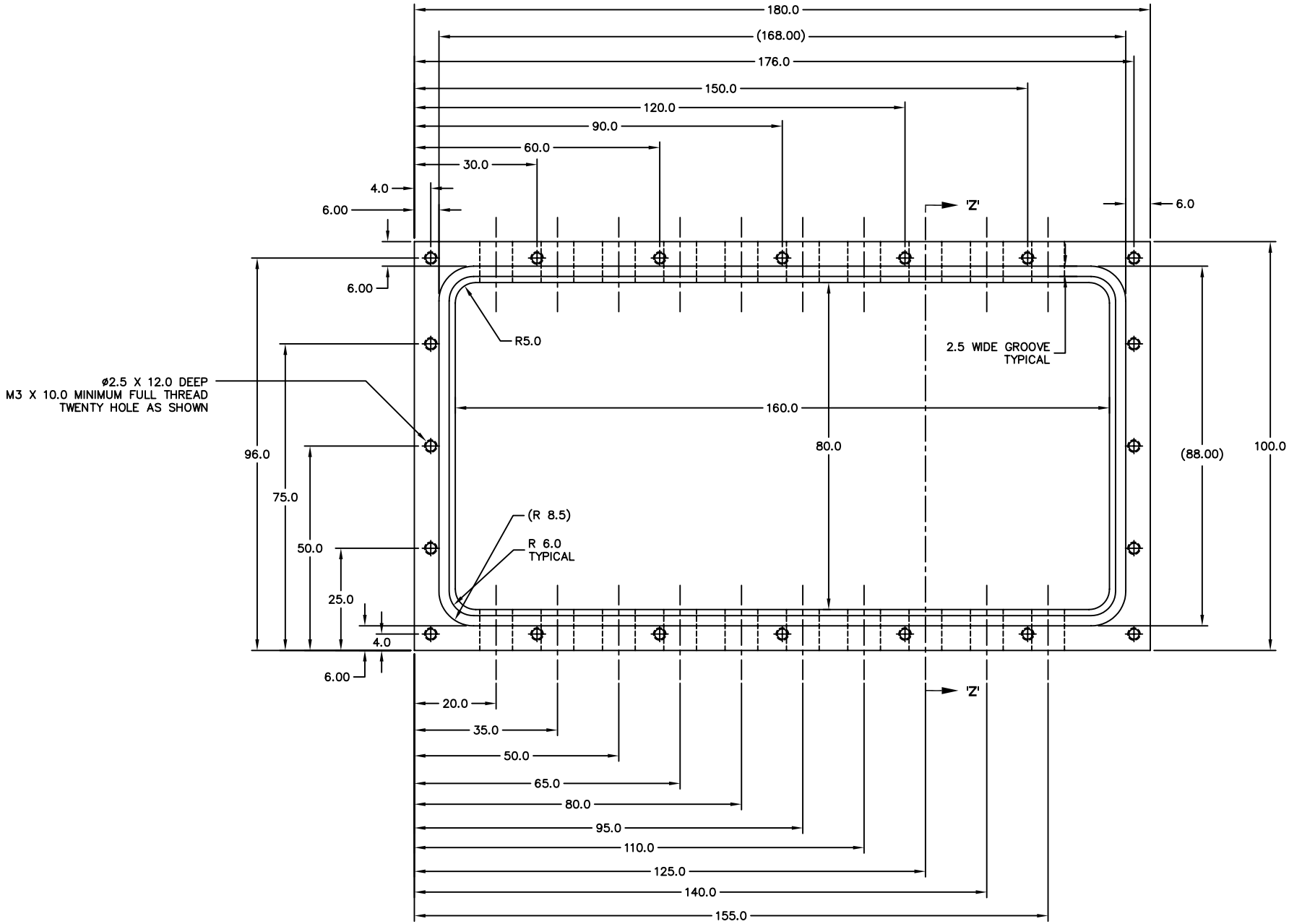

UNLESS OTHERWISE SPECIFIED: ALL DIMENSIONS ARE IN MILLIMETERS. BREAK ALL SHARP EDGES .01 – .03 R OR 45°

TOLERANCE UNLESS OTHERWISE SPECIFIED	SURFACE TREATMENT	NAYANG TECHNOLOGICAL UNIVERSITY
.X ± .1	AS MACHINED	
.XX ± .01	MATERIAL	PCB CASING
SHEET 1 OF 2 — ANGLES ± 1°	ACRYLIC	

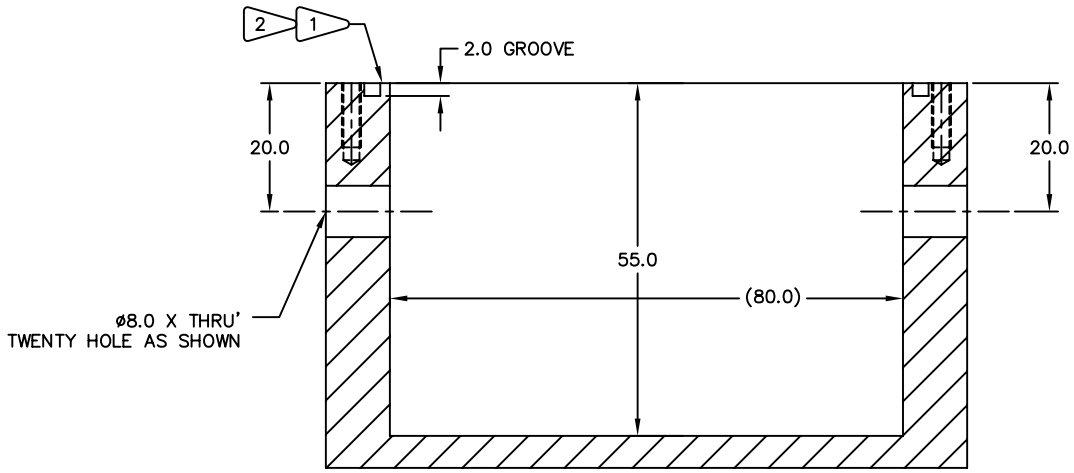

SECTION 'Z-Z'

NOTES:

1. SEALING SURFACE, NO INDENTATION OR DEFECTS ON THESE SURFACES
2. PROTECT THIS CIRCUMFENTIAL AREA WITH HEAVY TAPE AFTER MACHINING.
3. RECOMMENDED O-RING SIZE: ø2.50 MM, 470MM < ID < 480MM.
4. SPLICED O-RING MUST BE WATERPROOF TESTED WITHOUT COMPONETS INSIDE.
5. TO BE ASSEMBLED WITH PCB CASING COVER.

UNLESS OTHERWISE SPECIFIED: ALL DIMENSIONS ARE IN MILLIMETERS. BREAK ALL SHARP EDGES .01 – .03 R OR 45°

	TOLERANCE UNLESS OTHERWISE SPECIFIED	SURFACE TREATMENT	**NAYANG TECHNOLOGICAL UNIVERSITY**
	.X ± .1	AS MACHINED	
	.XX ± .01	MATERIAL	PCB CASING
SHEET 2 OF 2	ANGLES ± 1°	ACRYLIC	

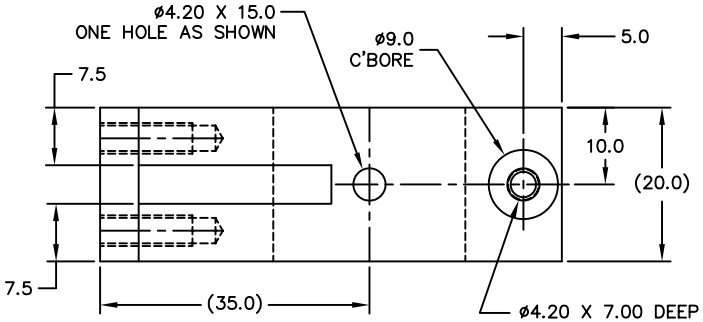

VIEW 'Y-Y'

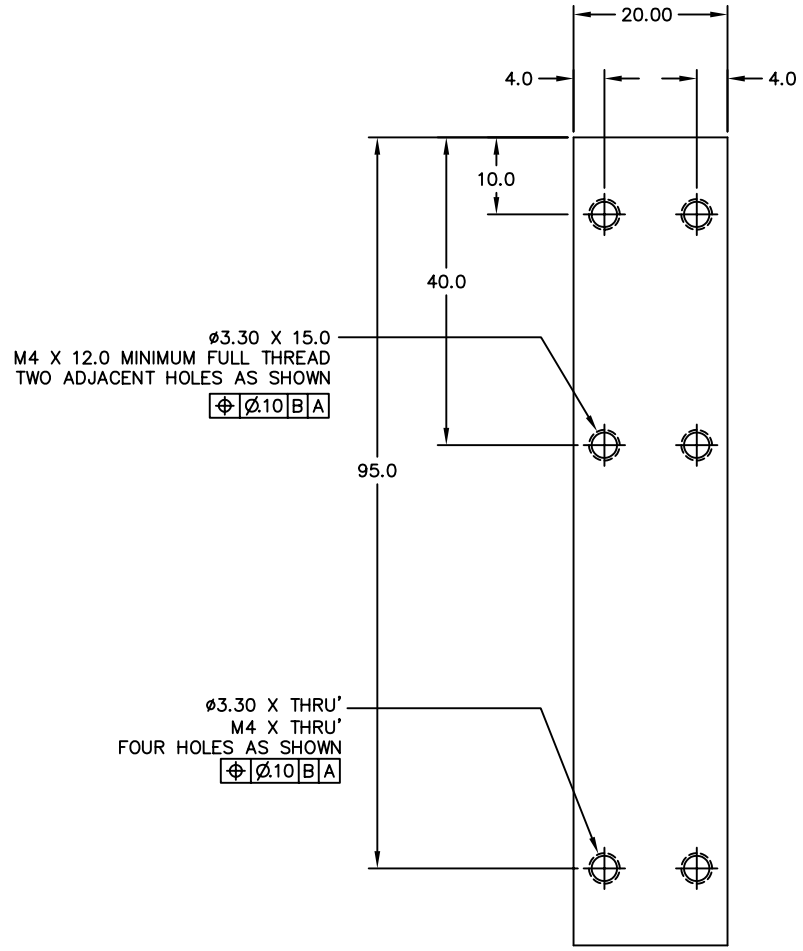

VIEW 'Z-Z'

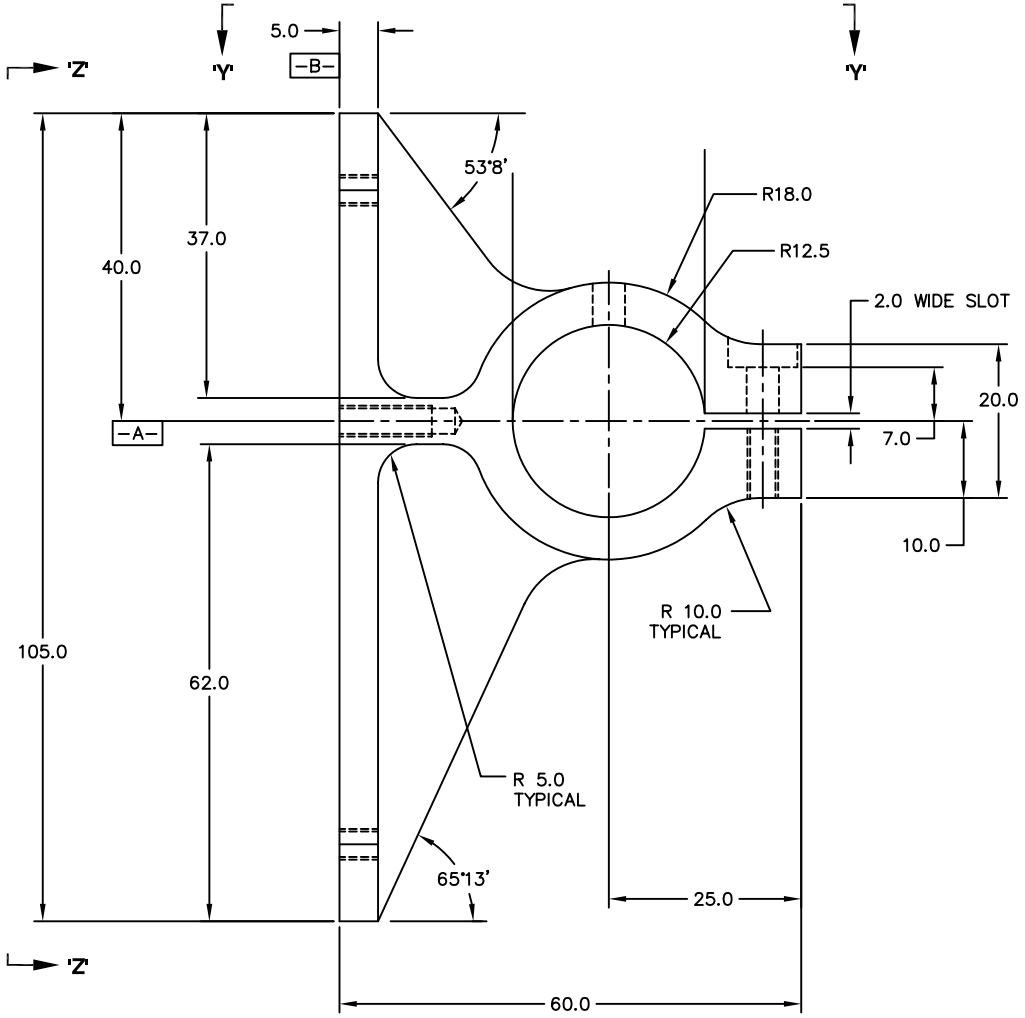

UNLESS OTHERWISE SPECIFIED: ALL DIMENSIONS ARE IN MILLIMETERS. BREAK ALL SHARP EDGES .01 – .03 R OR 45°

TOLERANCE UNLESS OTHERWISE SPECIFIED	SURFACE TREATMENT	NAYANG TECHNOLOGICAL UNIVERSITY	
.X ± .1	AS MACHINED		
.XX ± .01	MATERIAL	GUSSET–TO–SPINE CLAMP	
SHEET 1 OF 1	ANGLES ± 1°	ACRYLIC	

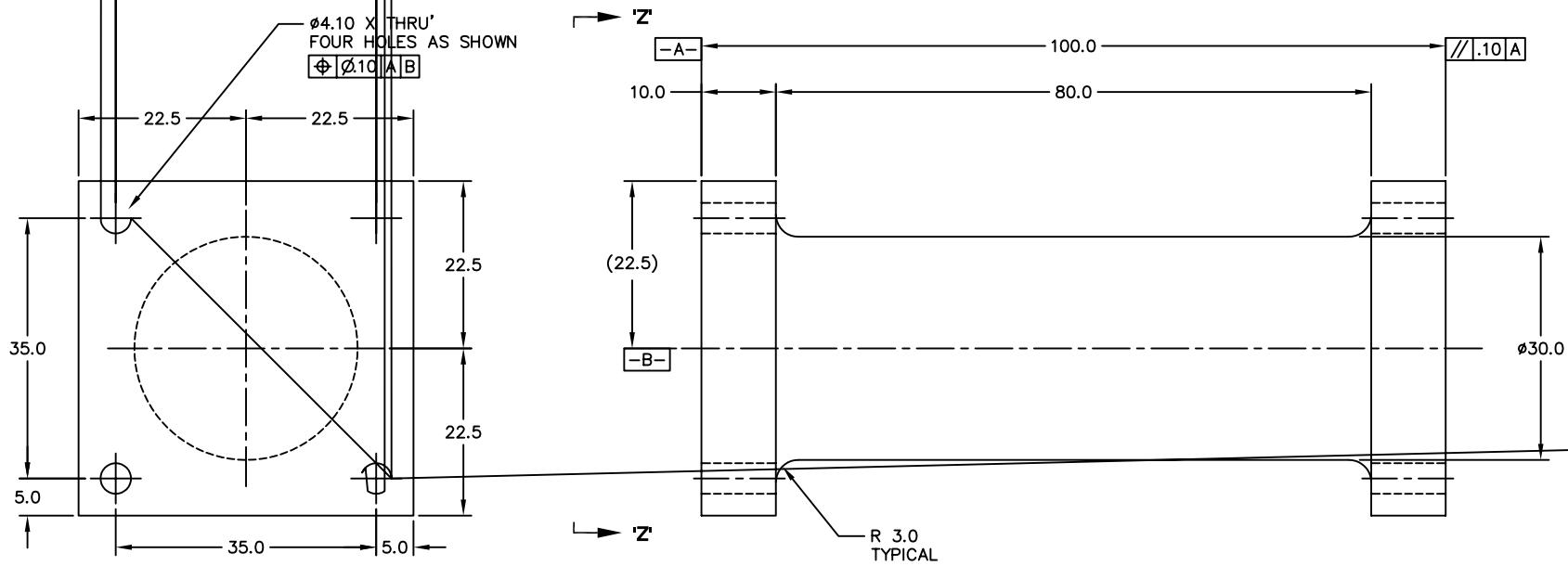

VIEW 'Z-Z'

UNLESS OTHERWISE SPECIFIED: ALL DIMENSIONS ARE IN MILLIMETERS. BREAK ALL SHARP EDGES .01 – .03 R OR 45°

TOLERANCE UNLESS OTHERWISE SPECIFIED .X ± .1 .XX ± .01 ANGLES ± 5°	SURFACE TREATMENT AS MACHINED MATERIAL ACRYLIC	**NAYANG TECHNOLOGICAL UNIVERSITY** SPINE CONNECTOR

SHEET 1 OF 1

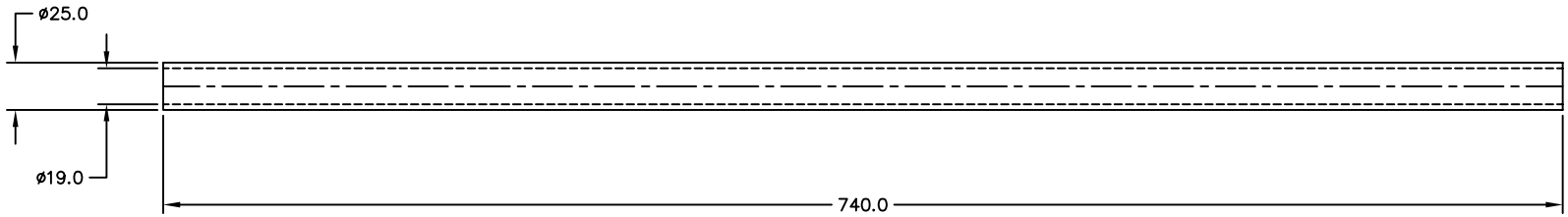

UNLESS OTHERWISE SPECIFIED: ALL DIMENSIONS ARE IN MILLIMETERS. BREAK ALL SHARP EDGES .01 – .03 R OR 45°

	TOLERANCE UNLESS OTHERWISE SPECIFIED	SURFACE TREATMENT	**NAYANG TECHNOLOGICAL UNIVERSITY**
	.X ± .1	ANODIZED	
	.XX ± .01	MATERIAL	SPINE
SHEET 1 OF 1	ANGLES ± 1°	ALIMINUM	

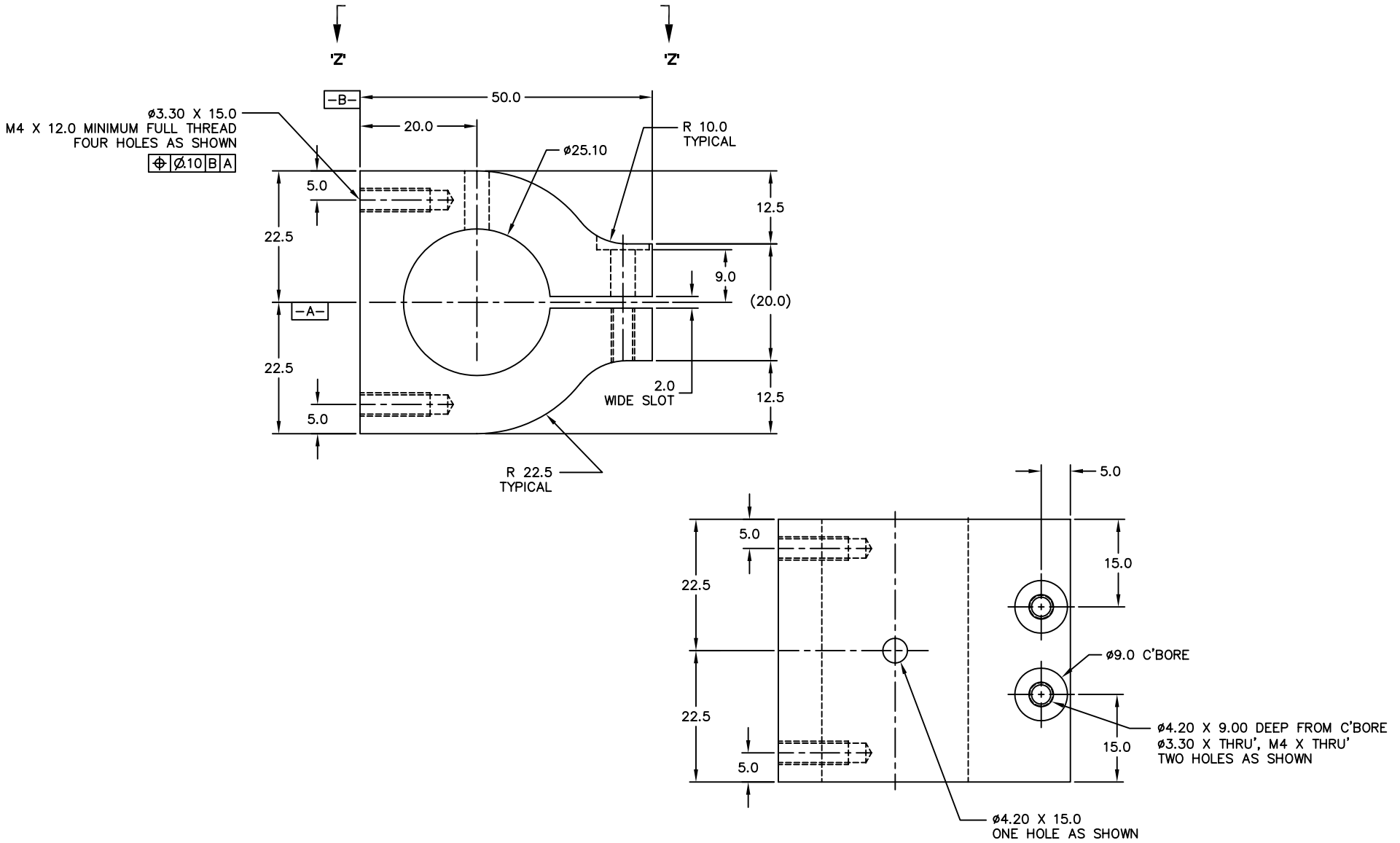

VIEW 'Z-Z'

UNLESS OTHERWISE SPECIFIED: ALL DIMENSIONS ARE IN MILLIMETERS. BREAK ALL SHARP EDGES .01 – .03 R OR 45°

TOLERANCE UNLESS OTHERWISE SPECIFIED .X ± .1 .XX ± .01 ANGLES ± 5°	SURFACE TREATMENT AS MACHINED MATERIAL ACRYLIC	**NAYANG TECHNOLOGICAL UNIVERSITY** SPINE CLAMP F/ SPINE CONNECTOR

SHEET 1 OF 1

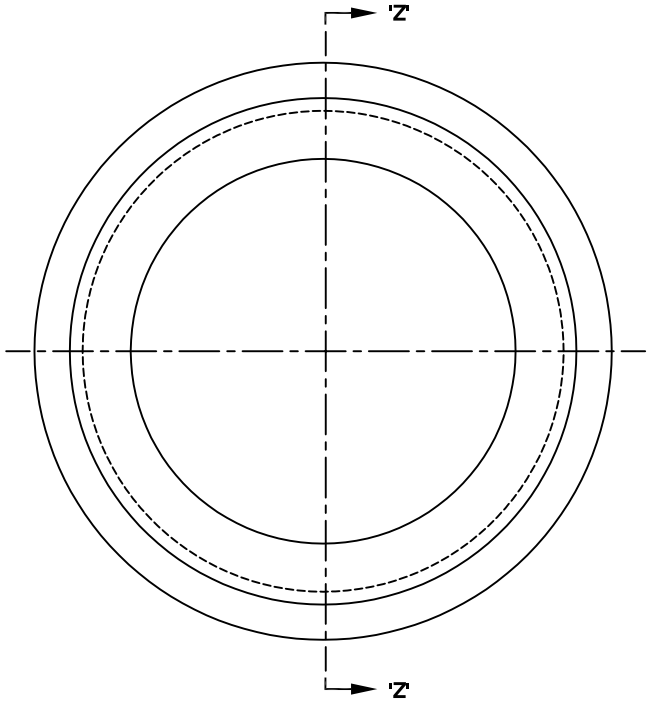

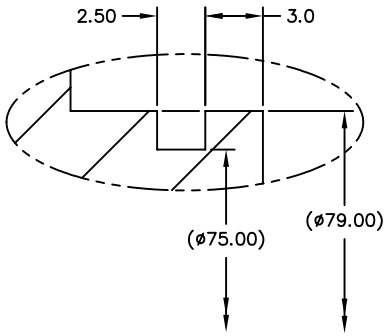

DETAIL 'A'
SCALE 3X
O–RING GROOVE

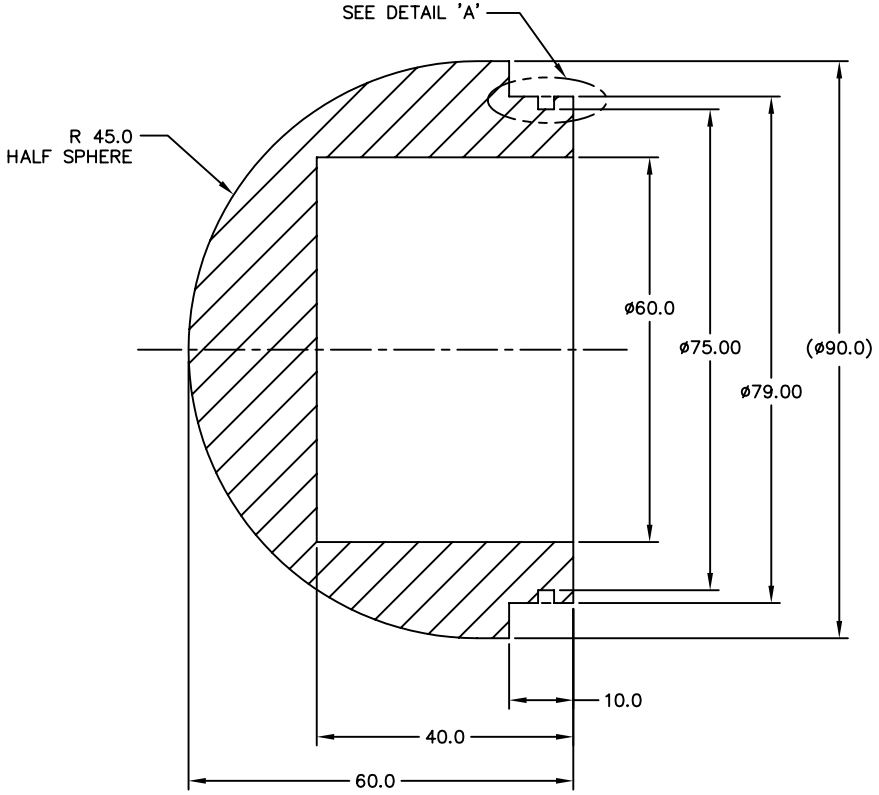

SECTION 'Z-Z'

NOTES:

1. SEALING SURFACE, NO INDENTATION OR DEFECTS ON THESE SURFACES
2. PROTECT THIS CIRCUMFENTIAL AREA WITH HEAVY TAPE AFTER MACHINING.
3. RECOMMENDED O–RING SIZE: ø2.50 MM, 70MM < ID < 75MM.
4. SPLICED O–RING NOT ALLOWED.

UNLESS OTHERWISE SPECIFIED: ALL DIMENSIONS ARE IN MILLIMETERS. BREAK ALL SHARP EDGES .01 – .03 R OR 45°

	TOLERANCE UNLESS OTHERWISE SPECIFIED	SURFACE TREATMENT	NAYANG TECHNOLOGICAL UNIVERSITY
	.X ± .1	AS MACHINED	
	.XX ± .01	MATERIAL	BUOYANT TUBE COVER
SHEET 1 OF 1	ANGLES ± 5°	ACRYLIC	